1994-06

Intraseasonal oscillations over the tropical western Pacific and eastern Indian Ocean for the northern summers of 1989-1991

Cardenas Amores, Jorge A.

Monterey, California. Naval Postgraduate School

NAVAL POSTGRADUATE SCHOOL
Monterey, California

THESIS

INTRASEASONAL OSCILLATIONS OVER THE TROPICAL WESTERN PACIFIC AND EASTERN INDIAN OCEAN FOR THE NORTHERN SUMMERS OF 1989-1991

by

Jorge A. Cardenas Amores

June 1994

Thesis Advisor: Chih-Pei Chang
Co-Advisor: Jeng Ming Chen

Approved for public release; distribution is unlimited

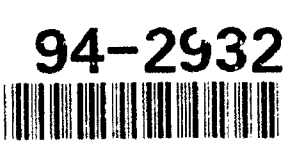

REPORT DOCUMENTATION PAGE

Form Approved OMB No. 0704-0188

1. AGENCY USE ONLY *(Leave blank)*	2. REPORT DATE	3. REPORT TYPE AND DATES COVERED
	June/1994	Master's Thesis

4. TITLE AND SUBTITLE

INTRASEASONAL OSCILLATIONS OVER THE TROPICAL WESTERN PACIFIC AND EASTERN INDIAN OCEAN FOR THE NORTHERN SUMMERS OF 1989-1991

5. FUNDING NUMBERS

6. AUTHOR(S) Cardenas Amores, Jorge A.

7. PERFORMING ORGANIZATION NAME(S) AND ADDRESS(ES)
Naval Postgraduate School
Monterey CA 93943-5000

8. PERFORMING ORGANIZATION REPORT NUMBER

9. SPONSORING/MONITORING AGENCY NAME(S) AND ADDRESS(ES)

10. SPONSORING/MONITORING AGENCY REPORT NUMBER

11. SUPPLEMENTARY NOTES The views expressed in this thesis are those of the author and do not reflect the official policy or position of the Department of Defense or the U.S. Government.

12a. DISTRIBUTION/AVAILABILITY STATEMENT
Approved for public release; distribution is unlimited.

12b. DISTRIBUTION CODE

13. ABSTRACT *(maximum 200 words)*

In this study we used data analyzed by the Navy Operational Global Analysis and Prediction System to study the intraseasonal oscillations other than Madden and Julian oscillation over the tropical western Pacific and eastern Indian ocean. The period of study is May-September of 1989,1990 and 1991. Multiple-set canonical correlation (MCC) ,single point correlation and composite analyses were used to determine the structure of the disturbances.

The results show that MCC mode#1 describes both the seasonal change and a near 20 day oscillation with a zonal half-wavelength around 3000-4000 km. The single point correlation and composites indicate that these oscillations are in gradient wind balance,transporting moisture northward,having upper level divergence over a surface low,and a warm-core structure. The seasonal change composite shows a quasi-stationary oscillation with May and June corresponding to the negative phase of MCC mode#1, and August corresponding to the positive phase of MCC mode#1. The near 20 day composite describes a westward propagation of 2.5-3° per day, with phase 2 corresponding to the negative phase of MCC mode#1 and phase 5 corresponding to the positive phase of MCC mode#1.

14. SUBJECT TERMS
INTRASEASONAL OSCILLATIONS, MULTIPLE-SET CANONICAL CORRELATION , SINGLE POINT CORRELATION AND COMPOSITE ANALYSIS.

15. NUMBER OF PAGES 117

16. PRICE CODE

17. SECURITY CLASSIFICATION OF REPORT	18. SECURITY CLASSIFICATION OF THIS PAGE	19. SECURITY CLASSIFICATION OF ABSTRACT	20. LIMITATION OF ABSTRACT
Unclassified	Unclassified	Unclassified	UL

NSN 7540-01-280-5500

Standard Form 298 (Rev. 2-89)
Prescribed by ANSI Std. 239-18

Approved for public release; distribution is unlimited.

Intraseasonal Oscillations Over the Tropical Western Pacific
and Eastern Indian Ocean for the Northern Summers of 1989-1991

by

Jorge A. Cardenas Amores
Lieutenant , Ecuadorian Navy
B.S., Ecuadorian Naval Academy, 1986

Submitted in partial fulfillment
of the requirements for the degree of

MASTER OF SCIENCE IN METEOROLOGY

from the

NAVAL POSTGRADUATE SCHOOL
June 1994

Author: _____
Jorge Cardenas Amores

Approved by: [redacted]
C.P. Chang, Thesis Advisor

[redacted]
Jeng Ming Chen, Co-Advisor

[redacted]
R.L. Haney, Chairman, Department of Meteorology

ABSTRACT

In this study we used data analyzed by the Navy Operational Global Analysis and Prediction System to study the intraseasonal oscillations other than Madden and Julian oscillation over the tropical western Pacific and eastern Indian ocean. The period of study is May-September of 1989, 1990 and 1991. Multiple-set canonical correlation (MCC), single point correlation and composite analyses were used to determine the structure of the disturbances.

The results show that MCC mode#1 describes both the seasonal change and a near 20 day oscillation with a zonal half-wavelength around 3000-4000 km. The single point correlation and composites indicate that these oscillations are in gradient wind balance, transporting moisture northward, having upper level divergence over a surface low and a warm-core structure. The seasonal change composite shows a quasi-stationary oscillation with May and June corresponding to the negative phase of MCC mode#1, and August corresponding to the positive phase of MCC mode#1. The near 20 day composite describes a westward propagation of 2.5 - 3° per day, with phase 2 corresponding to the negative phase of MCC mode#1 and phase 5 corresponding to the positive phase of MCC mode#1.

TABLE OF CONTENTS

LIST OF FIGURES

ACKNOWLEDGMENTS

The author wishes to express his appreciation and thanks for the invaluable assistance given by Prof. C.P. Chang and Dr. J.M. Chen without their assistance this researh could never have been completed.

Thanks also to Ms. Bao-Fong Jeng for providing extensive help with the computational support and to Dr. Patrick Harr for reading the manuscript.

This work was supported in part by the National Science Foundation Grant ATM-9106495. The NOGAPS data were provided by the Fleet Numerical Meteorology and Oceanography Center, Monterey,California.

I. INTRODUCTION

The existence of wave disturbances in the tropics was first recognized in the 1930's by tracing the movement of pressure changes across the tropical North Atlantic Ocean. Using surface data. Piersig (1936) and Regula (1936) were among the first to notice cyclonic circulation features (disturbances) traveling from western Africa towards the Atlantic at the rate of one every three or four days during the months of June to October, with wavelengths between 2000 km and 3000 km, and speed from 5 m/s to 10 m/s. Although waves occur in the easterlies over many parts of the tropics, observations in the Caribbean area have led to the formulation of wave models, defined as any scheme specifying the idealized or generalized space distribution of meteorological elements (clouds, precipitation, temperature, winds, pressure, etc.) with scales of 1000-2000 miles and a duration of days. Dunn (1940) found that a chain of isallobaric centers at sea level moved across the Caribbean islands from east to west in the hurricane season. These centers were accompanied by westward moving, wave-like oscillations (fairly sinusoidal) in the basic easterly current in the lower troposphere and were correlated with variations in the thickness of the moist layer between the inversion. As upper wind data began to increase, the knowledge of tropical synoptic processes increased too. During and after World War II using upper air data from the Caribbean area Riehl(1945) developed the waves in the easterlies model. He was

able to relate the wave disturbance in the trade easterlies to the surface pressure changes (isallobaric centers) that Dunn had previously studied with surface observations alone. Riehl described that wave disturbances reached their maximum intensity in the layer from 700 to 500 mb,and slopped eastward with height.

Yanai et.al.,(1968) used spectral analysis on radiosonde data over the equatorial central Pacific and observed westward propagating, 4-5 day period waves with an eastward tilt vertical structure. These waves are similar to the waves observed by Riehl over the Caribbean except that they have significantly longer wavelength on the order of 6000-10000 km. Subsequent studies often identified these waves with the mixed Rossby-Gravity waves. Wallace and Chang (1969) and Chang et.al.,(1970) also used spectral analysis on western Pacific stations, and found that the 4-5 day period dominates the equatorial zone over the tropical western Pacific within 10 degrees of the equator, but the waves, while propagating westward, have a zonal wavelength of 2000-4000 km in the lower troposphere and a vertical wave structure that changes systematically from east to west. The change is from an eastward tilt with height in the central Pacific to a slight westward tilt with height in the extreme western Pacific. In between, over most part of the western Pacific, the vertical structure is equivalent barotropic. They attributed this change to the longitudinal variation of the vertical shear in the ambient flow, which was verified in a linear model by Holton (1971). These

waves were also confirmed by Reed and Recker (1971) in a composite study. The term "easterly waves" are sometimes used to describe these synoptic disturbances, and their propagation characteristics are found to be close to Rossby waves. Chang and Miller (1977) later found that the east-west variation in vertical structure also shows up when comparing years with warm and cold sea-surface temperature anomalies over the central and eastern Pacific, with the warm year (El Nino) showing a more equivalent barotropic structure and the cold year a more eastward tilt with height.

Tropical synoptic waves over the North Atlantic were studied by Carlson (1969) and Burpee (1974), Reed et.al.,(1977) and Norquist et.al.,(1977). Along 11-12°N Reed et.al. showed that the average wavelength is near 2500 km, with a period of 3.5 days, which translates to a phase speed of 8 m/s (6-7 degree of longitude per day). The wave troughs are associated with cold anomalies at lower levels and warm anomalies at the upper levels. Most of the studies in the late 1960's and early 1970's were based on station radiosonde soundings and satellite cloud pictures. The expanded observations platforms of the 1979 First GARP Global Experiment (FGGE) and the availability of numerical global analysis from operational numerical weather prediction centers have facilitated further investigations into the behavior of tropical disturbances at locations where little or no station data were previously available. Nitta et.al.,(1985) and Nitta and Takayabu (1985) conducted a global survey of the tropical

transients using the FGGE observations for July and August. They showed a west-northwestward propagating disturbances in the western tropical Pacific. Reed et. al.,(1988) studied the synoptic evolution of African wave disturbances appearing in the European Centre for Medium Range Weather Forecasts (ECMWF) analyses for the summer of 1985. They concluded that ECMWF analyses are rather successful in depicting the African wave characteristics. Libeman and Hendon (1990) and Lau and Lau (1990) used the ECMWF initialized data and the Outgoing Long Wave Radiation (OLR) data during 1980-1987 to study the zonal variation of the 3-6 day equatorial synoptic scale waves. Their results indicate that Mixed Rossby Gravity Waves (MRG) dominate the equatorial eastern Pacific and Rossby type, west-northwest propagating waves dominate the western Pacific. Takayabu and Nitta (1993), using also the summer EC data (1980-1989) along with Japanese Satellite cloud data, found the same two wave patterns and concluded that the mean vertical shear and sea surface temperature gradient could be dominated by these two types of waves in certain regions, which is consistent with Chang and Miller's (1977) findings based on radiosonde data.

Chang et.al.,(1994) used multiple canonical correlation analysis (MCCA) with analyzed data from the Navy Operational Global Atmospheric Analysis and Prediction Model (NOGAPS) to study these northwestward propagating waves during the summers of 1989-1991 Because they were interested in the synoptic scale disturbances, the data were subjected to a high-pass filter where

oscillations with period greater than 12 days were removed. The waves have patterns that are similar to those found by Lau and Lau (1990) but the period is around eight days. They concluded that most of these waves are related to tropical cyclone activities, and postulated that nonlinear barotropic effects cause anticyclogenesis southeast of the main cyclone center, with the wave energy propagating to the southeast, which favors a continuous development of wave disturbances. These are Rossby waves as the beta effect plays a major role in the propagation and development.

In addition to synoptic-period waves discussed above, intraseasonal oscillations have been known to affect tropical weather significantly. The most well known is the 30-60 oscillation, or the Madden-Julian oscillation (MJO, Madden and Julian, 1971,1972). This is an eastward propagating planetary scale wave with zonal wavenumber one and dominant oscillations in the zonal (u) wind component. It is often associated with convection patterns along the equator all year round. Considerable observational studies on the MJO have established its key role in regulating the tropical convection, particularly in the Indian monsoon region (Krishnamurti and Subrahmanyan, 1982; Lorenc, 1984; Krishnamurti, 1985; Lau and Chan, 1986). Krishnamurti et.al.,(1985) clearly identifies a planetary-scale divergence wave that traverses around the globe eastward throughout the FGGE year. Its speed of eastward propagation is around 8 degrees of longitude per day . The amplitude of this

wave is largest during the summer season over the monsoon region and the western Pacific Ocean. The amplitude decreases somewhat as the wave traverses across the eastern Pacific and Atlantic oceans. The divergence or convergence centers usually appear over the western equatorial Indian Ocean. Then they propagate to the western Pacific, around 20 N, in 20 days. As suggested by the numerical studies of Hayashi and Sumi (1986) and Lau and Peng (1987), cumulus convection is an important factor in generating the 30-50 day low frequency mode. The northwestward propagation of the planetary-scale 30-50 day divergent mode might be attributed to the supply of available water vapor and cumulus convection over the entire Asian Monsoon region. Theoretical studies have suggested that the MJO is likely moist Kelvin waves (Chang, 1977; Lau and Peng, 1987; Chang and Lim, 1988), and may have a Rossby component that couple the convection with the planetary boundary layer (Wang, 1988).

Another intraseasonal signal in tropical oscillations occur in the period range between the synoptic waves and the MJO. Wallace and Chang (1969) found that while the meridional (v) winds at the tropical western Pacific stations show a dominant 4-5 day spectral peak, the u component show a 10-15 day peak at many of the stations. This quasi-biweekly periodicity also showed up in various studies of the Asian summer monsoon region, e.g., Krishnamurti (1973), Murakami and Frydrych (1974), Zangvil (1975), Krishnamurti and Bhalme (1976), Krishnamurti and Ardanuy (1980) and Krishnamurti et.al.,(1985), Wu and Li (1990), Li and

Zhou (1992) and Chen and Chen (1993). In these studies the term "10-20 day oscillation" is often used to describe these disturbances. In general, these disturbances propagate westward and have a near barotropic vertical structure. Many of the previous studies associated this oscillation with the activity of the Indian summer monsoon. In particular, Krishnamurti and Bhalme (1976) and Li and Zhou (1992), emphasized that the biweekly oscillation dominates the fluctuation of wind and surface pressure over the Indian monsoon region and documented its interaction with the MJO. Chen and Chen (1993) observed that in their 1979 summer data, which consisted of ECMWF analysis and satellite derived rainfall, the 10-20 day oscillation has a double-cell structure with one centered along 15-20°N and the other near the equator, and that significant rainfall occurs around the low center of the northern cell. They suggested that these disturbances develop from residual lows that propagate into the northern summer monsoon region from the western Pacific, as is the case with most monsoon depressions (Krishnamurti et.al.,1977; Saha et.al.,1981). Chen and Chen (1993) also emphasized the importance of the interaction of the 10-20 day oscillation with the MJO in the development of the former.

In a study of the effect of the variation of large scale circulations on tropical cyclone characteristics over the tropical western North Pacific, Harr (1993) identified six recurrent 700 hPa circulation patterns that represent large-scale variabilities associated with the monsoon trough and subtropical

ridge. There are a number of possible transitions between recurrent circulation patterns, but significant transitions occur over a very limited set of paths that are associated with interactions among topical and midlatitude circulation systems. Harr (1993) showed that the recurrent circulation patterns and their transitions can explain much of the observed intraseasonal variability in the occurrence and track types of tropical cyclones. His work may alternatively be interpreted as a description of the intraseasonal variations of the lower-tropospheric large-scale monsoon circulations. While the transition changes are not periodical and take a number of different paths, each transition occurs on a time scale of two to three weeks.

The strong signals of both the MJO and the quasi-biweekly oscillations over the northern summer monsoon region suggest that the intraseasonal oscillations may be the manifestation of a large-scale monsoon oscillation over the entire Indian Ocean-western Pacific region (Krishnamurti and Subrahmanyan, 1982; Lau and Chen, 1986; Chen et.al., 1988). The synoptic disturbances may have a period as long as 10 days (Chang et.al., 1994), which nearly overlaps with the short end of the period range of the quasi-biweekly oscillation. The spectrum of the quasi-biweekly oscillation is also nearly connected with that of the MJO. Since all are active in the tropical western Pacific, most previous studies have relied on time frequency filtering, typically band-pass filters, to separate the two systems. Such

an approach pre-determines the period window to be studied and may leave out structures that are outside of the pre-selected window. Chang et.al.,1994) have shown that the MCCA method, as proposed by Chen and Chang (1993) and Chen et.al.,(1994), can effectively isolate the synoptic-scale, west-northwestward propagating disturbances in the tropical westernmost Pacific from the NOGAPS analysis during summers of 1989-1991. Although intraseasonal frequencies were removed by a high pass filter that truncates the spectrum at a period of 12 days, narrow band pass filtering was not used by them. Because the MCCA technique is mainly a spatial decomposition, they were able to find the main structure of the synoptic waves whose period are actually closer to 8 day during these three summers rather than the typically assumed 3-6 day period.

The purpose of this study is to use the same MCCA on a domain larger than Chang et.al.,(1994), from Bay of Bengal to the tropical western Pacific, to study the structure of the intraseasonal oscillations during the same three summers. In particular, the focus of the study will be on intraseasonal oscillations other than the MJO. Therefore, as was done in Chang et.al.,(1994), the MCCA will be based on the meridional wind component. This will bring out the signals of non-MJO intraseasonal oscillations more effectively since the strongest signal of MJO is in the zonal wind component. It is expected that the same MCCA technique as applied by Chang et.al.,(1994) will separate out the tropical synoptic disturbances from the

larger-scale intraseasonal oscillations in this domain, therefore allowing a focused study on the latter without the reliance of a pre-determined band-pass filter.

Section 2 will briefly discuss the NOGAPS data and the analysis methods used. Section 3 will show the primary MCCA-decomposed modes base on v winds at 850 hPa that include both the intraseasonal oscillations and the synoptic scale waves. Section 4 will show the structure of this intraseasonal mode. Section 5 will discuss the results of a composite study where a submonthly oscillation that is identified with the intraseasonal v mode is compared with the summer seasonal trend. Section 6 includes a summary and the conclusions.

II. DATA AND METHODOLOGY

The data used on this study are the un-initalized objective analysis produced by the Navy Global Atmospheric Prediction System (NOGAPS), for three summers (May-September): 1989, 1990 and 1991, available twice daily on 2.5 X 2.5 grids. The domain of the study is shown in Figure 1. A core region of 100-180E, 10S-25N is embedded in the large domain of 20S-40N, 70-180E. Use of NOGAPS data allows us to make a preliminary evaluation of an additional data set for the study of tropical waves. Due to a major upgrade in software and the availability of large amounts of data different statistically methods have been used in the meteorology and oceanography fields. One of those is the Principal Component Analysis (PCA) which was first suggested by Pearson (1901) in a biological context when he recast linear regression analysis into a new form so as to avoid the usual asymmetrical relationship between "dependent" and "independent" variables in linear regressions. Later Hotelling (1933) applied PCA in Psycrometry. Lorenz (1956) made prediction studies of the 500 mb height anomaly field, and term the weighting function coefficients as empirical orthogonal function (EOF).

The basic idea of PCA is to find a linear combination (or component) of the original data variable such that the principal component (PC), which is a function of time over a set of grid points (17*15 in our study) and is also referred to as an "amplitude", has the maximum possible variance under the

condition that the weighting function, which is a function of space over a set of grid points, is orthogonal to those of all preceeding PC's. Subsequent PC's can be found under the same maximum variance, unitary weighting function,and orthogonality requirements. If a data pattern is proportional to its own weighting function, all other PC's will vanish due to the spatial orthogonality. Therefore the weighting functions can be viewed as the spatial patterns associated with each PC. These weighting functions are often called EOF's in meteorological studies. Chang et.al.,(1993) have shown that direct application of PCA to data from a well chosen network is particularly efficient.

PCA gives us the internal variation within one data field to the leading component, but doesn't tell us information about relationship between different fields. The relationships between two fields in terms of correlation coefficient can be found using the Canonical Correlation Analysis (CCA) (Hotteling, 1935, 1936; Glahn, 1968; Prohaska, 1976). The CCA is basically a search for optimal correlation between two variable fields by linearly combining the elements of each field. These combinations are called canonical components (CC). The method also gives a pair of patterns (one for each field) that soley correspond to each optimized correlation, and their respective variance contributions. Conventional CCA can be used for investigating the correlation between two fields, but often it can only reveal maximum correlations without regard to the variance significance. Therefore truncation with PC's is often recommended before CCA is

performed. It is hoped that with PCA the leading components (those with larger variabilities) may indeed represent different physical processes. Or at least, component truncation can help to delete noise and errors that we beleive to be associated with small variabilities.

The Multiple-set Canonical Component Analysis (MCCA) method is a generalization of the traditional two fields CCA to multiple fields (e.g. Steel, 1955; Horst, 1965; Kettenring, 1971; Gifi, 1990). The method seeks the optimal correlation among more than two data fields. Through a diaganolization of the product or the squared product of the correlation matrices, Chen et al.,(1994) not only greatly simplify the MCCA procedures to be use in studies with large dimensioned data, but also enable to select correlations only between desired field pairs. Chen and Chang (1994) tested the sensitivities of the MCCA technique in the 850 hPa meridional wind data over the tropical western Pacific to study tropical synoptic wave disturbances during summer. Their results indicated that the method is stable to sampling changes when the data contain significant signals of physical phenomenon, and not stable when the data are random. For our study, the MCCA is used on V_{850} within the core region to find the basic disturbance structure mode,and other variables at various levels over the large domain are correlated with the basic structure mode to delineate the entire structure of the disturbance.

The data on 255 grid points within the core domain are first pre-processed with an PC analysis, which allows a truncation that

includes only the first 18 principal components (80.6 % of total variance). The MCCA is then applied to twelve data sets from 00h (time T1) to 132h (time T11) as a 12 h window is used. The squared product of correlation matrices between fields of adjacent times are optimized after transformation matrices from principal components to canonical components are obtained, spatial patterns of V_{850} at each time step are computed as weighting functions which converts the canonical components back to the original V_{850} field. The reliability of the method for the unfiltered data set has been tested by Chen and Chang,1994.

To describe the space-time evolution of the tropical transients, we have applied MCCA analysis on the summertime data for the 850 hPa v component. On the basis of one-point (component) correlation maps at various pressure levels we are able to delineating the vertical structure, time evclution, phase propagation speed and the growth/decay rates of the synoptic disturbances. The temporal lags used in our study range from 0 to 6 days. Here negative (positive) lags refer to computations with the time series at individual grid points leading (lagging) time series.

Comparisons between the patterns in different panels will reveal the characteristics of transient phenomena occuring in the area covered in this study. The space-time evolution of selected meteorological variables associated with the quasi-biweekly oscillations in different active regions are described in Section 4, using the composites constructed on the basis of the temporal

MCC amplitudes.

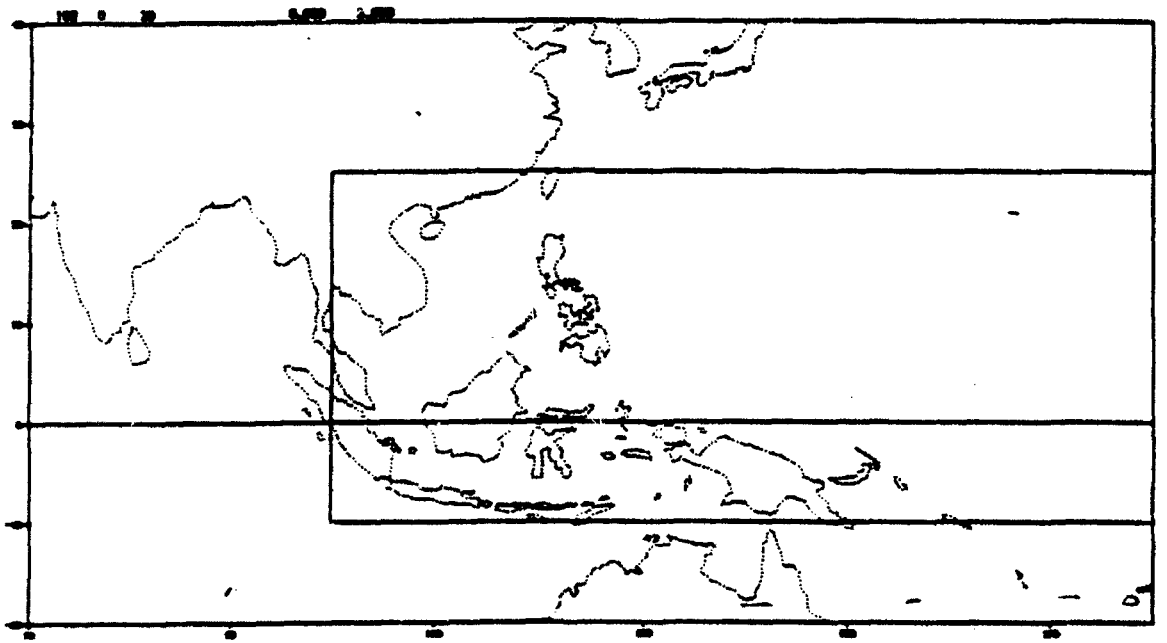

Figure 1: Map of data area (showing core domain for MCCA and large domain for single point correlation and composites).

III. LEADING MCC MODES BASED ON V_{850}

A. STRUCTURE OF THE LEADING MODES

The first three MCC modes of V_{850} are shown in Figs. 2, 3 and 4, respectively. In each figure the structure for 12 consecutive twelve-hourly time frames, from 00 h to 132 h (5.5 day), is displayed. For MCC mode 1 (Fig. 2) the average correlation between the adjacent times is 0.89, with an average fractional variance of 17.6% and a maximum residual correlation of 0.015. The smallness of the last value relative to the average correlation is an indication that the solution is reliable (Chen and Chang, 1994). This mode shows a near stationary large-scale pattern with four major centers, a pair of positive and negative areas whose centers are near the northern boundary of the core domain along 25°N, and an opposite pair of negative and positive areas just north of the equator. The centers of these couplets line up more or less longitudinally, with the western centers over southern China coast and the Philippines, and the eastern centers over the westerm Pacific. The gross pattern is roughly stationary, with a slight indication of a slow westward propagation. The propagation signal is particularly evident for the southeast center near the equator, which has the smallest amplitude of the four centers and propagates from 155°E to 140°E over 5.5 days, which is faster than the other three centers that

propagate westward by about one third of this speed (less than 5° over the 5.5 days). These two pairs of couplets give a pair of cyclonic/anticyclonic circulations that are aligned in the north-south direction.

Fig. 2 indicates that for the positive phase of mode 1 there will be a slowly westward propagating, anticyclonic longitudinal shear of meridional wind in the northern equatorial region of the western Pacific, and a slower westward propagating, or almost stationary,cyclonic longitudinal shear of meridional wind north of 10°N between 130°E-140°E. For the negative phase the reverse is true. The large zonal scale, which is about 30° longitude for a half wavelength near 25°N, suggests that the northern pair of anomaly centers may be a manifestation of alternating presence or strength of the East Asian monsoon trough (Tao and Chen, 1977) and the western North Pacific subtropical ridge. The southern pair of anomaly centers near the equator have about 20° longitude between them, and may represent the alternating strength of the equatorial monsoon trough associated with the northern summer intertropical convergence zone (ITCZ) in the tropical western Pacific. This variation of the monsoon trough is also influenced by a slowly propagating system that propagates westward at approximately 3° longitude per day.

MCC mode 2 (Fig. 3) shows a time sequence of a northwestward moving wave with a period around eight days and a half wavelength of about 14° longitude. The northeast-southwest elongated wave patterns which emanate from the eastern part of the equatorial

western Pacific east of 160°E are very similar to those found by Chang et.al.,(1994) using the same data set with a smaller MCC analysis domain and those observed by Lau and Lau (1990) in the same area during summers of 1980-1987. The average correlation between the adjacent times is 0.871, with an average fractional variance of 15.3% and a maximum residual correlation of 0.049. The time sequence of MCC mode 3 (Fig. 4) resembles that of mode 2, except that there is a phase shift of about two days in time and a quarter-cycle shift in space. Mode 3 has an average fractional variance of 16% and a maximum residual correlation of 0.033, again very small compared to its average correlation of 0.86.

Both modes 2 and 3 indicate an eight-day period as can be seen from the reversal of the phase of the entire pattern between any two panels that are four days apart. The quarter-cycle time and spatial phase shift between modes 2 and 3 is consistent with the 8-day periodicity and the combination of these two modes describe this northwestward propagating wave pattern. This is the same wave modes found and studied extensively by Chang et.al., (1994). Here modes 2 and 3 together describe a total fractional variance of 31.3%, which is only slightly smaller than the total variance of 35.1% found be Chang et.al.,(1994) in a smaller domain of 110°E-150°E and 10°S-25°N, which is one half the area of the present MCC domain. Thus the 8-day northwestward propagating wave pattern, which Chang et.al.,(1994) proposed to be a manifestation of a wave-tropical cyclone interacting system, is a

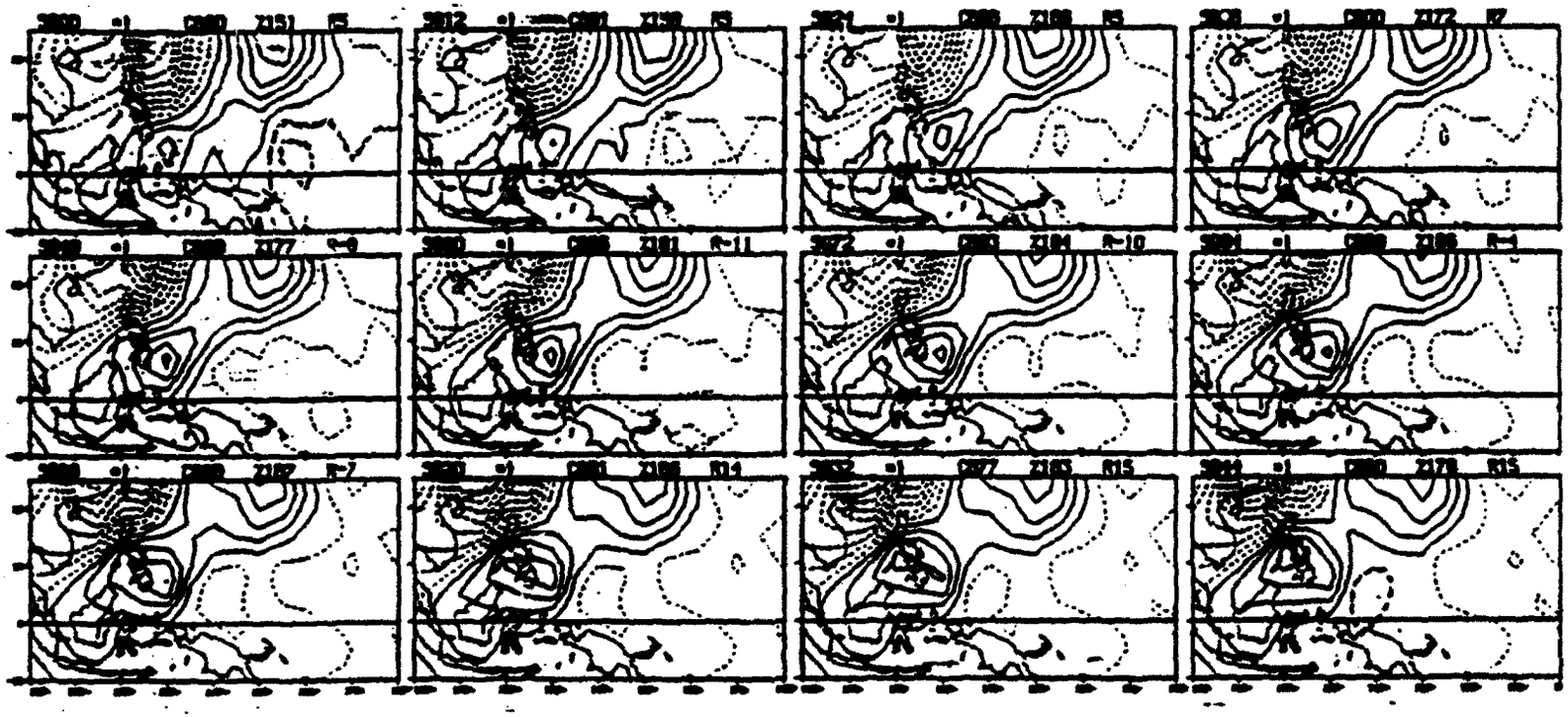

Figure 2: Weighting function for MCC mode#1 (equivalent to MCC mode #1 structure) of 850hPa meridional wind (V) for 12 consecutive twelve-hourly frames from 00h to 132h (5.5 days). Contour interval is 0.03 and dashed lines correspond to northerly winds when MCC mode#1 amplitude is positive.

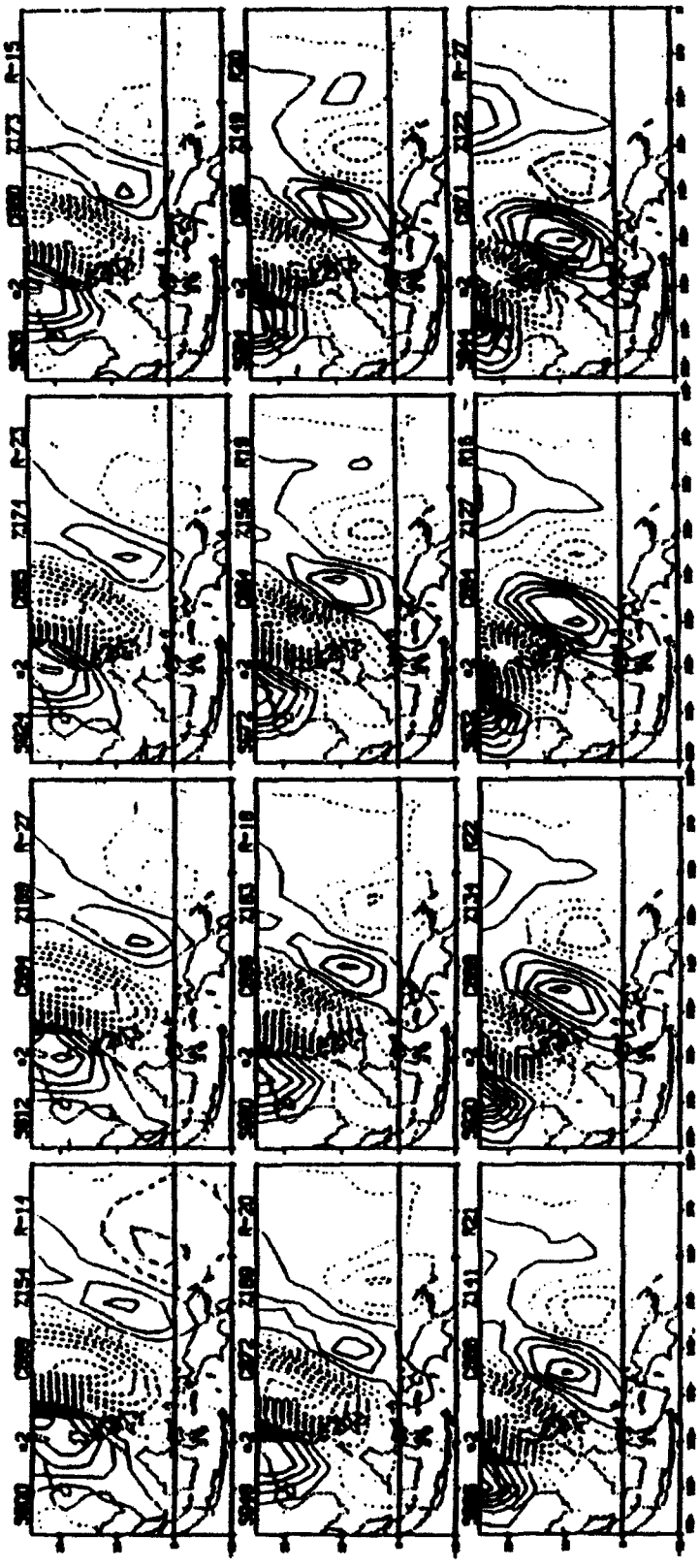

Figure 3: Same as figure 2 except for MCC mode#2.

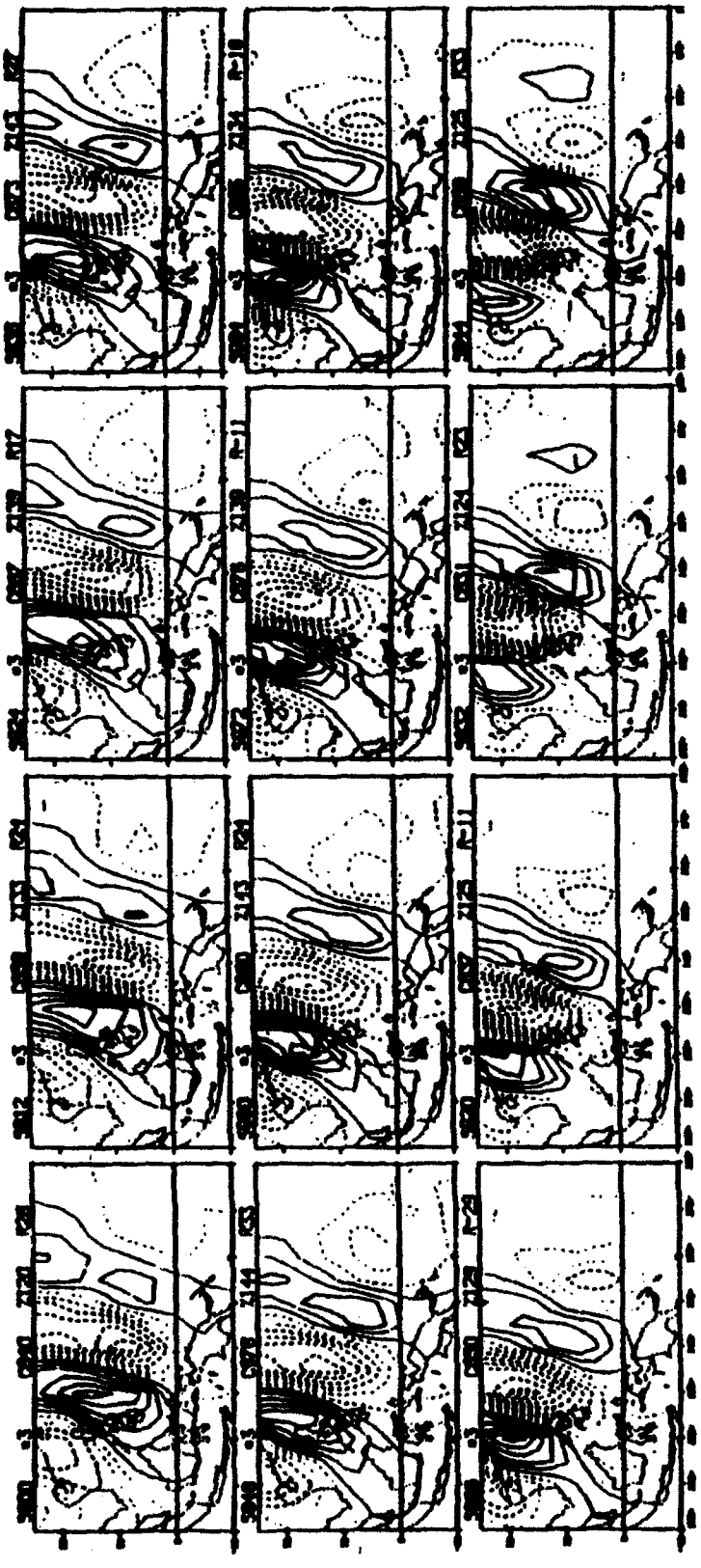

Figure 4: Same as figure 2 except for MCC mode#3

substantial synoptic scale motion system over the entire tropical western Pacific and its effects, according to Figs. 2-3, may extend to southern China and the Indochina Peninsula.

B. TIME VARIATION OF THE COEFFICIENTS OF THE LEADING MCC MODES

At any given time a mode contains both horizontal and time structures, with the latter encompassing 12 consecutive twelve-hourly frames from day 0 to day 5.5. Thus, the time variation of each mode should be described by considering the fact that each mode is a space-time volume function that covers not just the horizontal spatial domain but also a time domain of 5.5 days. In order to take into account this time domain, the coefficient of each mode is constructed by producing a time-integrated amplitude coefficient. This coefficient is the average amplitude of the 12 consecutive twelve-hourly structures, and is plotted in the time domain according to the time of the first (day 0) time frame.

Fig. 5. shows the time series of the time-integrated amplitude coefficient of mode 1 for the three summers. To the right of each series is its power spectrum. In each year there is a general tendency of increasing coefficient from the early part of the season to latter part of the season, although near the very end (September) there is a slight trend of decreasing coefficient, particularly in 1991. Superimposed to this seasonal trend are shorter time scale oscillations, whose amplitude is

more pronounced in the latter half of each season. These two time scales are represented in the spectral distribution with two power "peaks": a seasonal trend at the lowest frequency, clearly shown in the 1989 and 1991 spectra, and an intraseasonal oscillation at about 20-day period, clearly shown in the 1989 and 1990 spectra.

Figs. 6-7 show the time series of the time-integrated amplitude coefficient of modes 2 and 3, respectively, for the three summers. The two time series are nearly one-quarter cycle out of phase just as shown in the spatial structure patterns of the two modes (Figs. 3-4). A prominent spectral peak at a narrow period band centered around 8 days is clearly indicated for all three summers. This is the same periodicity that is evident in Figs. 3-4. The power peak is sharp and concentrated around this period band, with the 1989 and 1990 summers both showing a peak between 7-8 day and 1991 summer a peak at 9 day. Both the time series and the spectral distribution of these two modes closely resemble those of the two leading modes in Chang et.al.'s high-pass filtered data, and clearly reconfirms the existence of the 8-day northwestward propagating wave patterns studied by them.

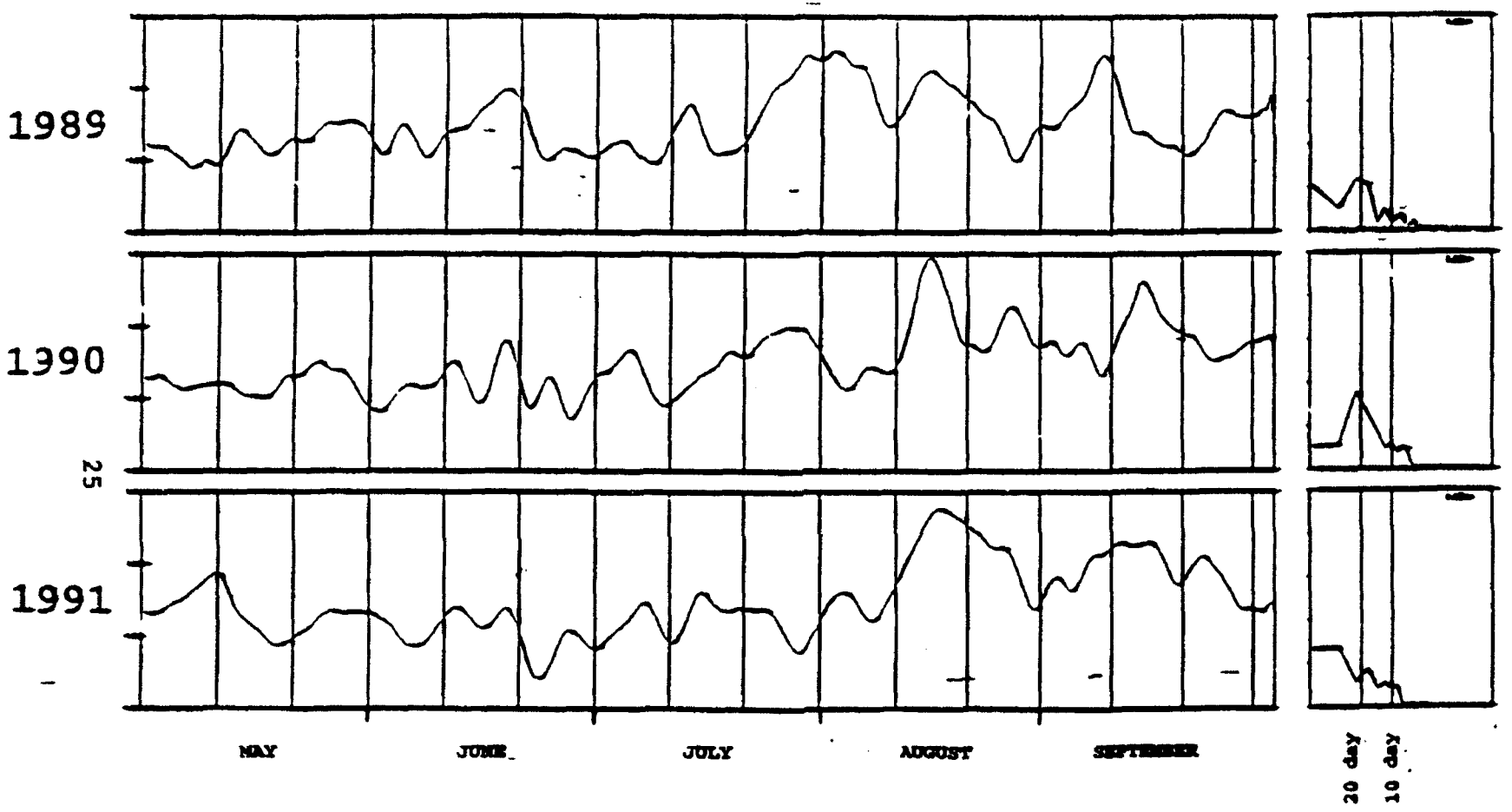

Figure 5: Time series of time-integrated amplitude coefficients of MCC mode#1 for the three summers. Power spectrum of the time series is shown at right.

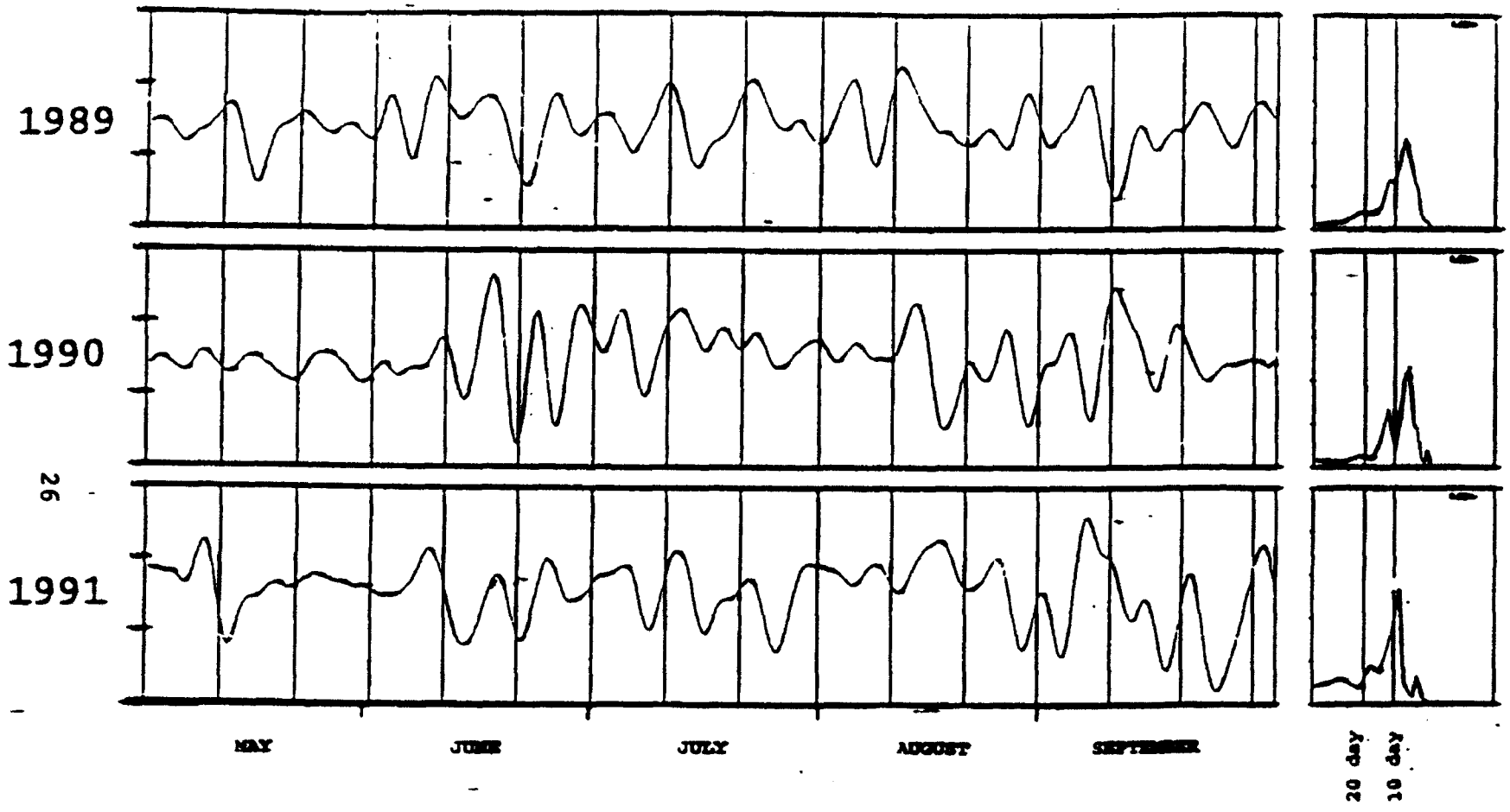

Figure 6: Same as figure 5 except for MCC mode#2.

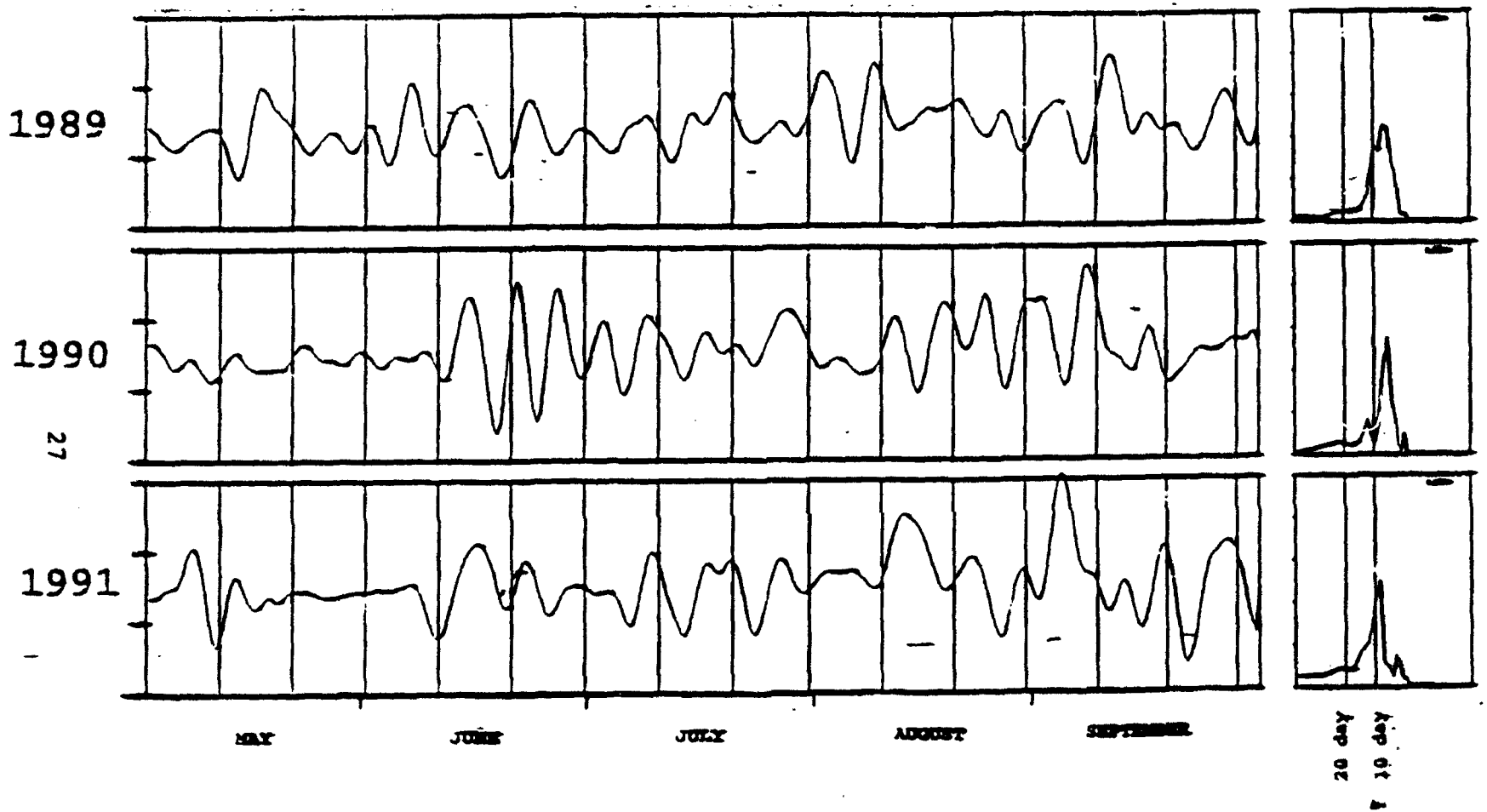

Figure 7: Same as figure 5 except for MCC mode#3.

IV. SINGLE POINT CORRELATION OF MCC MODE #1

As discussed in the previous section, MCC modes 2 and 3 are the same eight-day northwestward propagating wave pattern studied in detail by Chang et.al. using the same data set. Therefore, we will focus on an analysis of the MCC mode 1 in this thesis. The spatial patterns of this mode over the larger domain (70°E-180°, 20°S-40°N) in several variables, including the zonal (u) and v wind components, temperature, and dew-point depression at several levels, and the surface pressure, are determined by the single point correlation between these fields and the time-integrated amplitude coefficient of mode 1.

A. CORRELATION PATTERNS OF VELOCITY COMPONENTS

Fig. 8a shows the correlation patterns of V_{850} with mode 1, at four different lags: 0, 2, 4 and 6 days, respectively. Since the MCC modes are calculated based on V_{850}, the correlation pattern at zero lag closely resembles the structure of mode 1 shown in Fig. 2. The four centers of alternating signs line up approximately as four corners of a rectangular, indicating two pairs of opposite signs, of correlated zonal shear of meridional wind along 25°N and the latitudinal belt between 5°N-10°N. For the positive phase of this mode, the two positive cells are connected to show a northeast-southwest orientation for the positive area. The

gross pattern of the lag 0 correlation remains the same through the other three lag patterns, with very little movement of the positive and negative areas over the six days, even though the centers have shifted slightly to the west or northwest (the positive cell near Philippines).

The northeast-southwest orientation is slightly better defined in the lagged correlations where the negative area in the northwest corner of the core domain shows a more clear orientation. Thus the V_{850} correlation pattern indicates the same alternating subtropical ridge and monsoon trough strength variations along 25°N and the northern equatorial ITCZ region as shown by the MCC mode 1 structure, with a more clear indication that the anomaly features are tilted in a northeast-southwest orientation. The correlation coefficients for the feature centers are in the range of 0.4-0.6 for the northern cells and smaller for the equatorial cells, particularly the southeastern cell. The correlation seems to increase somewhat with lag as the lag changes from 0 to 4 days, resulting in the most clear pattern being displaced at days 2-4. This may be related to the time integration of the amplitude coefficient of MCC mode over the twelve 12-hourly time volume, as day 3 is the central point of the time volume.

Fig. 8b is the U_{850} correlation patterns, for lags 0, 2, 4 and 6 days, respectively. The figure is dominated by a pair of zonally-elongated cells with opposite signs and separated at a latitude just south of 25°N. Both cells occupy the entire

longitudinal span of the core domain, and appear to extend beyond the core domain boundaries of 100°E and the dateline. A slow westward propagation at a speed of about 2.5° longitude per day is indicated by the movement of the two center locations, around 10°N and 30°N, respectively. The northern center appears to propagate slightly faster than the tropical one. However, because of the long zonal scale, the entire pattern as defined by the longitudinally elongated positive and negative areas appears to be near stationary. The correlation coefficient is in the range of 0.6-0.7 for the southern center and 0.5-0.6 for the northern center. These values are somewhat higher than the V_{850} correlation pattern shown in Fig. 8a despite the fact that the basic MCC mode is computed from V_{850}. The reason for this seems to be the fact that in the V_{850} MCCA process the eight-day, northwestward propagating wave pattern, which has a substantial variance, has been separated out in other MCC modes. Chang et.al.,(1994) found that this propagating wave pattern is less prominent in the u component, therefore U_{850} has relatively smaller correlated variations that are associated with the northwestward wave pattern compared to V_{850}. As a result, it has a relative higher variance, and therefore correlation, in other motions, particularly the mode-1 correlated motion.

There is also a minor, third cell near 132°E and 5°S which is to the south, and lined up in about the same longitudinal zone, of the other two centers. It has much lower correlation coefficients, in the range of 0.2-0.3, and a smaller "area of

apparent influence". This center does not appear to move at all, resulting in the appearance that the axis connecting the three centers changes from a very slight northeast-southwest orientation on day zero to almost north-south on day 3. For the positive phase of mode 1, the zero lag U_{85C} correlation pattern indicates a cyclonic shear zone between 15°N-25°N, and an anticyclonic shear zone between 5°S-10°N over the western Pacific. This distribution of correlated vorticity variations is in phase with the patterns deduced from the V_{850} correlations. Therefore the correlated variation is principally a rotational circulation.

Figs. 9-13 shows the lag correlation patterns for v (a) and u (b), for 700, 500, 300, 200 and 150 hPa, respectively, also for lags 0, 2, 4 and 6 days. The V_{700} patterns (Fig. 9a) closely resemble those of V_{850} (Fig. 8a), except for somewhat smaller correlation coefficients, particularly for the southwestern cell near Philippines. The U_{700} patterns (Fig. 9b) also resembles the U_{850} patterns (Fig. 8b). The only detectable difference is along the equator, where the correlation coefficients are very small. The in-phase relationship between 850 and 700 hPa indicates little vertical tilt, for both the quasi-stationary pattern and the slow westward propagation, between the two levels.

As expected, the correlation coefficients continue to decrease at higher levels. At 500 hPa, both u and v patterns (Fig. 10) are still closely in-phase with 850 hPa, although a slight westward tilt with height can be seen for the center near

Philippines. There are two main differences in U_{500} (Fig. 10b). The westward propagation of the main centers appears more distinct, and over the northern equatorial region east of about 150°E the narrow zone of very small positive correlations is replaced by small negative correlations. This negative area extends west-southwestward to connect with the small southern equatorial negative center. It thus appears that from the tropical western North Pacific to the Bay of Bengal the zonal wind anomaly associated with MCC mode 1 is near barotropic up to 500 hPa, but in the eastern part of the western Pacific and the central Pacific around the dateline it is baroclinic with a significant phase tilt between 700 and 500 hPa.

The phase shift in u correlations continues upward to 300 hPa (Fig. 11b) where the low-latitude positive correlation area shrinks substantially to a weak and narrow zone that is oriented east-northeast to west-southwest extending from the South China Sea to about 140°-150°E and 20°N. The tendency of a slight westward propagation of the pattern can still be detected by following the center of features, although the correlation coefficients are very low (magnitudes 0.2-0.3). Comparing the U_{300} pattern with the u at lower levels, it appears that the barotropic (vertically in-phase) part of MCC mode 1 correlated variations is gradually replaced by baroclinic structures from the southeastern region of the domain. This trend continues to U_{200} (Fig. 12b) U_{150} (Fig. 13b) and U_{100} (Fig. 14b), where the entire domain is occupied by negative correlation coefficients.

Thus north of 25°N the vertical structure of the u anomaly is in phase throughout the troposphere, while south of 25°N in the equatorial region there is a phase reversal between the lower troposphere and upper troposphere. The phase reversal takes place around 500 hPa. It probably starts around 600 hPa in the eastern region near the dateline, and propagates westward to occupy the entire domain when 400 hPa is reached. For the positive phase mode 1, the zonal wind at 200 hPa (Fig. 12b) indicates a west-east elongated ridge over the western Pacific between 10°N-20°N, which is situated to the south of the cyclonic zone near 20°N-25°N. The maximum correlation coefficient for U_{100} reaches 0.5 in the equatorial region of Borneo and southeastern Philippines, indicating that the deep vertical structure is maintained fairly well.

The correlation pattern for V_{500} (Fig. 10a) is also in phase with the lower troposphere. The westward phase shift from the eastern region of the tropical western Pacific shown in U_{500} (Fig. 10b) is not seen here. This is probably due to the lack of correlated v variations there. Above 500 hPa a phase reversal between the lower and upper tropospheric levels in the equatorial maritime continent region, similar to that indicated in u, may be seen in the upper level v correlation patterns starting from 300 hPa (Fig. 11a). In fact, this reversal takes place over the entire tropical western Pacific and South China Sea at 200 hPa (Fig. 12a) and above (Figs. 13a, 14a). Comparing V_{200} (Fig. 12a) with V_{850} (Fig. 8a), it is seen that the lower tropospheric

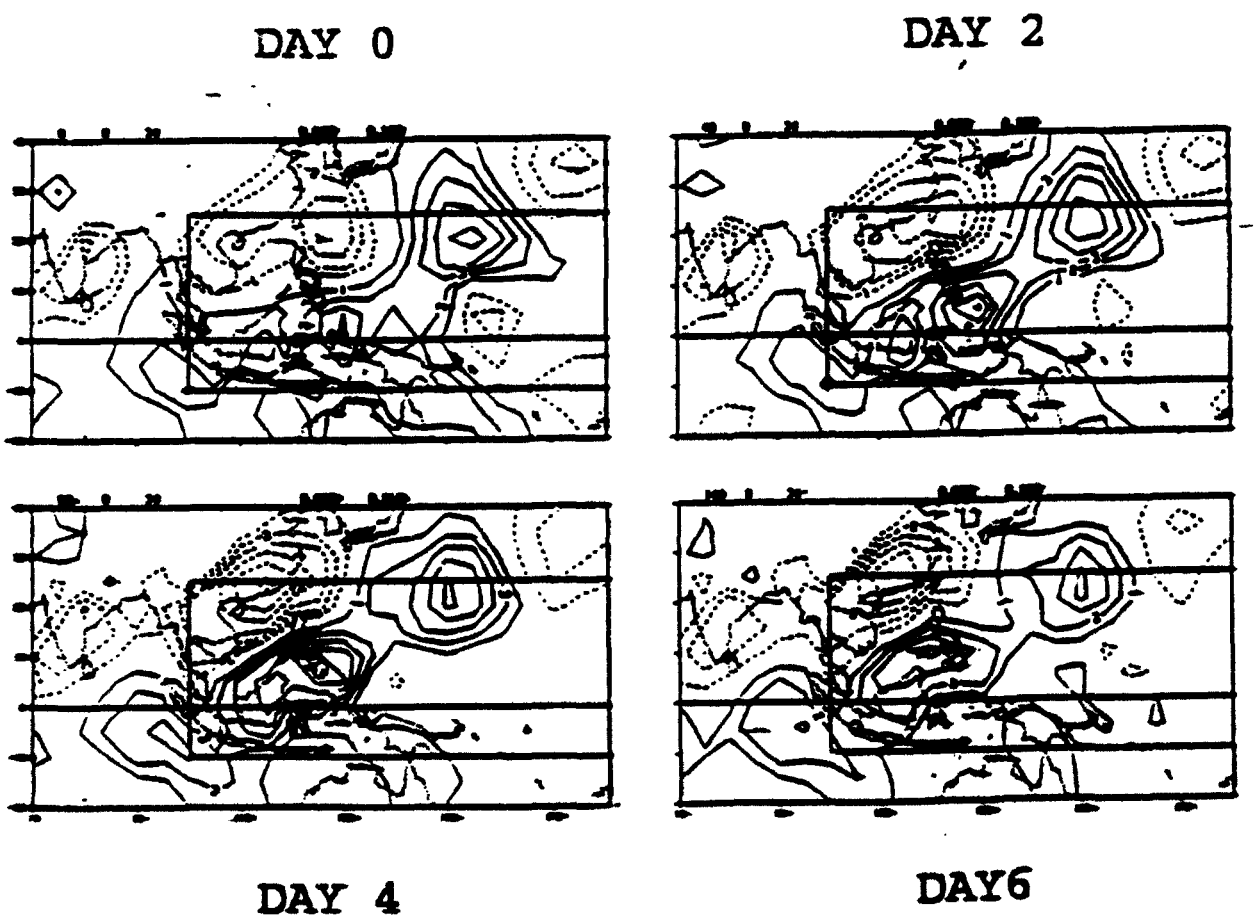

Figure 8a: Single point correlation patterns of V_{850} with MCC mode #1,at four different lags: 0,2,4 and 6 days. Contour interval is 0.1 and negative values are dashed.

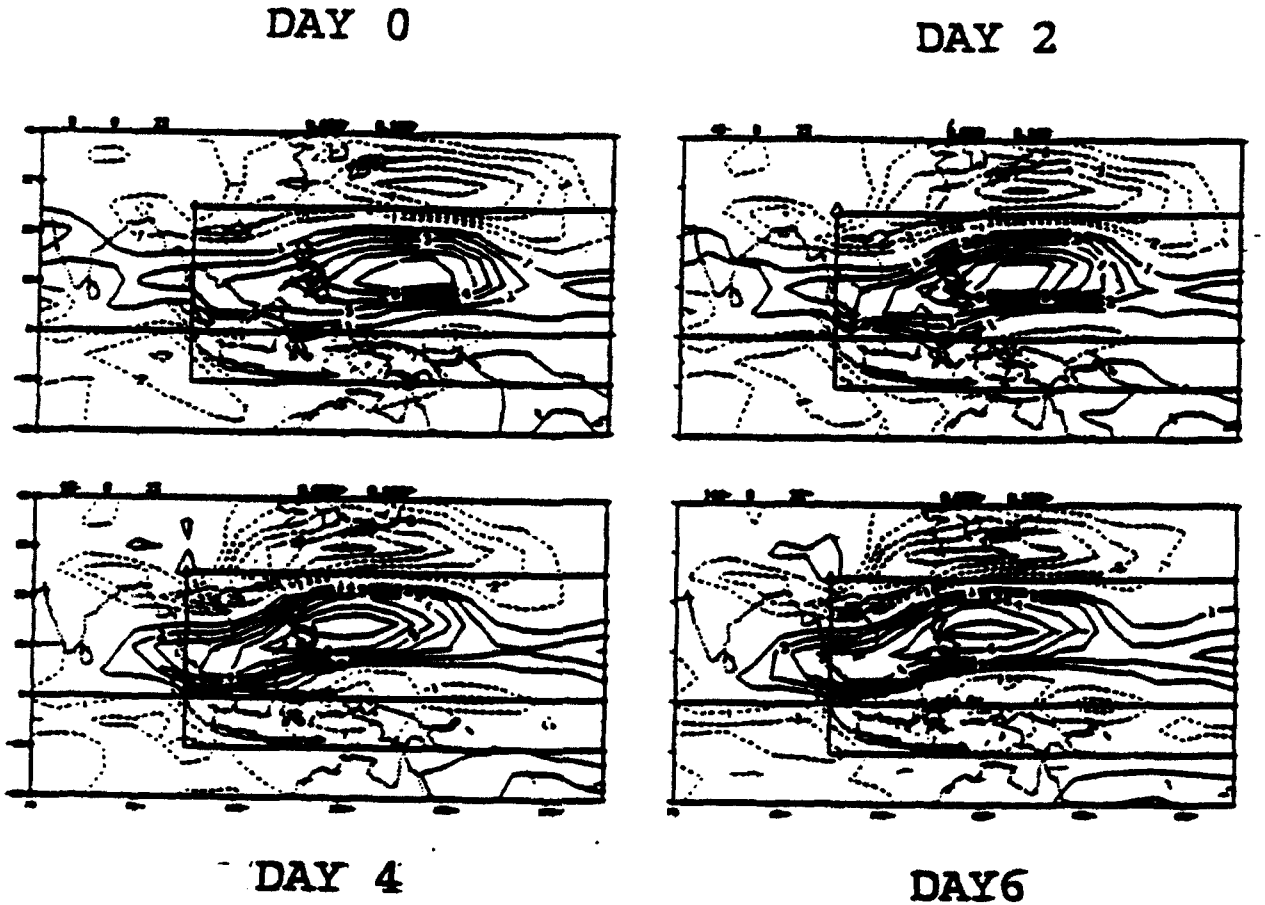

Figure 8b: Same as figure 8a except for U_{850}.

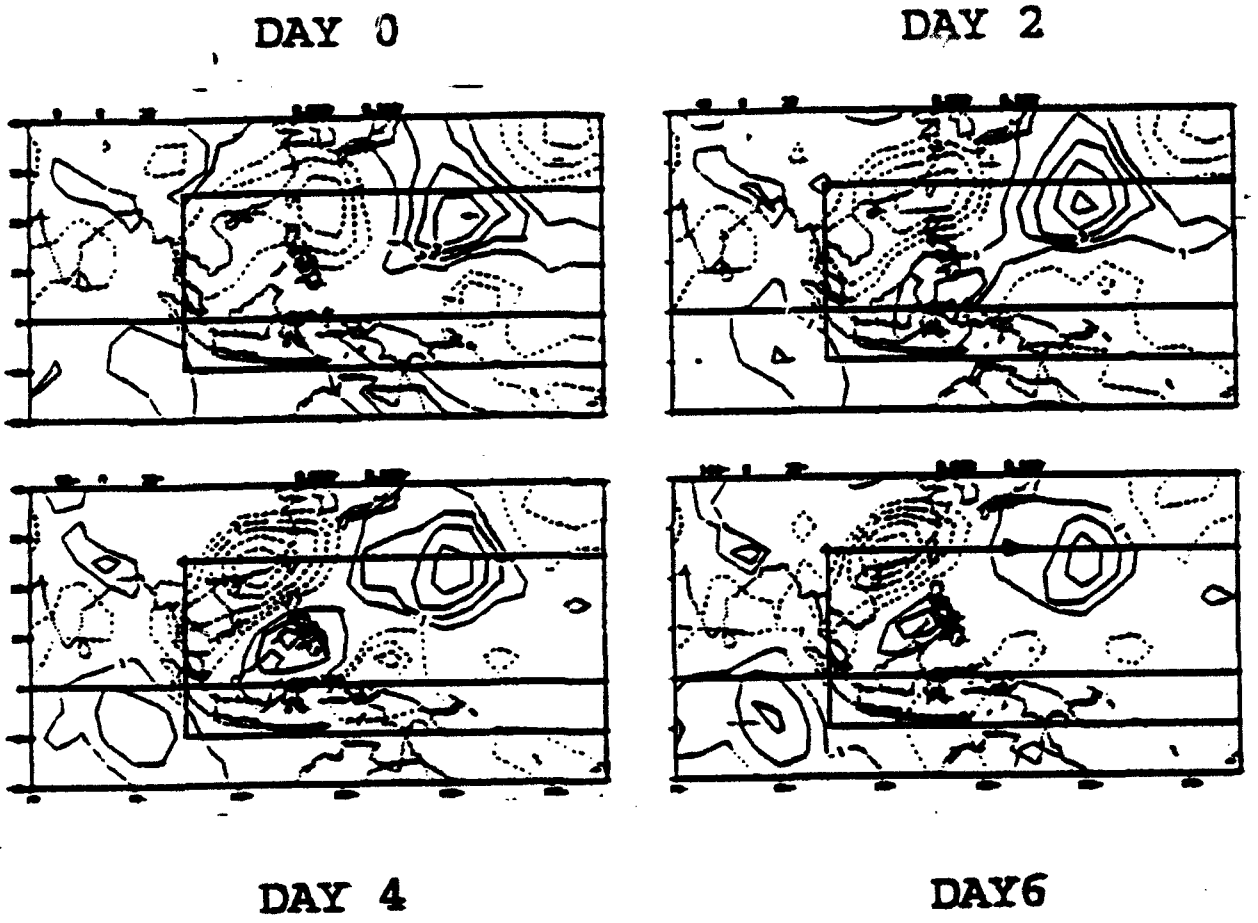

Figure 9a: Same as figure 8a except for V_{700}.

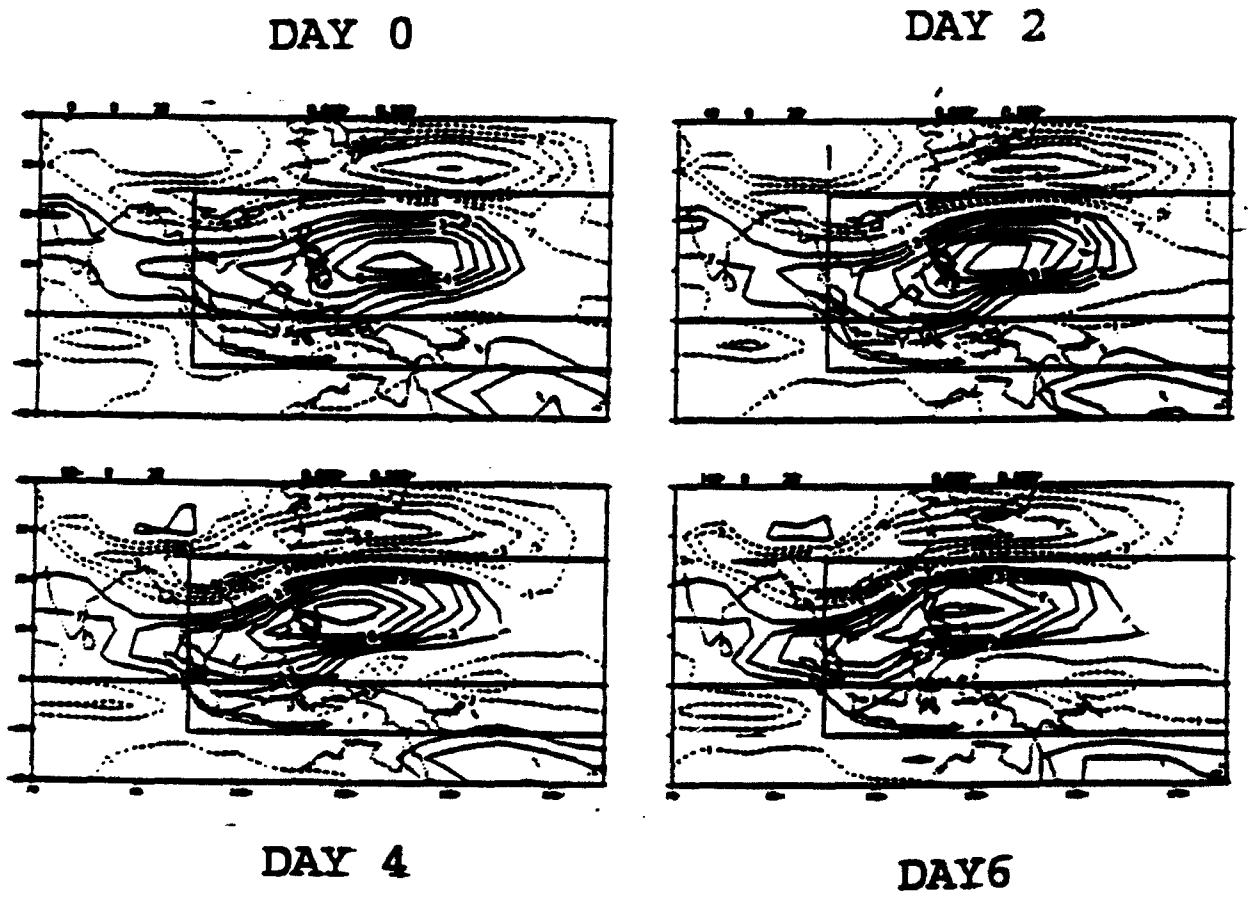

Figure 9b: Same as figure 8a except for U_{700} .

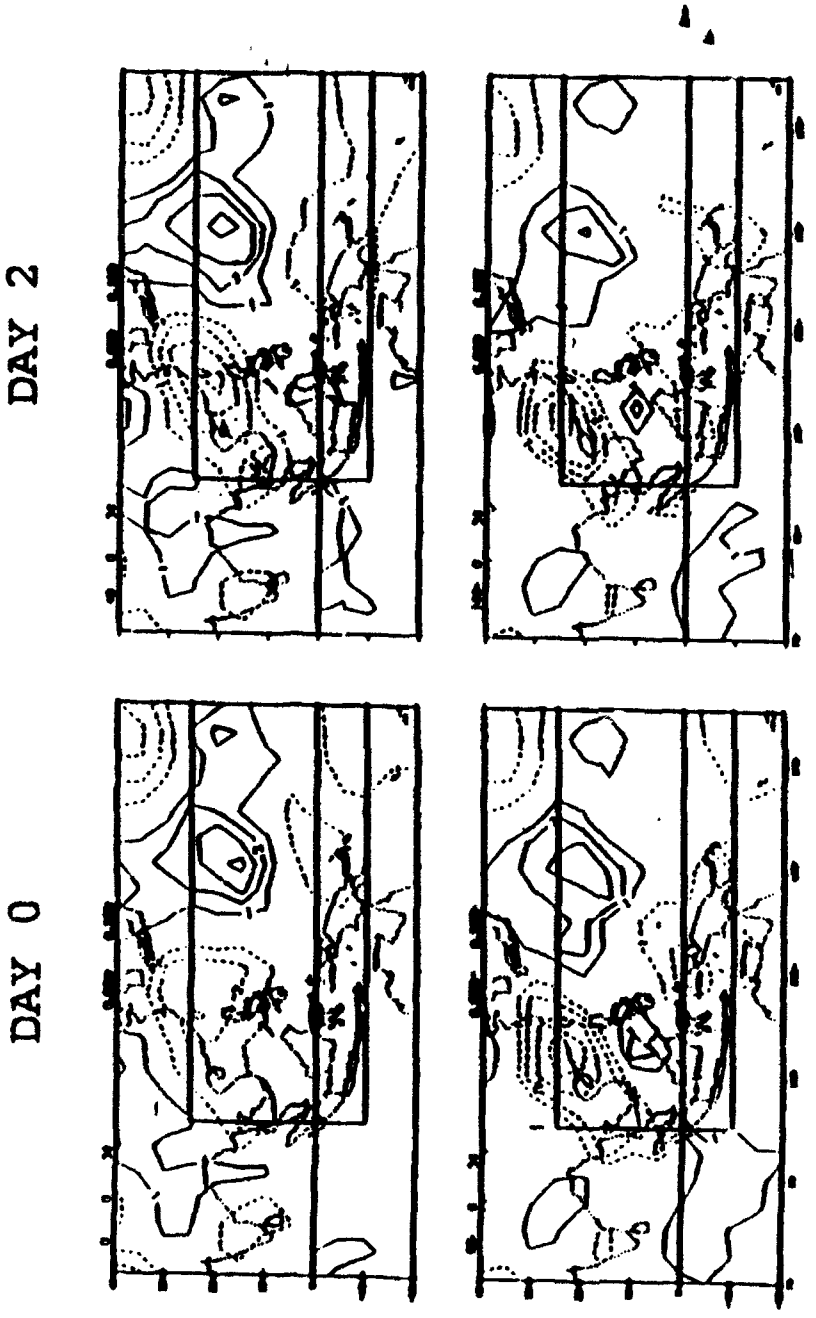

Figure 10a: Same as figure 8a except for V_{500}.

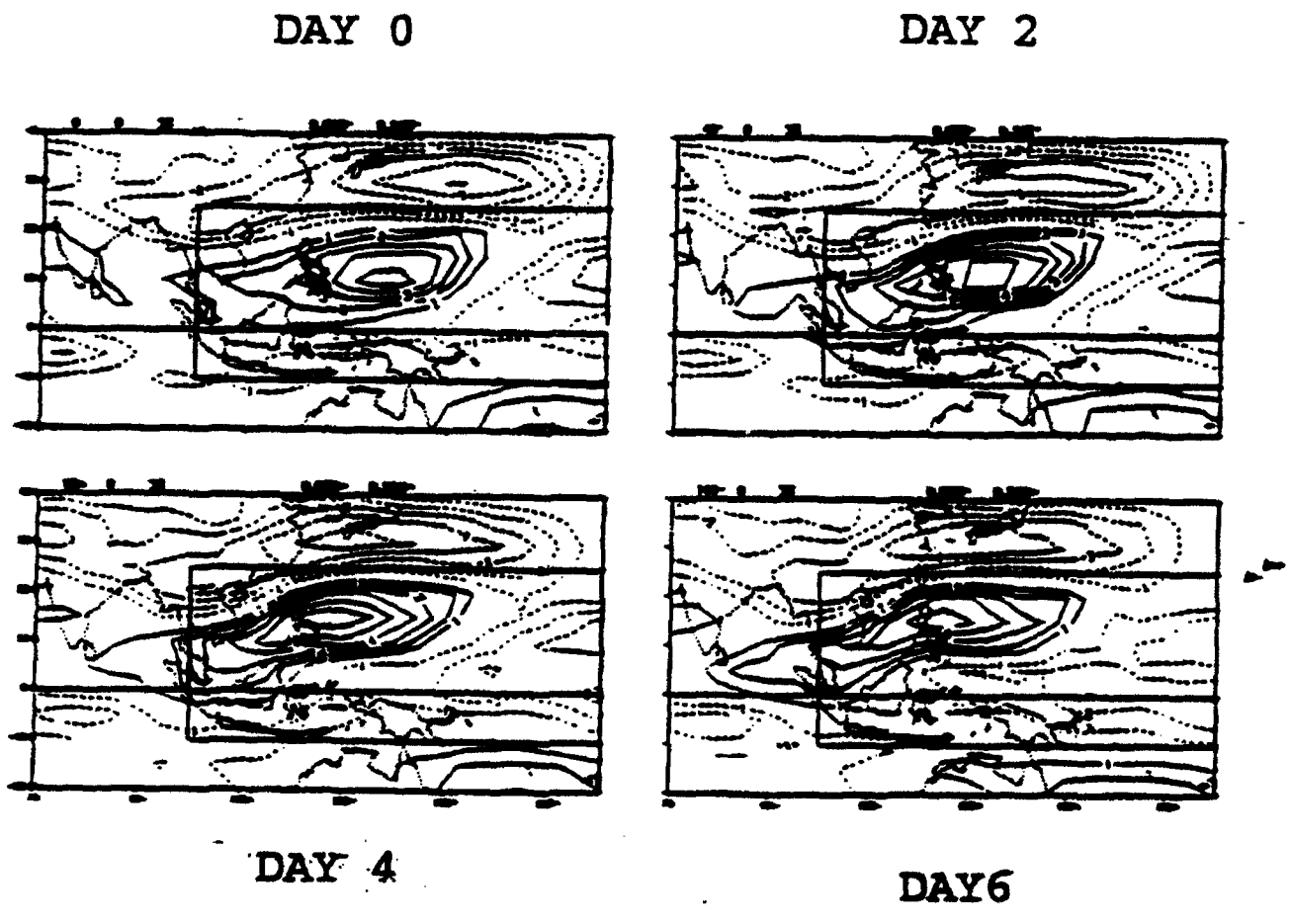

Figure 10b: Same as figure 8a except for U_{300}.

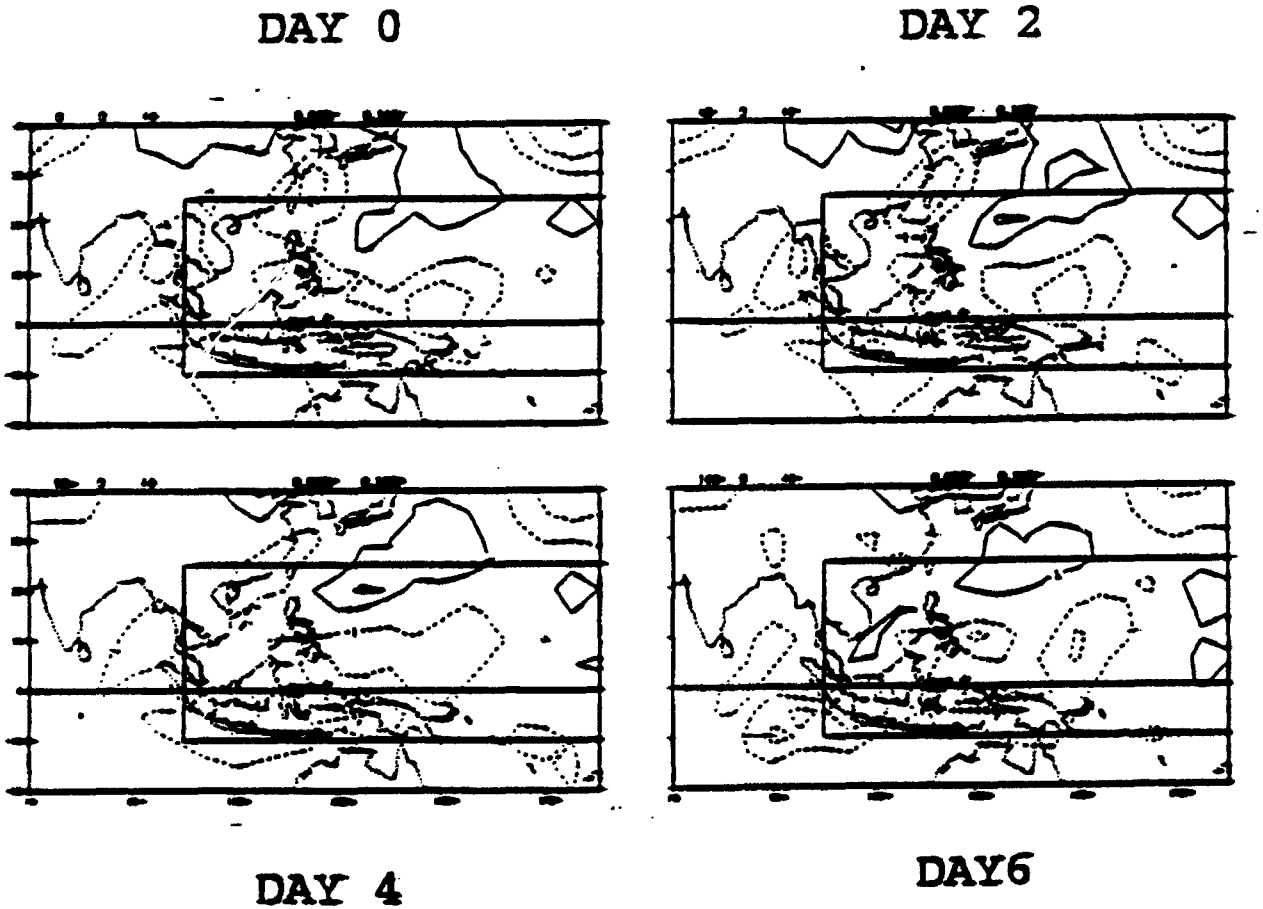

Figure 11a: Same as figure 8a except for V_{300}.

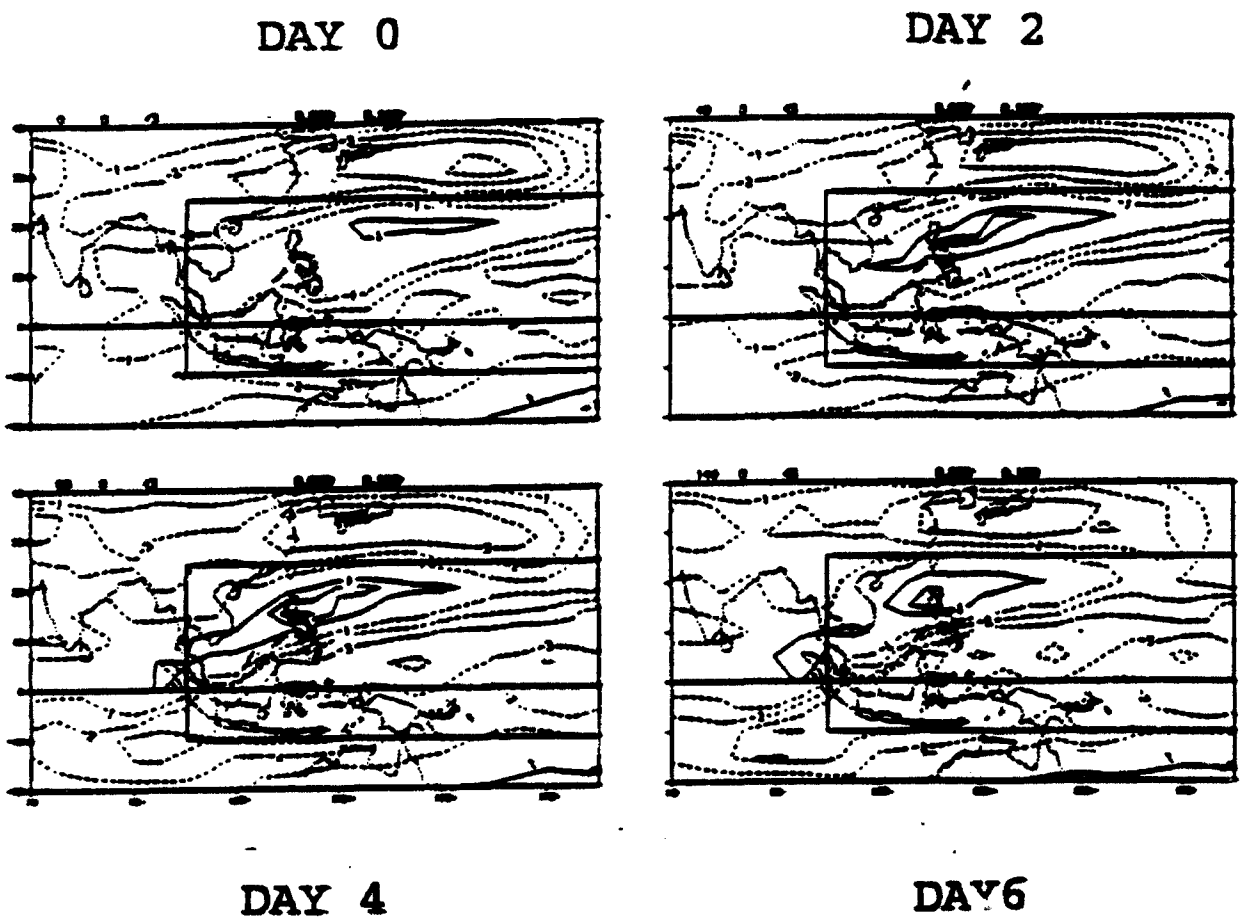

Figure 11b: Same as figure 8a except for U_{300}.

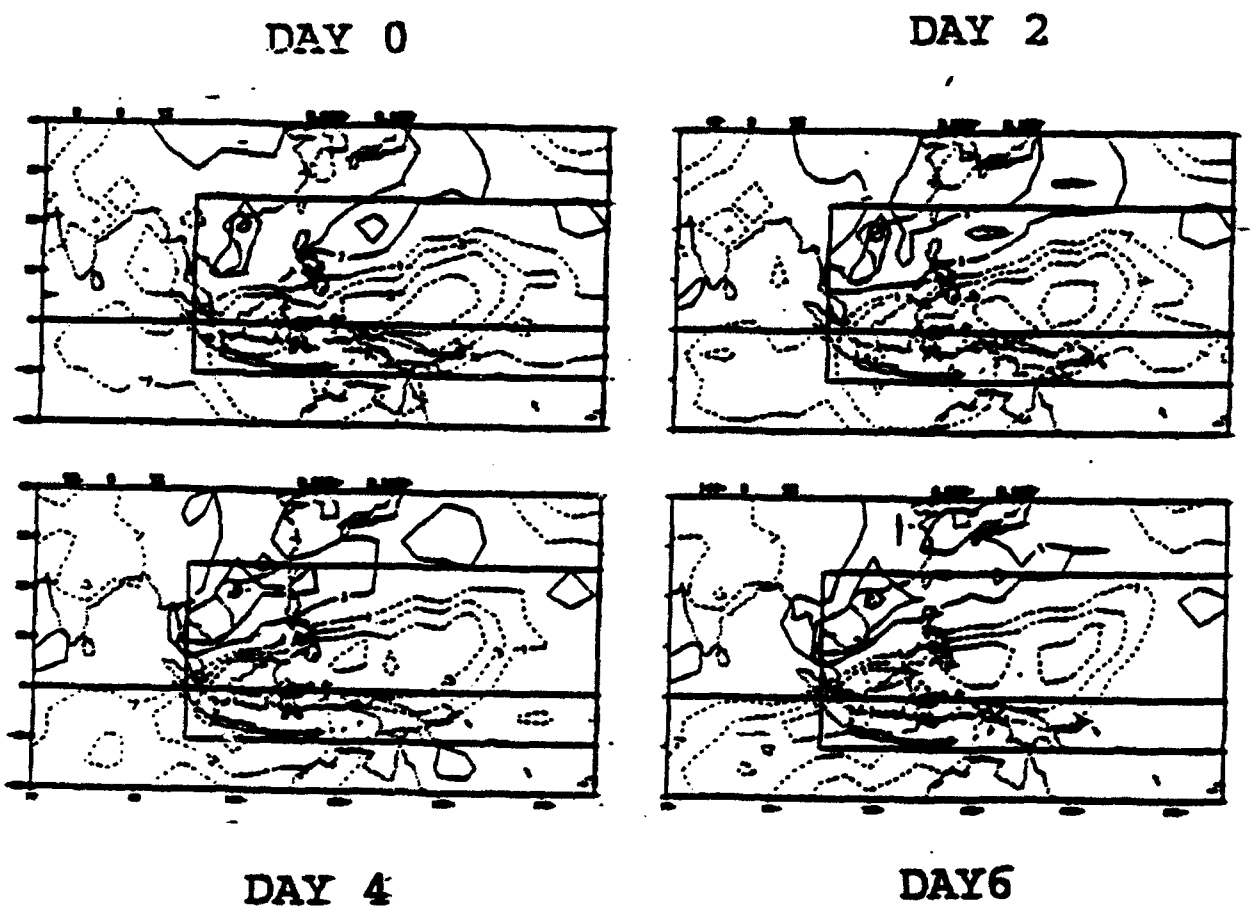

Figure 12a: Same as figure 8a except for V_{200}.

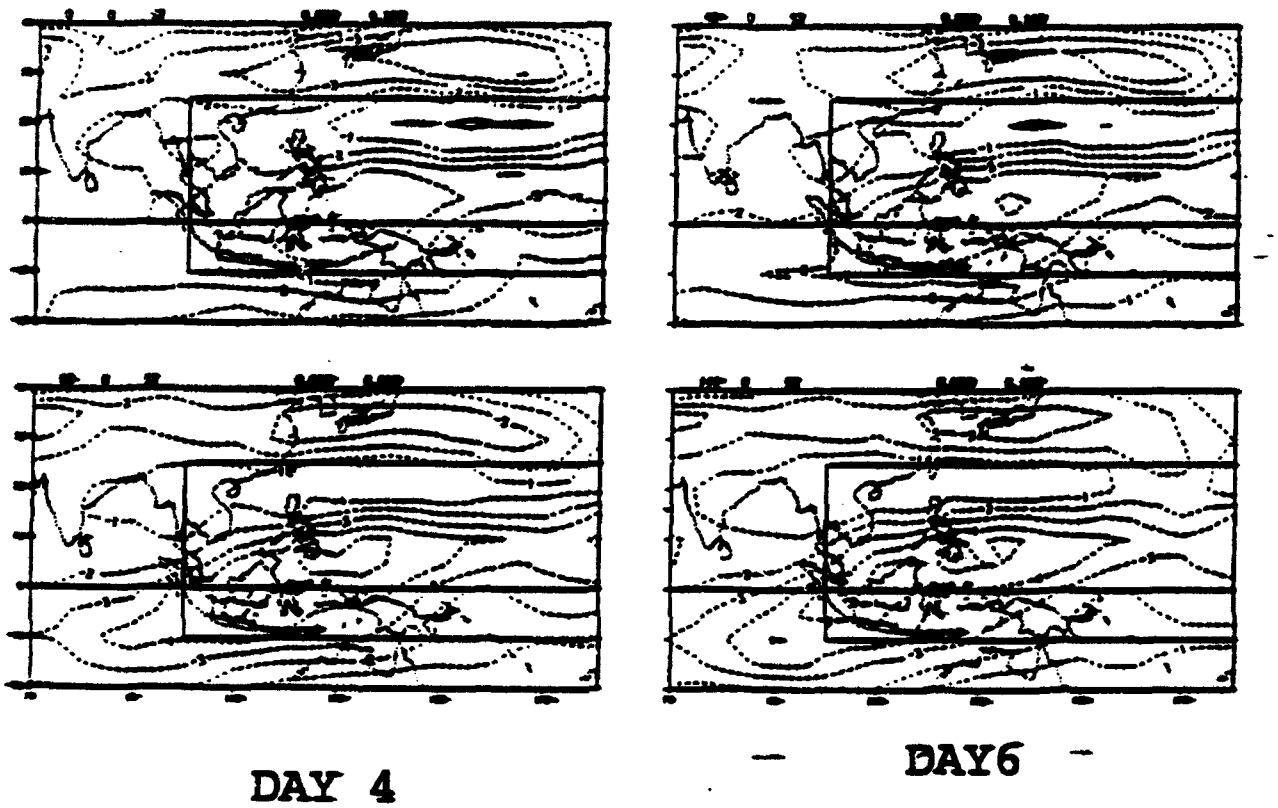

Figure 12b: Same as figure 8a except for U_{200}.

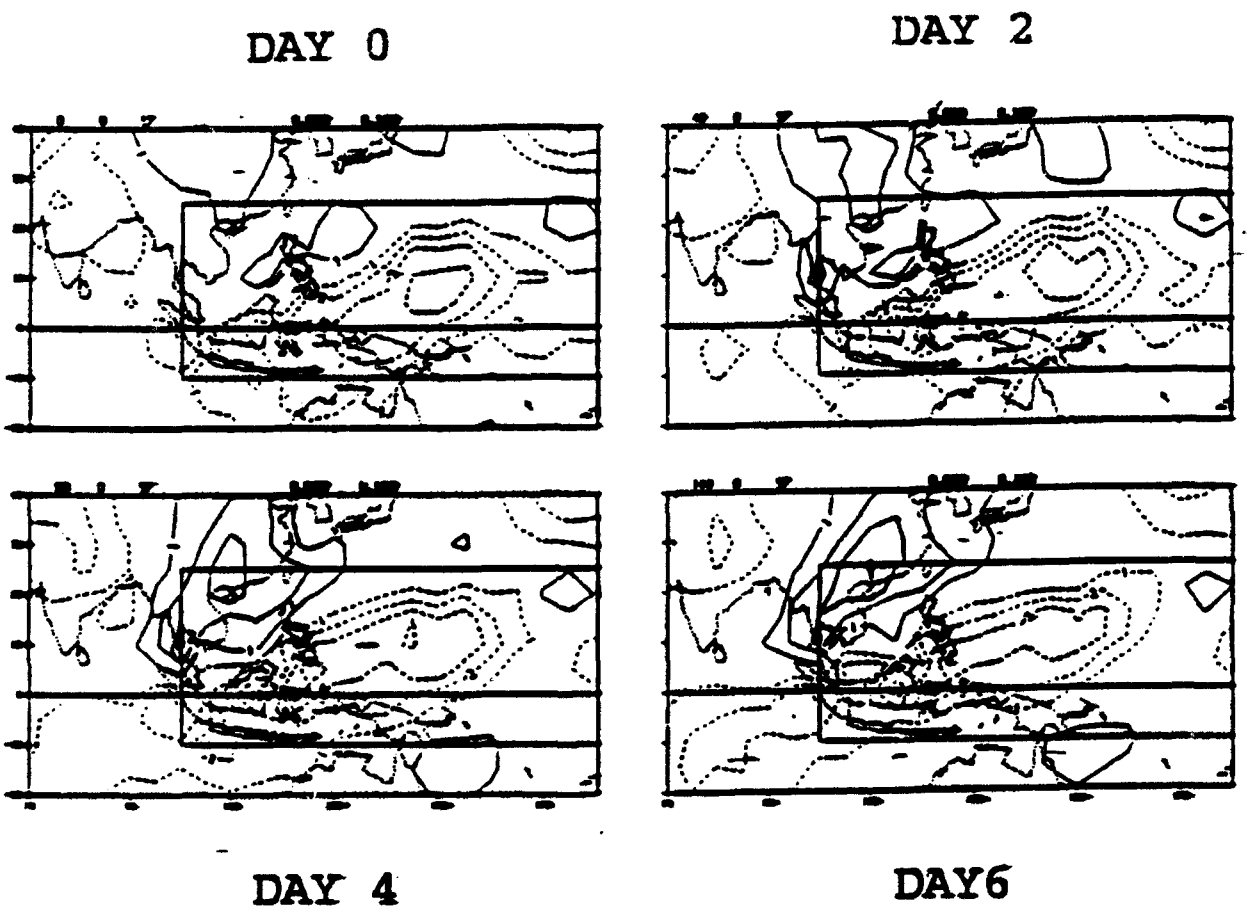

Figure 13a: Same as figure 8a except for V_{150}.

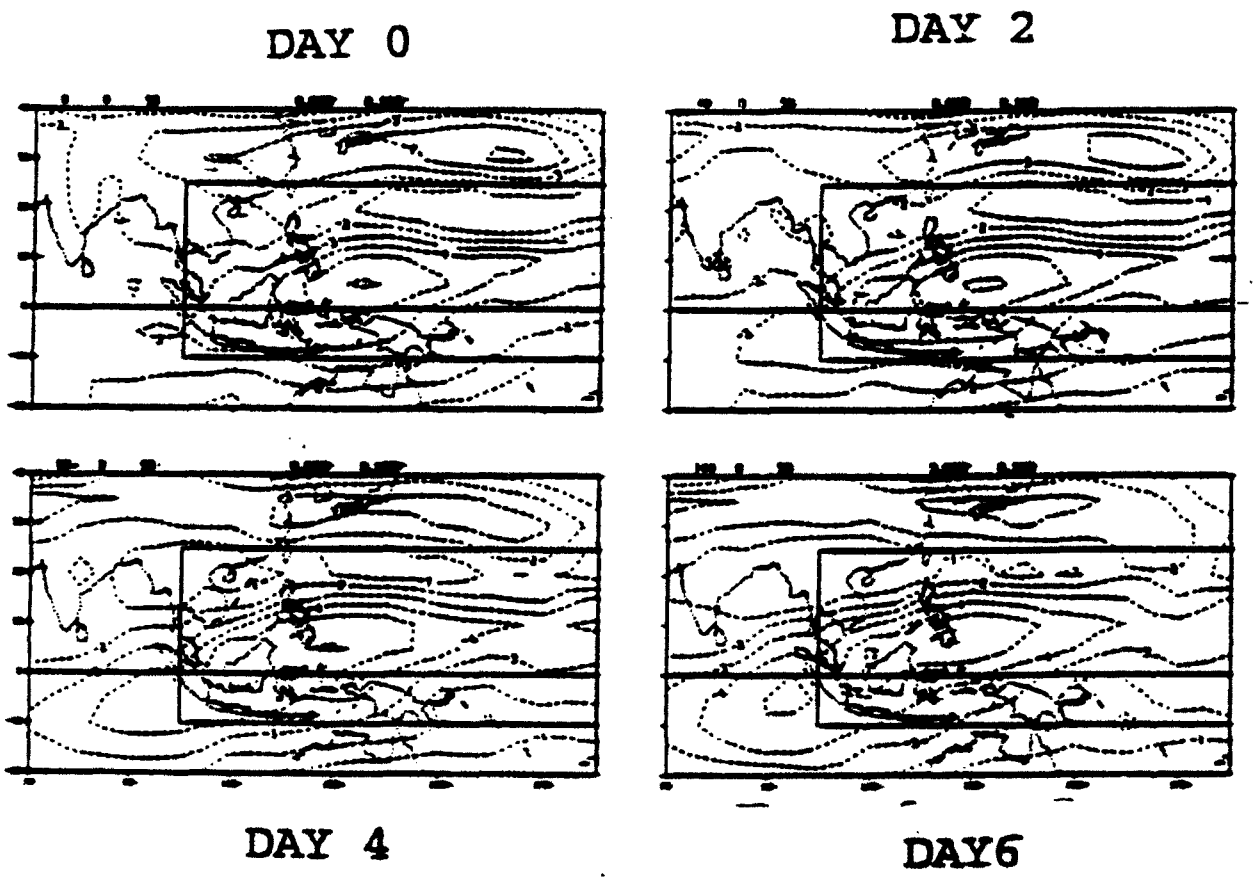

Figure 13b: Same as figure 8a except for U_{150}.

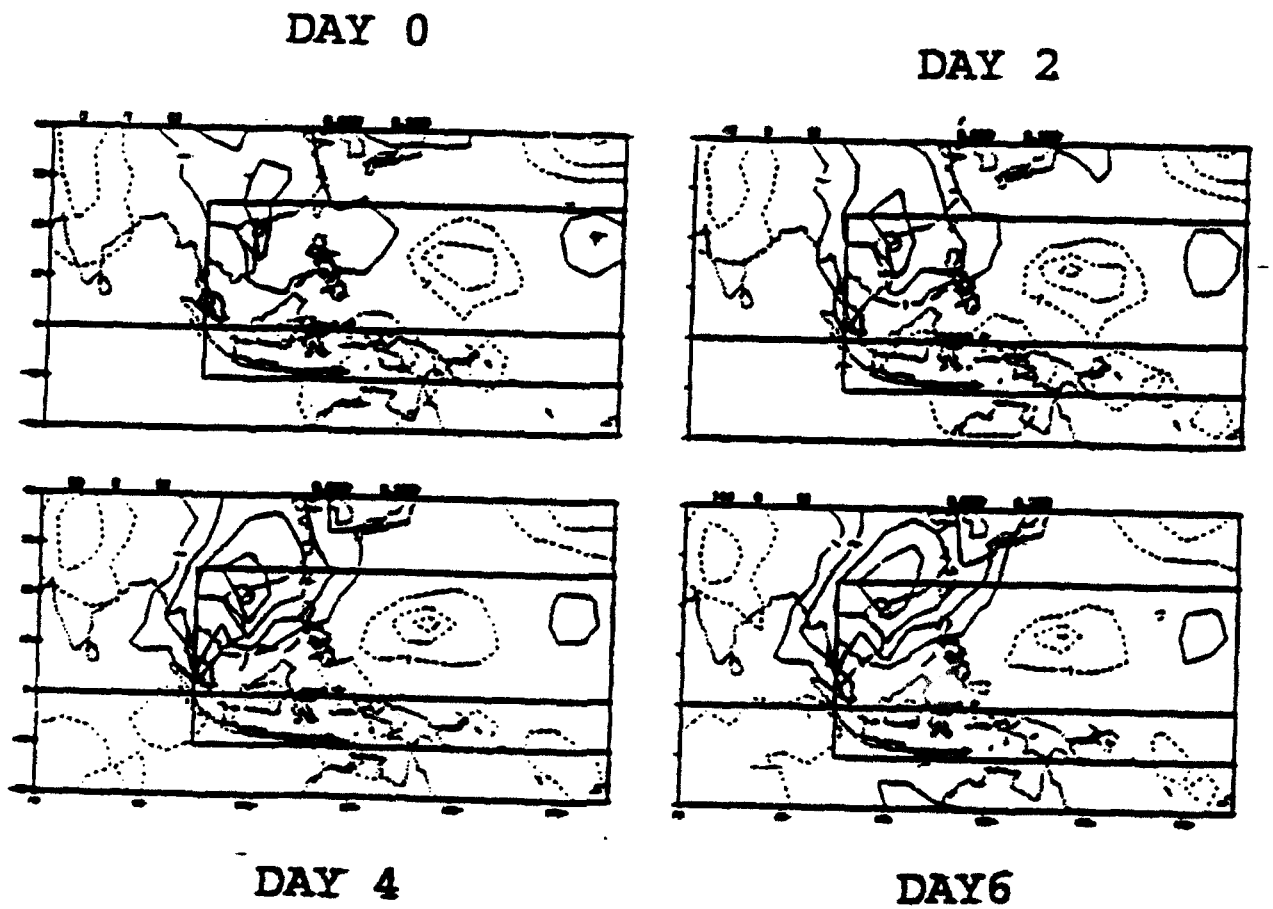

Figure 14a: Same as figure 8a except for V_{100}.

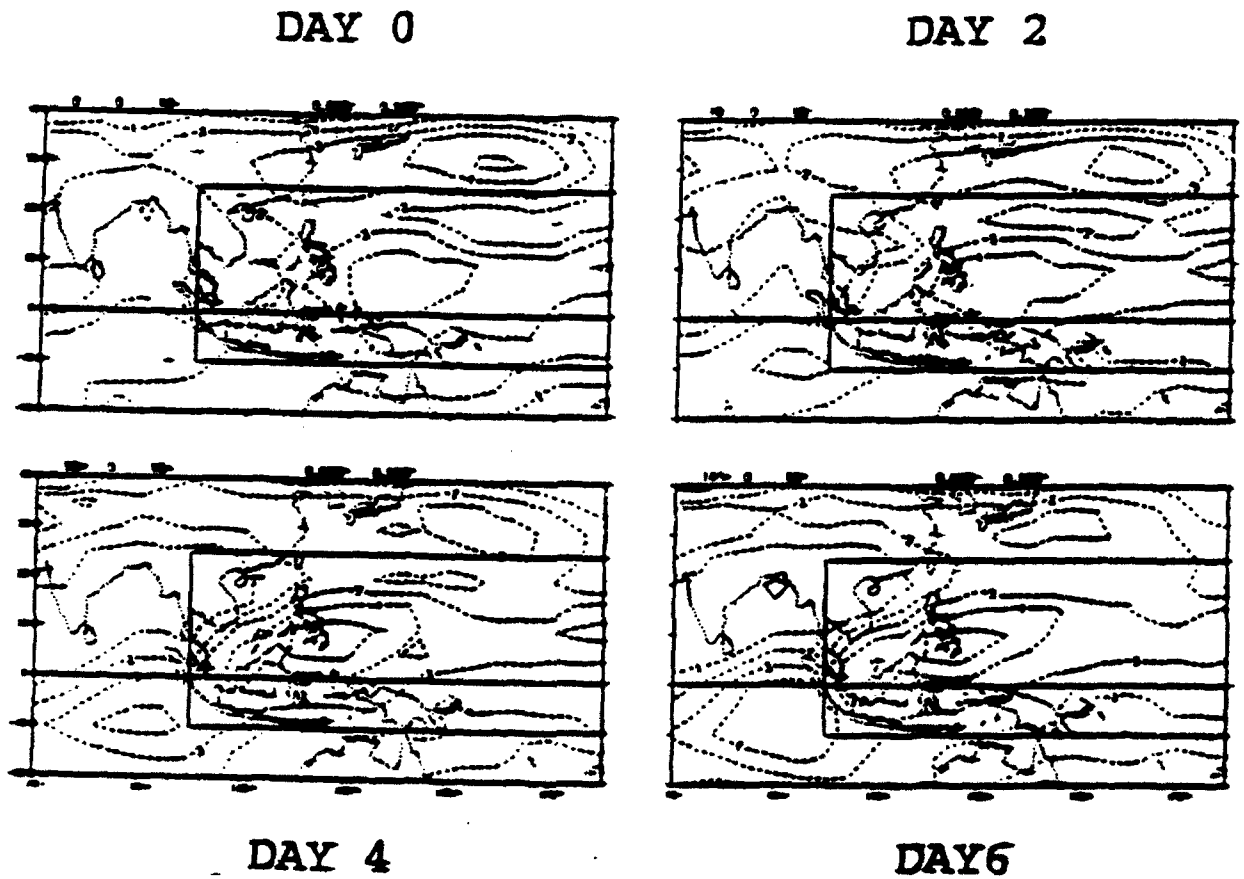

Figure 14b: Same as figure 8a except for U_{100}.

variation, which is mostly rotational, changes to a pattern with significant divergence along a west-southwest to east-northeast extended narrow region between the equatorial Sumatra-Malay Peninsula and the subtropical western North Pacific. For the positive phase mode 1, this is near the 200 hPa ridge line indicated by the U_{200} correlation pattern, and is in the general vicinity of upper-level outflow associated with the northern summer ITCZ. It may be worth noting that the orientation of this outflow zone is contrary to the climatological mean west-northwest to east-southeast orientation of the ITCZ over western Pacific during northern summer monsoon.

B. CORRELATION PATTERNS OF PRESSURE, TEMPERATURE AND MOISTURE

The correlation patterns of sea-level pressure (P_{sfc}) with MCC mode 1 at lags 0, 2, 4 and 6 days are shown in Fig. 15. The principal feature is a well-defined, negatively correlated cell in the western North Pacific whose western edge extends to the South China Sea and Indochina. The center near 20°N shows a slow westward movement of about 2° per day from 142°E at day 0 to 130°E at day 6. The well defined negative cell is consistent with the low-level rotational circulation anomaly implied from the u and v patterns discussed in the previous sub-section. It clearly indicates the existence of a pressure variation pattern that is probably a manifestation of the strength and domain changes of the subtropical ridge-monsoon trough complex, together

with a possible slow westward moving component.

The correlated temperature variations at three levels, 925, 700 and 300 hPa, are shown in Fig. 16. At 925 hPa (Fig. 16a), the temperature pattern shows very small correlation coefficients with positive values in the northeast region of the domain and negative values elsewhere. This weak pattern does not seem to be correlated with the psfc cell or the V_{850} MCC mode 1. However, it resembles the general positive-negative pattern shown in both T_{700} and T_{300}. The T_{700} (Fig 16b) and T_{300} (Fig. 16c) both show a positive cell over the negative psfc cell, displaying a consistent hydrostatic relationship. Both the area enclosed by the positive temperature correlations and the correlation coefficients are larger at 300 hPa than 700 hPa. Thus, the temperature structure may be described by an equivalent barotropic circulation structure whose vertical shear is in speed only. This is consistent with the deep barotropic phase structure of the u and v correlation patterns near 25°N discussed in the previous sub-section.

The correlated dew point temperature depression patterns at 925 hPa (D_{925}) and 700 hPa (D_{700}), are shown in Fig.17a-b. At 925 hPa a negative cell with small correlation coefficient coincide with the negative psfc cell, indicating a near 180° out-of-phase relationship between psfc and moisture in the boundary layer. This relationship means that if the subtropical ridge is stronger (or monsoon trough weaker) the boundary layer is drier, and vice

versa. This is reasonable because the prevalence of subsidence over the subtropical ridge and rising motion in the monsoon trough. Fig. 17a also shows some other features. There is a negative area in the western region of the domain from the Tibetan Plateau to the Bay of Bengal.

Over the Tibetan Plateau and most of India this an artifact as 925 hPa is under terrain, so only this feature may only be valid over the Bay of Bengal and equatorial eastern Indian Ocean, where is the correlation is low (near 0.2).

Another feature is a small positive-negative couplet whose sign changes between the southern China coast and the South China Sea. This pattern indicates an out-of-phase relationship between the moisture variations over the subtropical ridge-monsoon trough variation cell shown prominently in the P_{sfc} pattern (Fig. 15), and the coastal region north of the South China Sea. All these features are basically stationary over the northern equatorial belt of the western Pacific, a positive area extends to the Borneo, and it be a manifestation of the westward propagation features shown in other fields.

The D_{700} pattern (Fig. 17b) resembles D_{925}, and appears more organized. The main feature is the negative cell associated with the negative psfc cell, with a higher maximum correlation coefficient of about 0.4. It is out-of-phase with the southeastern China coastal area and in-phase with the Bay of

Bengal and the equatorial Indian Ocean.

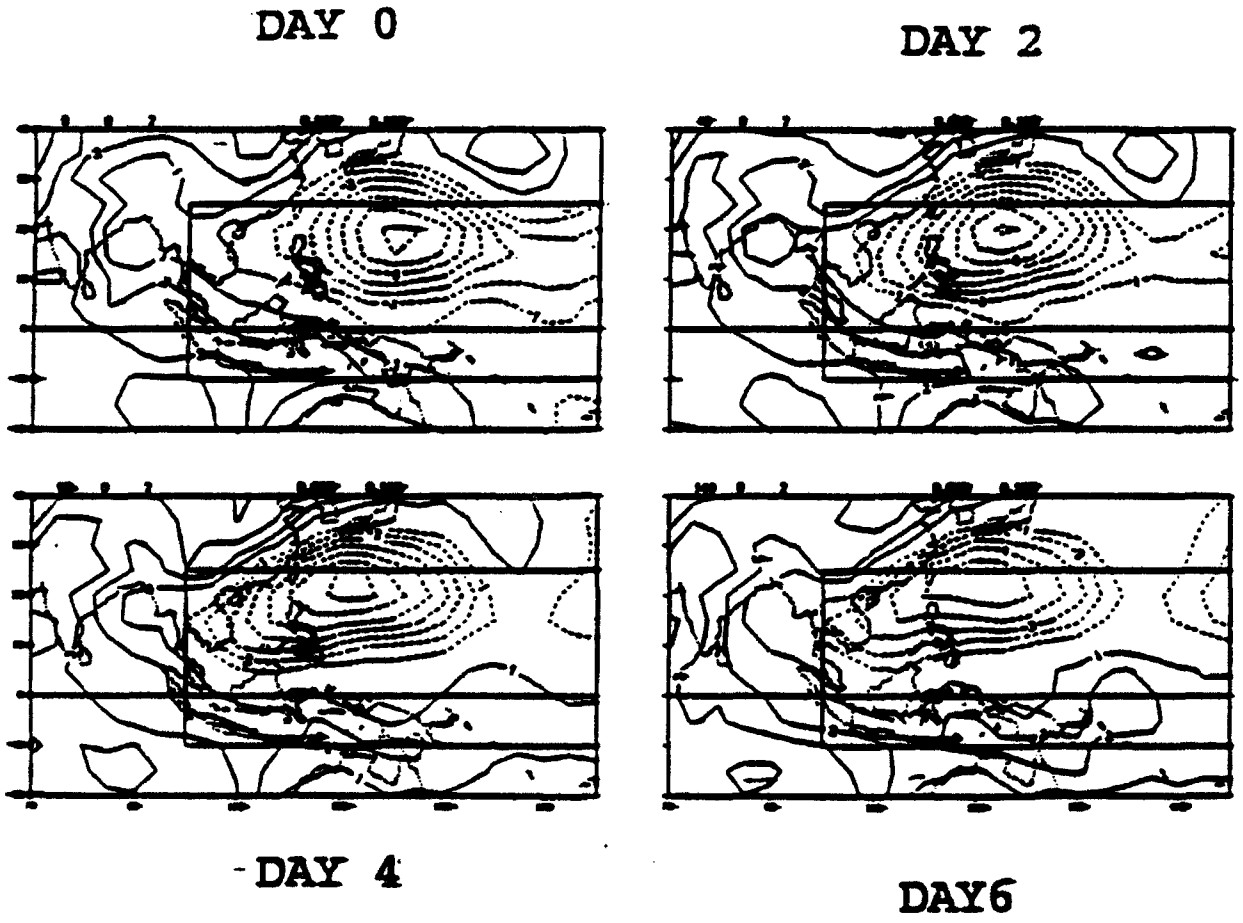

Figure 15: Same as figure 8a except for P_{sfc}.

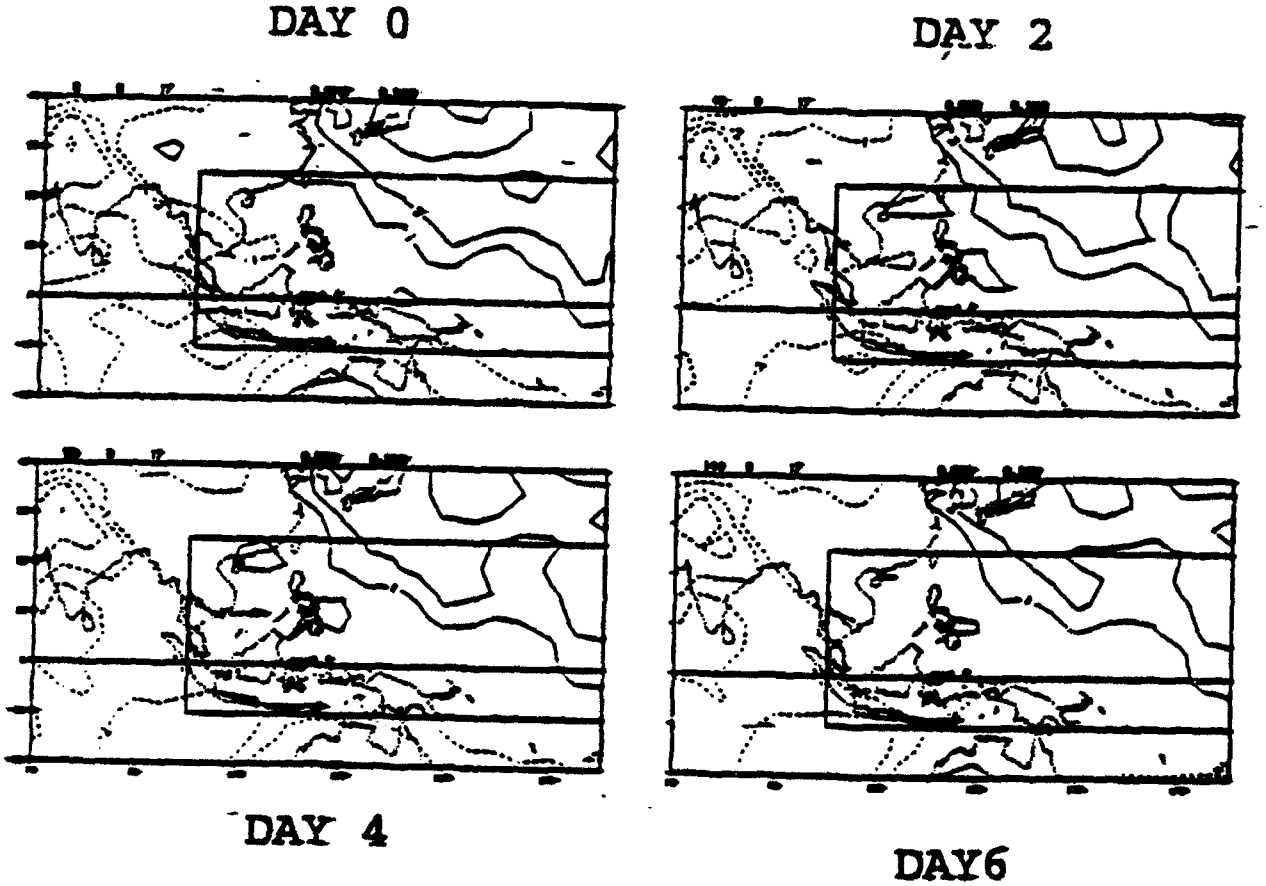

Figure 16a: Same as figure 8a except for T_{925}.

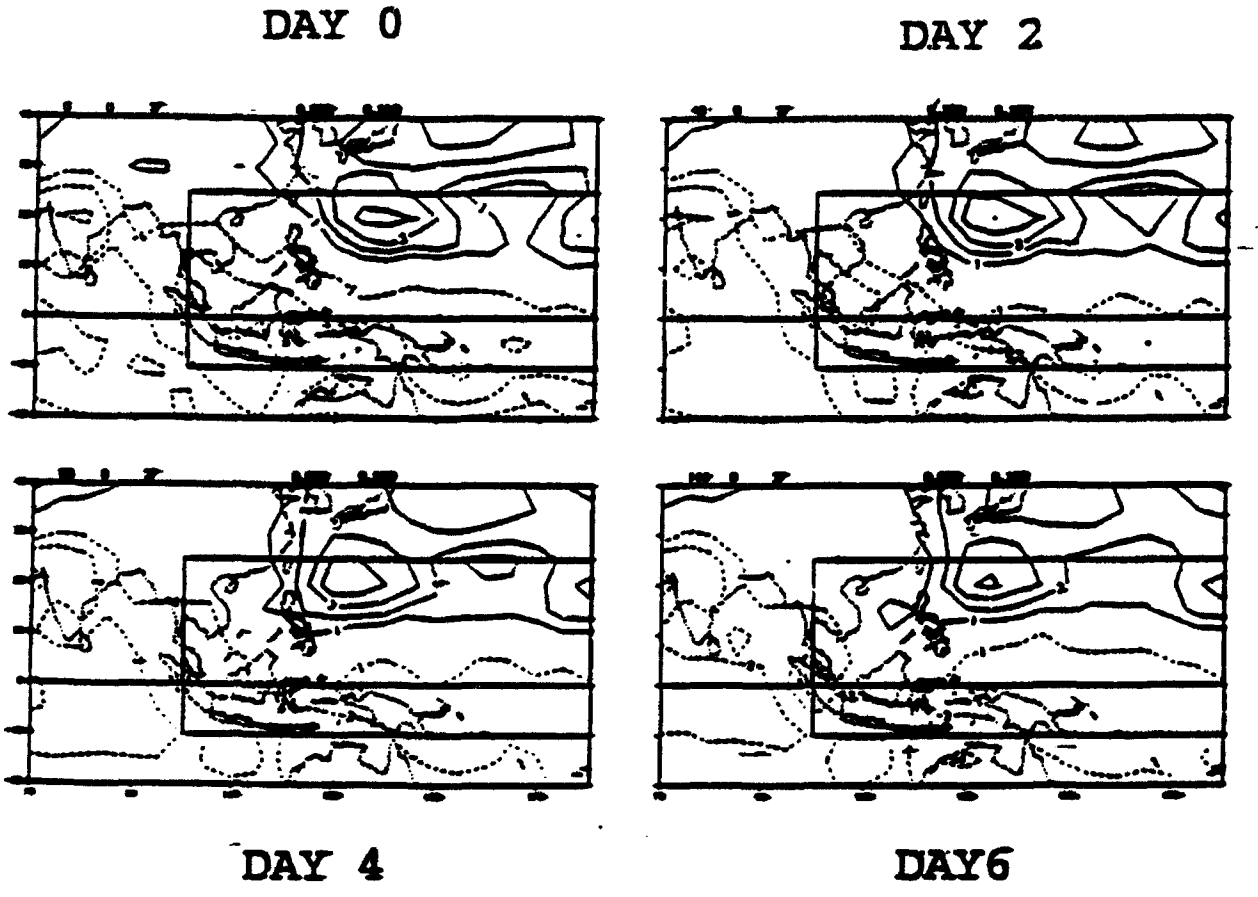

Figure 16b: Same as figure 8a except for T_{700}.

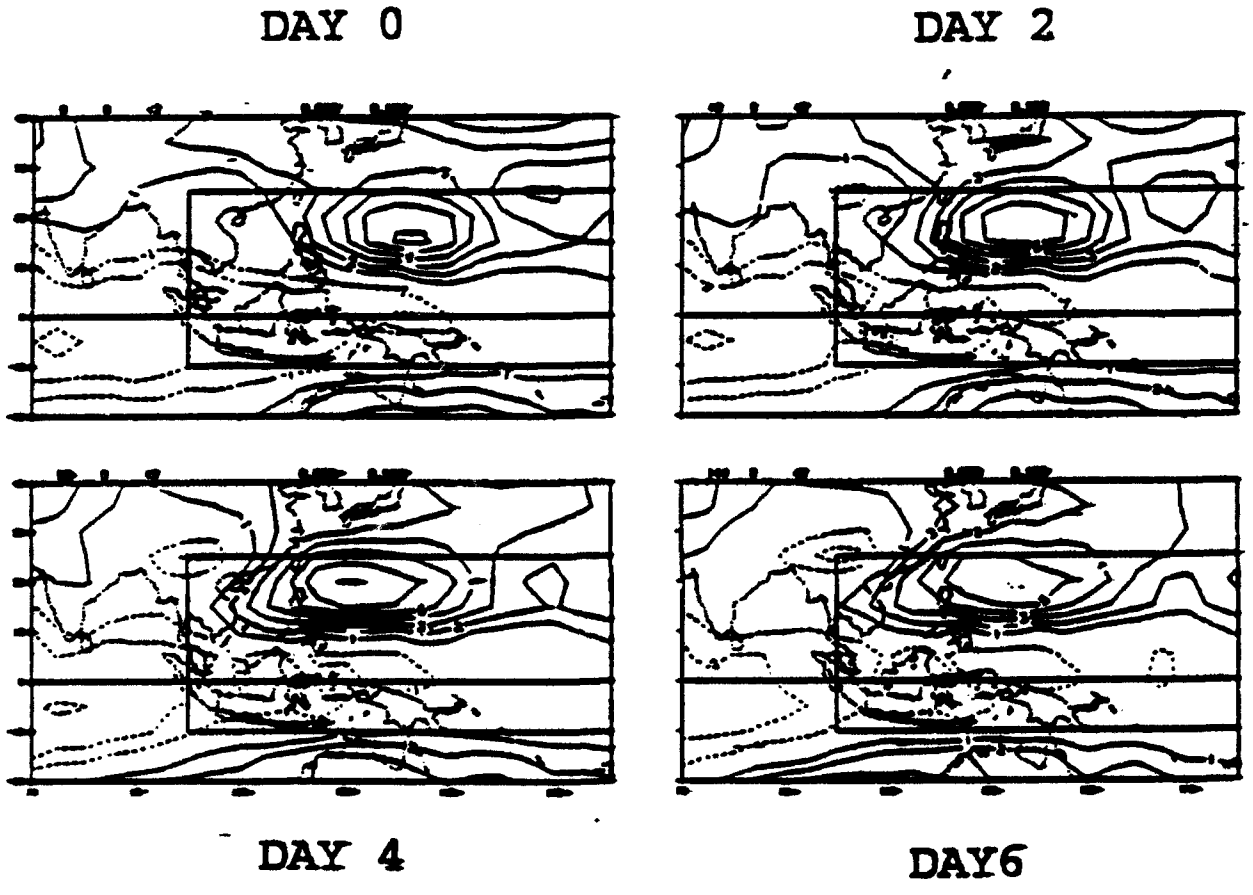

Figure 16c: Same as figure 8a except for T_{300}.

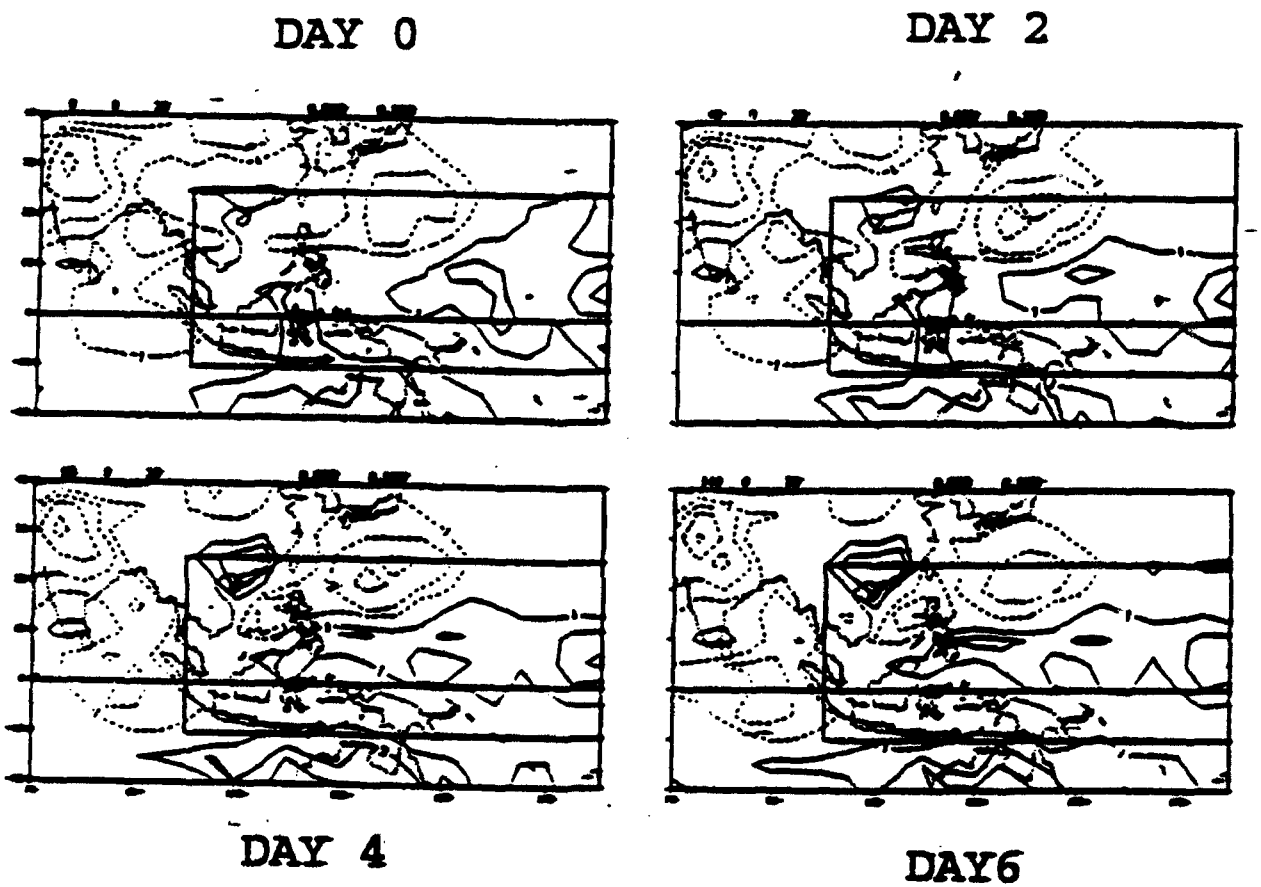

Figure 17a: Same as figure 8a except for D_{925}.

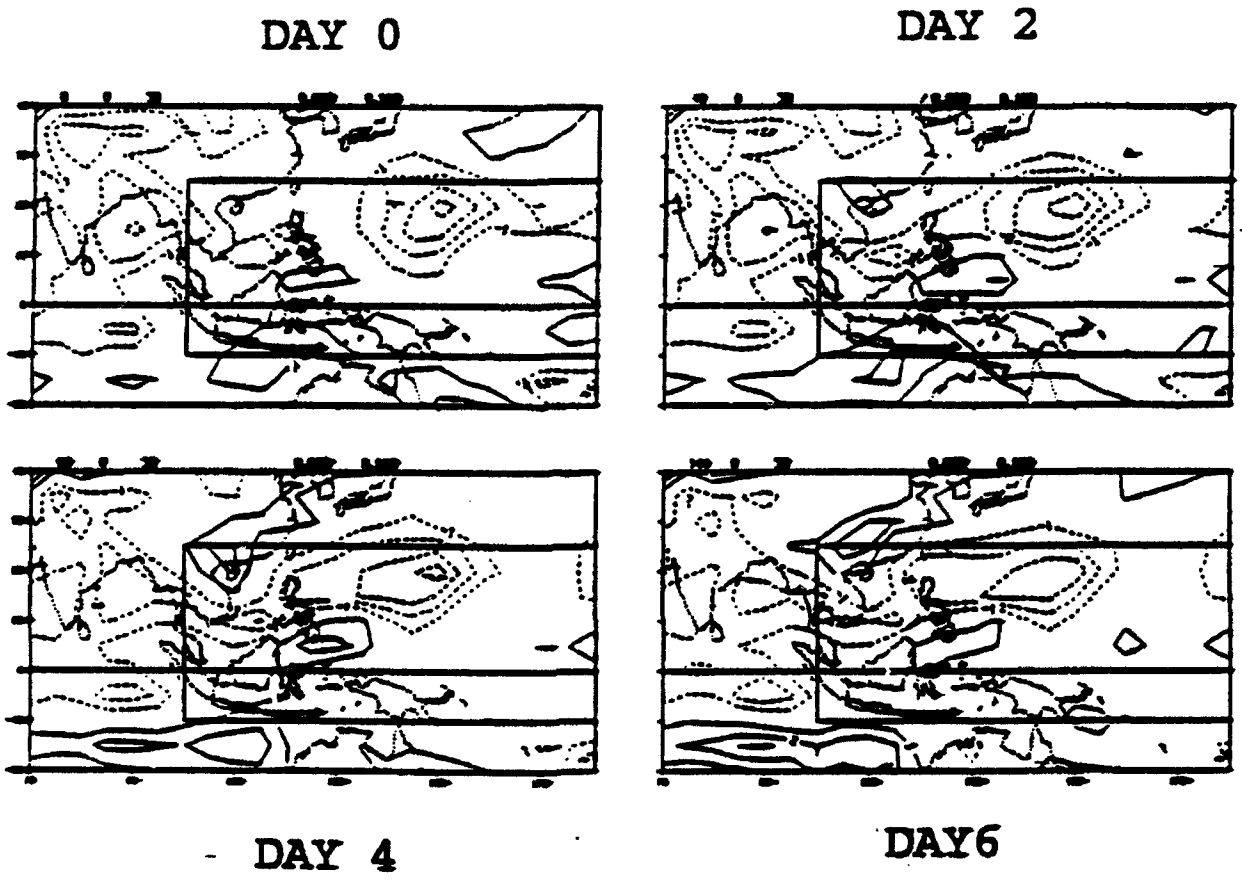

Figure 17b: Same as figure 8a except for D_{700}.

V. COMPOSITE ANALYSIS

Two important time scales can be seen in the time series of coefficient for MCC mode 1 shown in Fig. 5 . There is a seasonal trend with an increase in the coefficient from May towards the late season. In addition, there is another faster intraseasonal oscillation at a time scale around 20 days. The power spectrum diagrams clearly shows a concentration of power at the lowest frequency for 1989 and 1991, and a spectral peak near 20 day period for 1989 and 1990. The two different time scales make the interpretation of the spatial structure of mode 1 shown in Fig. 2, and the the single point correlation patterns described in Section 4 a complex task.

The simplest interpretation is that there is a stationary oscillation pattern that occurs at the two intraseasonal time scales. The slow westward propagation of some features may be an easterly wave disturbance that is superimposed on both intraseasonal quasi-stationary oscillations, or it may represent a westward propagating oscillation around 20 days. In order to see how the MCC1 mode represents both oscillations, we carry out a composite study to compare the structures of both oscillations and that of the MCC1 mode as determined by the correlated patterns. The composite for the seasonal change is done simply by producing the monthly averages of various fields for May through September, respectively. The composite for the 20-day oscillation is done by identifying different phases of selected

cycles whose signals are strong.

In the following subsections we discuss the composite diagrams for the three dimensional structures, including thermal and moisture structures, of both the seasonal change and the near-20 day oscillation.

A. SEASONAL COMPOSITE STRUCTURE

Fig. 18 shows the monthly average departures of V_{850} from the seasonal mean (average of all 15 months) for the five months from May to September . The main departure features in May are in the western part of the large area from India to the South China Sea, with alternating southern and northern cells. The southern cells are over India-western Bay of Bengal and the Indochina Peninsula, the northern cells are over eastern Bay of Bengal and between Philippines and Indonesia. Compared to the single-point correlation map for V_{850} (Fig. 8a), the May pattern resembles the negative phase of MCC mode 1 over the western half of the large area. The pattern signifies the fact that in May the India summer monsoon has not developed. In June and July the departure features are in the northwestern Pacific and southeastern China centered around 25-30°N, where the patterns correspond to the negative phase of mode 1. The features signify the strong southerly monsoon winds that start in May over southeast Asia then move to southeastern China near 25°E in June and extend northeastward to Korea and Japan in July. These movements are

manifestations of the progression of the East Asian summer monsoon rain belt, or Mei-Yu (Tao and Chen, 1987). In August, the departure diagram has features over most part of the area, and in general they correspond to the positive phase of mode 1 over almost the entire domain. The northern departure cell over southeastern China intensifies in September and extends southwestward over Indochina and eastern Bay of Bengal. This prominent northern departure pattern signifies the weakening of southwesterly monsoon winds as the summer season withdraws.

Overall, May-June-July are the negative phase and August-September are the positive phase of MCC mode 1. May is the western half of the negative phase of mode 1, covering the equatorial Indian Ocean, Bay of Bengal, and Southeast Asia, and June-July covers the northwestern Pacific and southeastern China. August is the only month that represents a near complete mode 1 structure (and in positive phase). Superimposed on this quasi-stationary phase reversal is a westward propagating feature in the northeastern region of the large area. A small positive area at the northeastern corner near 35°N and the dateline in June appears to move westward to south of Japan near 140°E in September. A weak negative area to the west, centered near 25°N, 155°E in June, appears to move westward and intensifies in August and September over southeastern China near 115°E, to become the dominant feature that gives these two months prominent positive phase mode 1 characteristics. Both areas move approximately 40° longitude from June to September, or about 0.5° per day. This is

considerably slower than the estimated 2.5° per day westward propagation signals in the MCC mode 1 structure and correlation patterns. Thus, the intraseasonal change contributes only to the stationary oscillation shown in mode 1.

Figure 19 shows the departures of U_{850} from the seasonal mean for the five months from May to September. The May pattern is dominated by zonally-elongated easterlies in the entire northern tropics south of 25°N. Compared to the U_{850} correlation pattern shown in Fig. 8b, it clearly correspond to the negative phase of MCC mode 1. This correspondence continues into June for the western Pacific and the South China Sea, and gives an overall negative correspondance in spite of the phase shift near India. By July, the negative phase mode 1 feature is limited to a smaller area between 110°E-140°E, 15°N-40°N. While this area from southeastern China to southern Japan and a limited region of the subtropical western North Pacific still resembles the negative phase of mode 1, the large westerlies over India and nearby oceans are not features associated with mode 1.

The weakening of the negative phase of mode 1 from May to July corresponds to the eastward withdraw of the subtropical ridge as the summer season evolves. The August departure is again a near complete representation of the positive phase of mode 1, signifying the strong and widespread southwest monsoon winds over the entire tropical northern summer monsoon region from Indian Ocean to the western Pacific. The positive phase remains in September, except over India and southeastern Asia

where the southwesterly monsoon weakens. The appearance of a southeastward movement of the trough over the western North Pacific is due to two seasonal trends. The first is the southward withdrawal of the trough from August to September. The other is the continuous weakening of easterlies in the northern equatorial Pacific from May to September, resulting in the extension of the westerly departure cell eastward towards the central Pacific in September. This latter aspect makes the September pattern resembling the eastern edge of the positive phase mode 1.

The seasonal 850 hPa flow change from May to September is also represented in wind vector plots shown in Fig. 20. The departure from the seasonal mean is presented mainly for the purpose of comparing with the composites of the near 20-day oscillation.

In order to avoid showing actual sea-level pressure field over the large land area of Asia included in the diagrams, the departures of geopotential height at 850 hPa(Φ_{850}) from the seasonal mean for the five months, shown in Fig. 21, are compared with the sea level pressure (P_{sfc}) mode 1 correlation pattern (Fig. 15). Similar to the general trend of the monthly average 850 hPa u and v departure fields, there is an evolution in the Φ_{850} departure patterns that correspond to the change of negative phase mode 1 from May and June to positive phase in August. The signals during July and September are too weak. The location and sign of these Φ_{850} departure patterns are consistent, in the sense

of gradient wind balance, with those of the 850 hPa winds.

Fig. 22 shows the departure fields of the dew-point depression at 700 hPa(D_{700}) indicating a change from a drier (positive D_{700}) May and June to a more moist August (negative D_{700}). The northeast-southwest orientation of the departure patterns over the western North Pacific is in the same sense as that shown in the D700 mode 1 correlation pattern. It may be concluded again that the monthly averages of this low-level moisture filed resemble a mode 1 evolution from negative (dry) phase to positive (moist) phase through the summer season. The moist regions overlap with southerlies and the dry regions overlap with northerlies, this overall pattern transports moisture from the tropical western Pacific to the north.

The departures from the seasonal mean of T_{300} are shown in Fig. 23. As expected, the departure gradients are concentrated in the midlatitudes, with a trend of increasing upper tropospheric temperature from May to August. Only in August is there a distinguishable warm departure over the subtropical western North Pacific, and this is consistent with the positive phase mode 1 correlation pattern shown in Fig. 16c.

The departures from the seasonal mean of the upper-tropospheric winds for the 5 months are represented by V_{200} (Fig. 24) and U_{200} (Fig. 25). Compared to the mode 1 correlation patterns for V_{200} (Fig. 12a), the May V_{200} departure field (Fig. 24) resembles somewhat the negative phase of mode 1 in the maritime continent and equatorial Pacific region, but not

southern China and northern Indochina. The resemblance over the latter area improves in June with the establishment of northerly departures, indicating a convergence zone elongated in the zonal direction. In July the western tropical Pacific departure field is flat. The August field is again a very good representation of the positive phase of mode 1, with an east-northeast to west-southwest oriented northerly departure area covering the maritime continent and western Pacific, and a southerly departure area that branches from Indochina to the north and northeast, with a small northerly area near the East China Sea and Korea. The elongated divergence outflow zone over the tropical western North Pacific is well indicated.

While the averaged U_{200} fields show an easterly jet axis that extends east-southeastward from South Asia towards the equatorial western Pacific, the departure fields (Fig. 25) exhibits an east-northeastward orientation from the maritime continent to the central tropical Pacific. This latter orientation agrees better with the MCC mode 1 correlation patterns for U_{200} shown in Fig. 12b. The May and June averages correspond to the negative phase of mode 1 and the July, August and September averages correspond to the positive phase. This is somewhat different from the lower tropospheric zonal wind fields, where July is still a weak negative phase (see U_{850}, Fig. 19).

In general, the seasonal change from May to September correspond approximately to the reversal of phase of MCC mode 1 from negative to positive. May is normally a "developing stage"

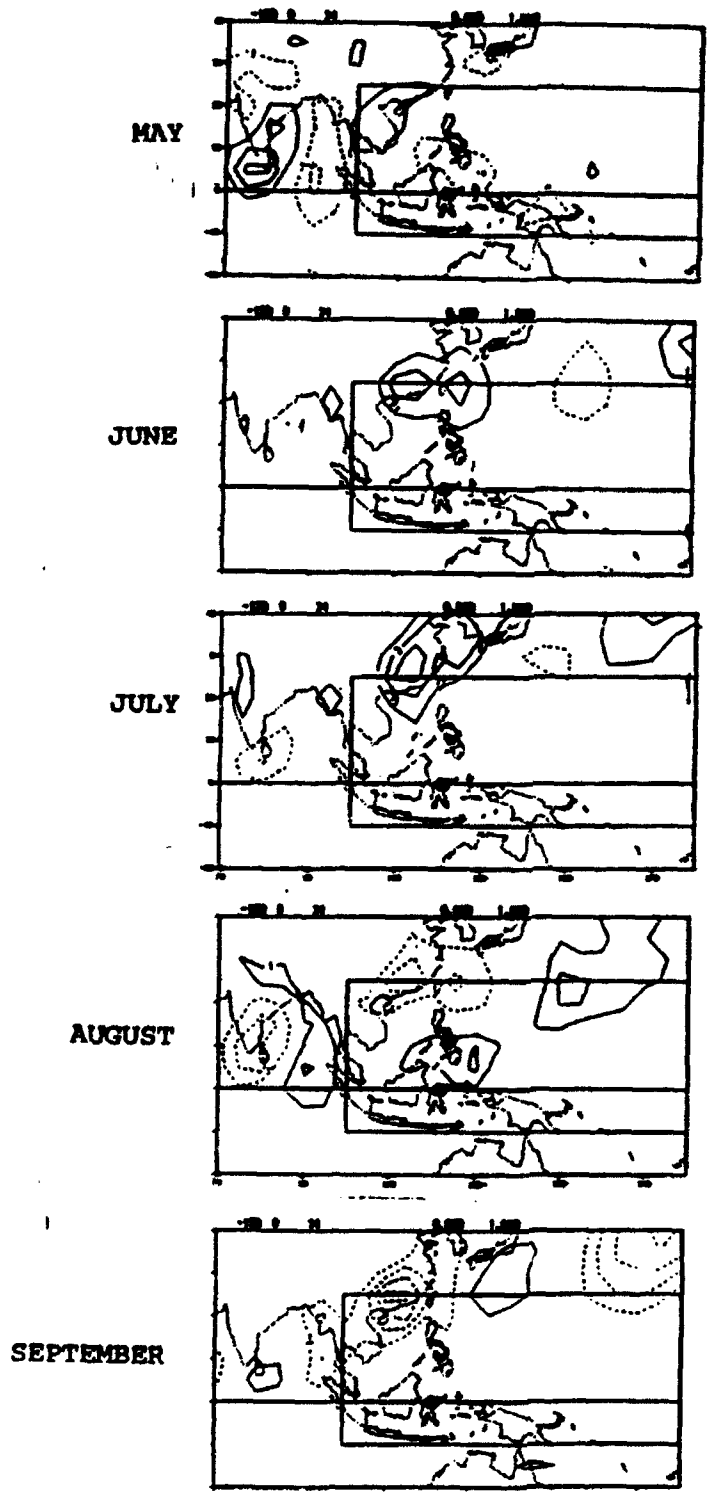

Figure 18: Departures of V_{850} from the seasonal mean for the five months from May to September. Contour interval is 1.0 m/sec. and negative values are dashed.

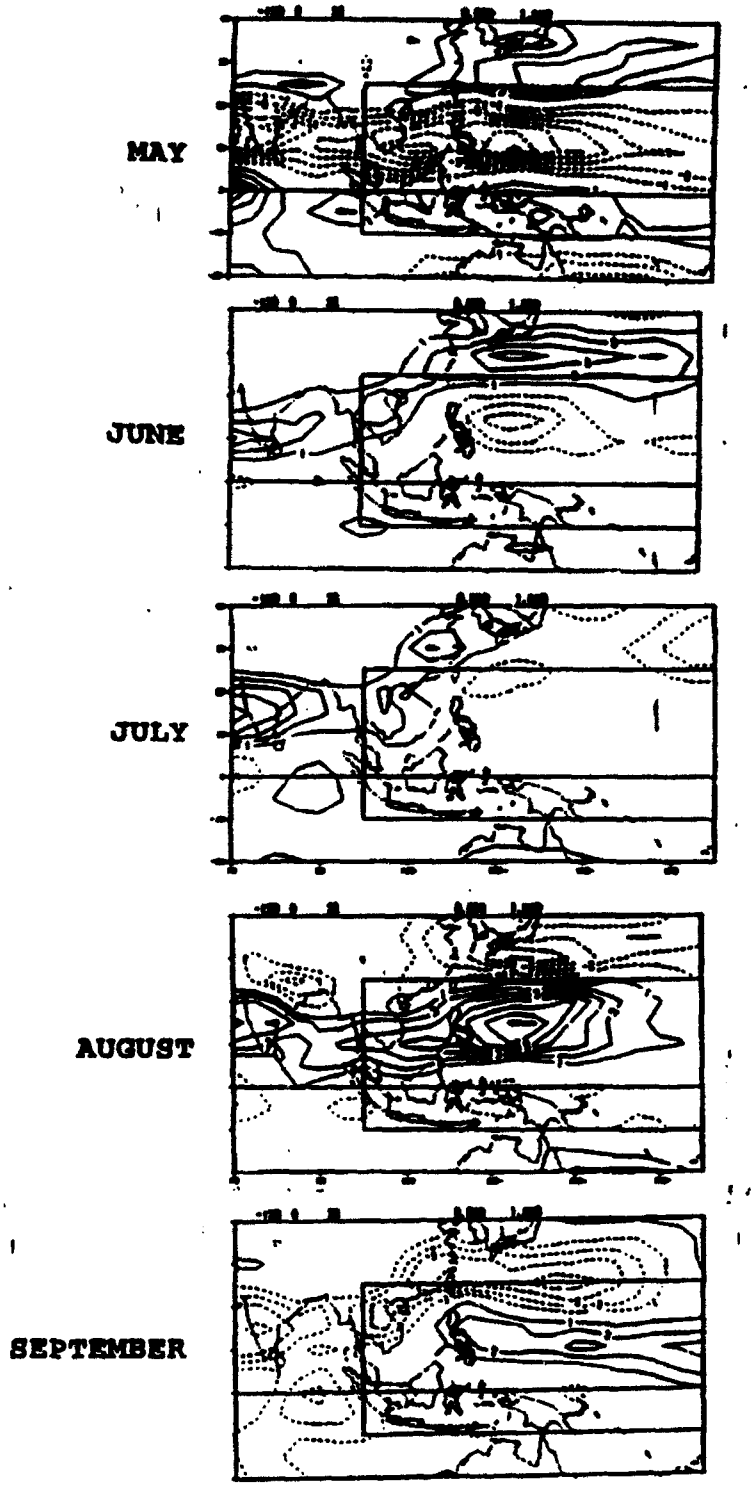

Figure 19: Departures of U_{850} from the seasonal mean for the five months from May to September. Contour interval is 1.0 m/sec. and negative values are dashed.

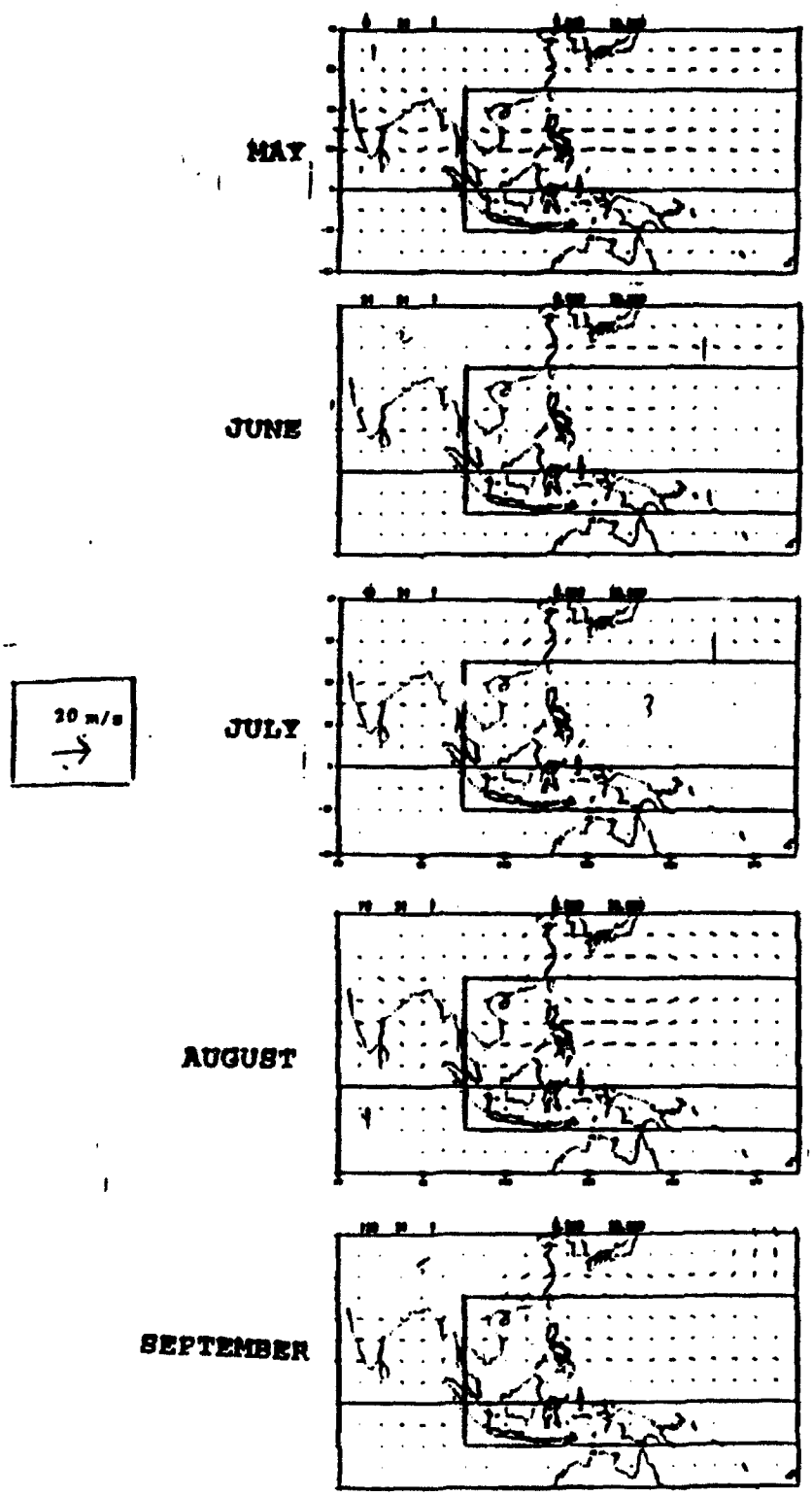

Figure 20: 850 hPa wind vector plot (from figures 18 and 19). Vector scale shown on center of the diagram.

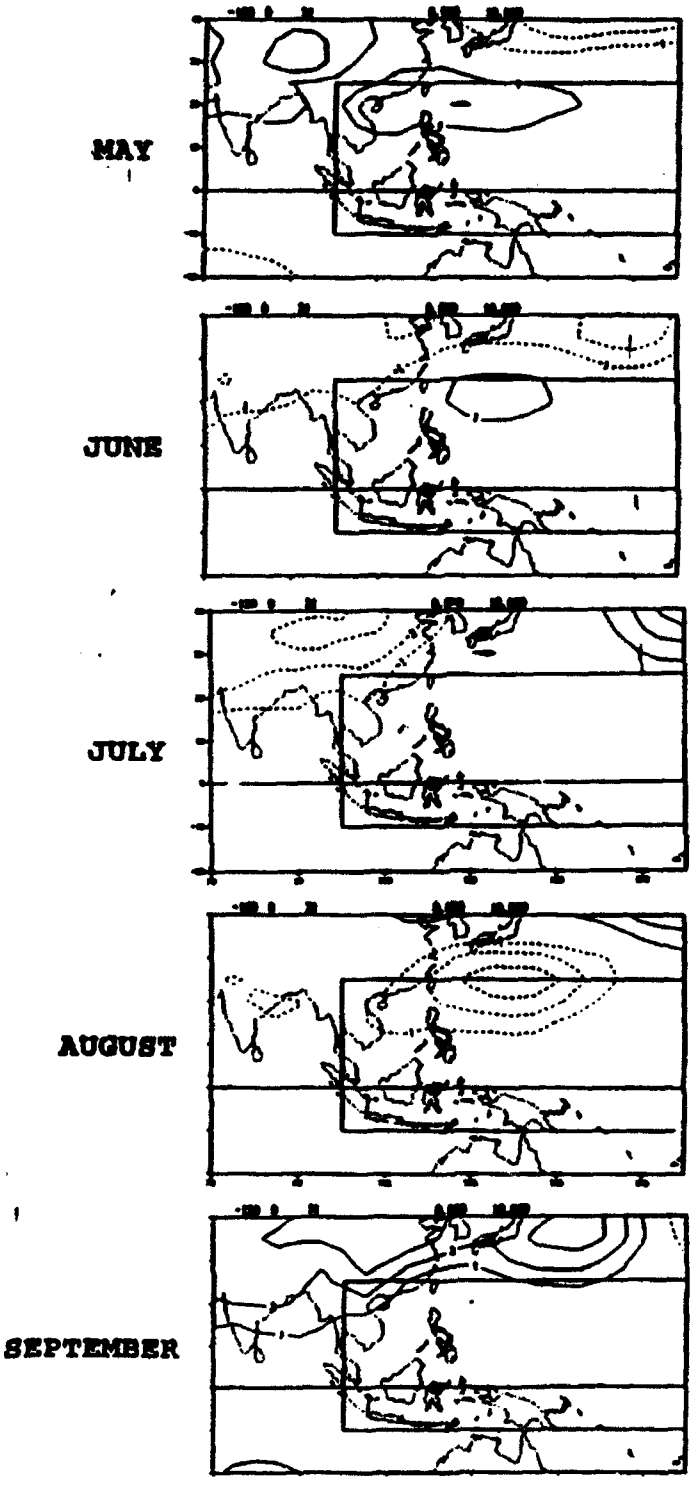

Figure 21: Departures of geopotential height at 850 hPa from the seasonal mean for the five months from May to September.Contour interval is 10 m and negative values are dashed.

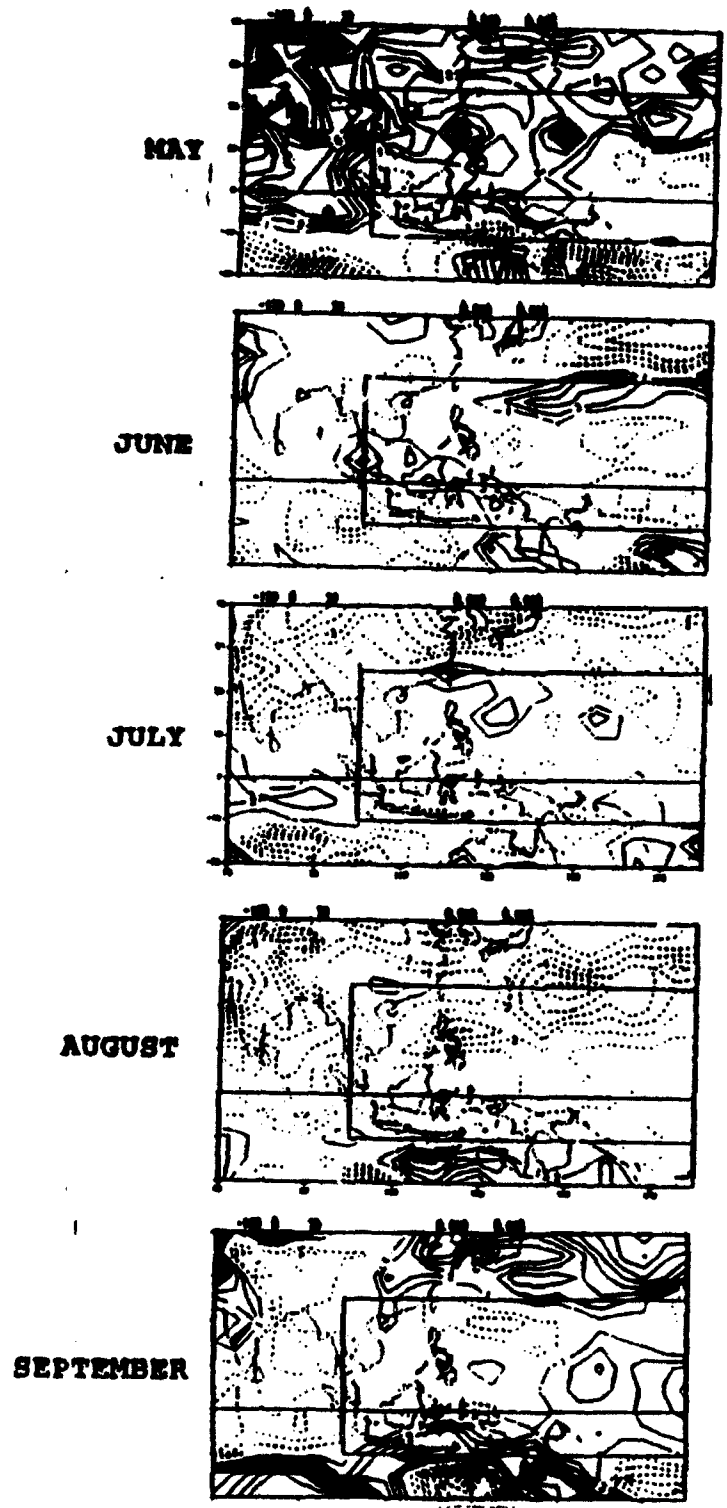

Figure 22: Departures of dew point depression at 700 hPa from the seasonal mean for the five months from May to September. Contour interval is 0.005 °C and negative values are dashed.

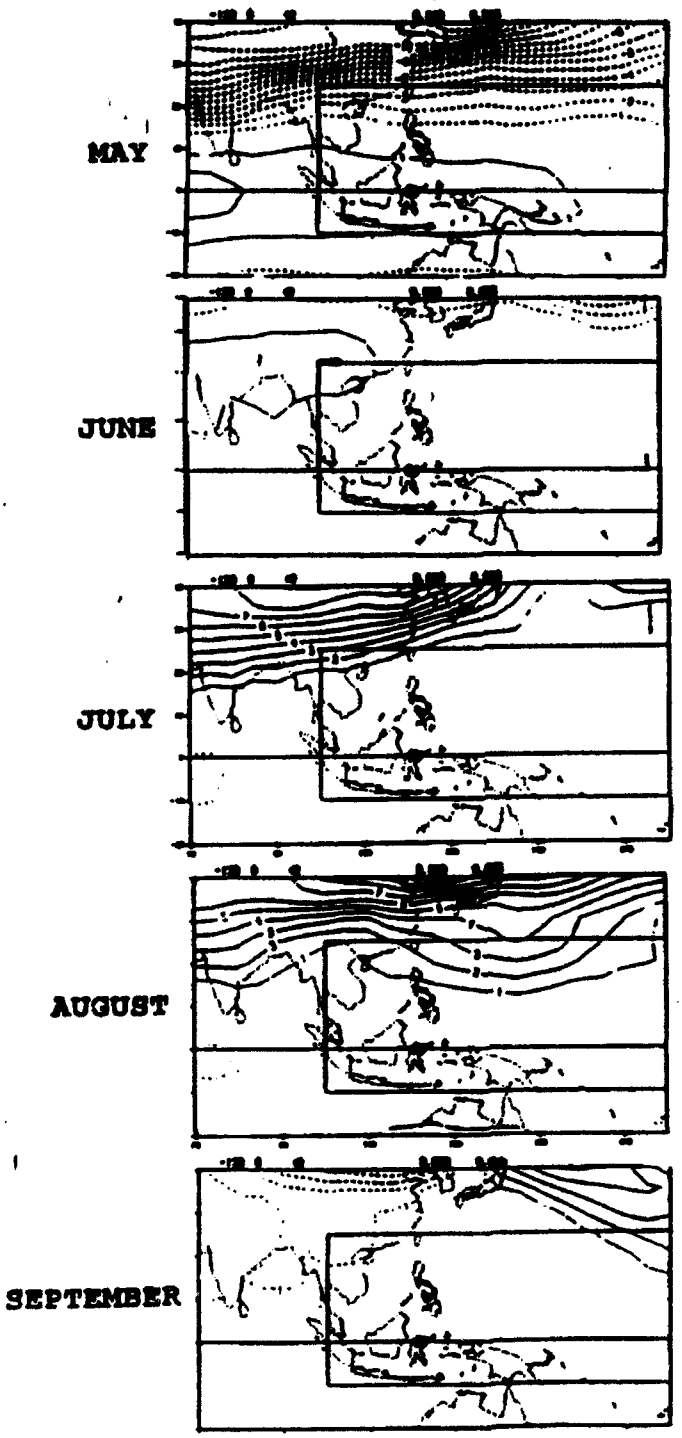

Figure 23: Departures of T_{300} from the seasonal mean for the five months from May to September. Contour interval is 0.005 °C and negative values are dashed.

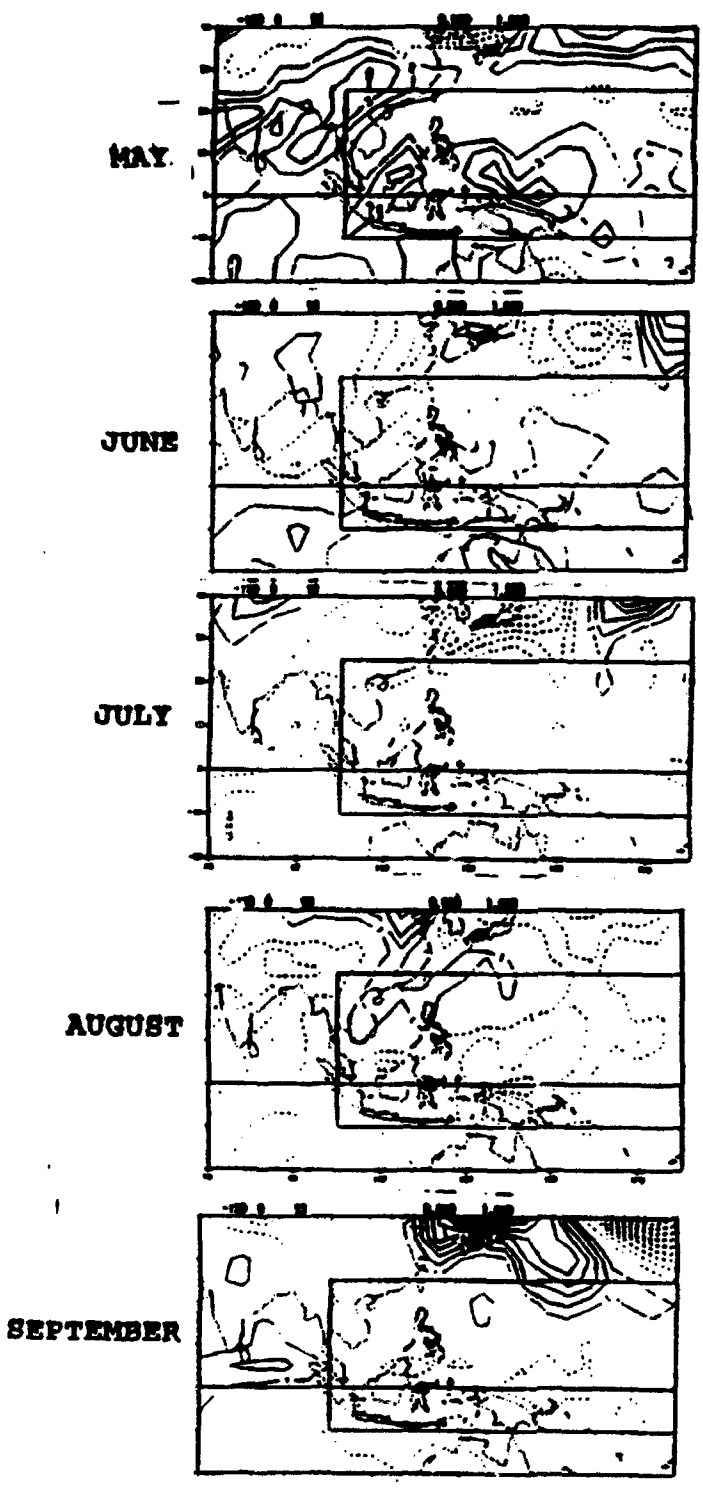

Figure 24: Departures of V_{200} from the seasonal mean for the five months from May to September. Contour interval is 1.0 m/sec. and negative values are dashed.

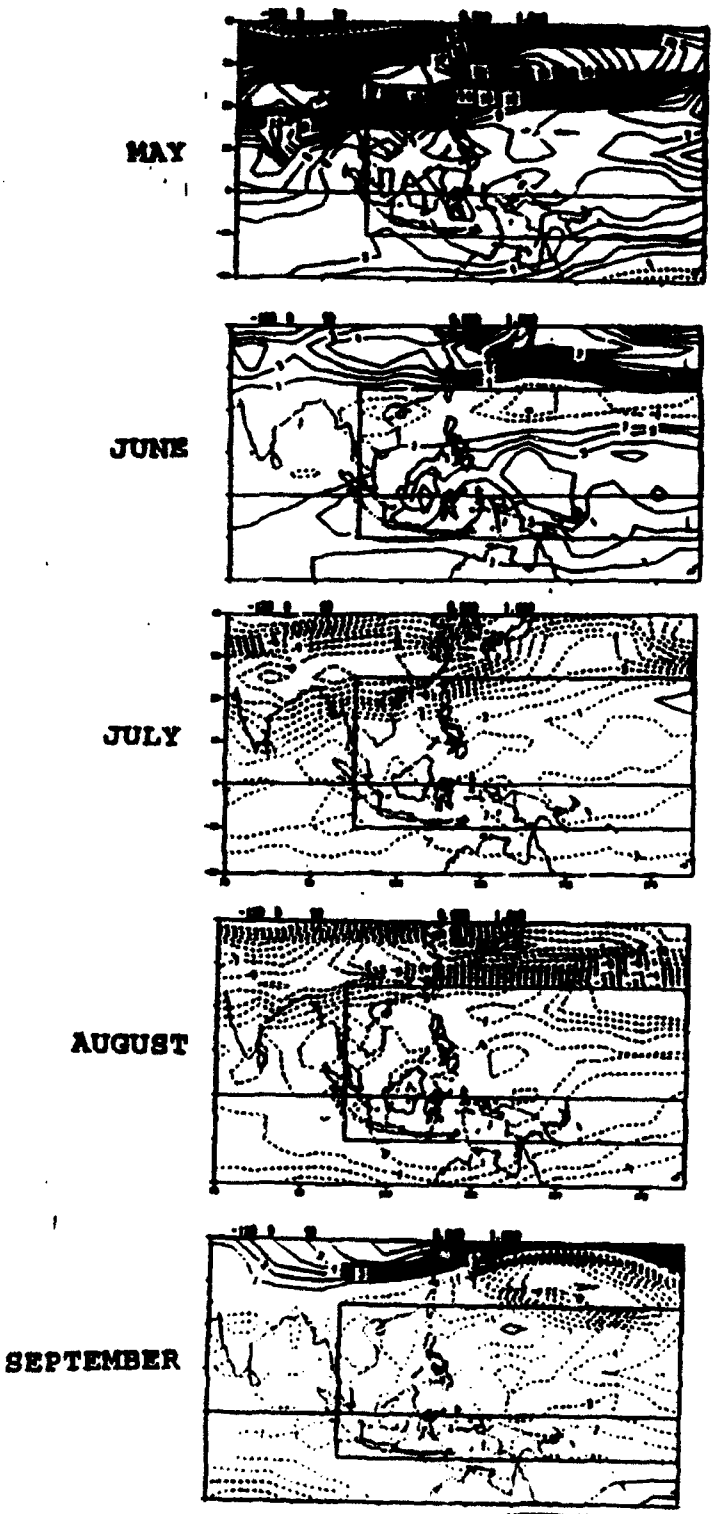

Figure 25: Departures of U_{200} from the seasonal mean for the five months from May to September. Contour interval is 1.0 m/sec. and negative values are dashed.

of the negative phase with a partial mode 1 structure. June has a somewhat more developed negative phase of mode 1. July is near a neutral node in the phase reversal. August shows the most complete mode 1 structure with a pattern that resembles closely the positive phase. September appears to be a remnant of the positive phase with a partial structure in the wind fields.

B. NEAR 20-DAY COMPOSITE STRUCTURE

For the near 20 day period oscillation, the composite structure is based on selected case whose signals are strong in the time series of the MCC mode 1 coefficient. The selection of cases is shown in Fig. 26, which is the same MCC1 coefficient time series (Fig. 5) with each selected case marked by six phase categories. Phase 1 is the minimum, phases 2 and 3 are intermediate times that mark the 1/3 and 2/3 points of the interval from minimum to maximum, phase 4 is the maximum, and phases 5 and 6 are intermediate times that mark the 1/3 and 2/3 points of the interval from maximum to minimum. A total of eight cases are selected, all in the second half of summers. The composite structure of the oscillation is produced by averaging all fields of the selected cases with respect to each phase category, and then compute the departures from the case means for each phase. For each variable field, the results are shown as a time sequence of the six phases of the departure patterns.

Fig. 27 shows the composite of V_{850}. At phase 1, an anticyclonic circulation dominates the western North Pacific between the equator and 30°N and 120°E-160°E. A westward propagating pattern is clearly indicated, with the northerly wind region at 25°N, 155°E in phase 1 moving steadily westward to 110°E in phase 6. This translates to a propagation speed of 45° longitude per 5/6 cycle. If a 20-day period is assumed, the propagation speed is 2.7° per day, which is very close to the speed of westward propagation noticed in the MCC mode 1 structure and correlation patterns. The diagram also shows clearly that there is a near 180° phase reversal between phase pairs 1-4, 2-5, and 3-6, respectively. However, the propagation pattern is somewhat limited to the longitudinal range of the western Pacific and the South China Sea, the core domain of the MCCA. The structure of phase 1 seems to only partially continue from phase 6. In phase 6 the anticyclonic circulation east of 150°E is only defined by the southerly near 25°N, 150°E, northerly winds are not evident to the east. Thus, there seems to be an intensification of the anticyclonic circulation in the subtropical western North Pacific in phase 1.

To the west of the core domain, a weaker pattern of alternating southerly and northerly cells with a smaller spatial scale continues to propagate slowly westward over the Bay of Bengal and India. This propagation pattern is clearly detectable from phases 3 to 6, and has a movement of about 10-15° longitude between them. This translates to 1-1.5° per day. Over India an

180° out-of-phase relationship can be seen between phases 2-5 and also phases 3-6, thus there is a westward propagation at the same near 20-day period. This shorter scale, slower propagation can be traced from the longer and faster propagation from the western Pacific and the South China Sea.

In addition to westward propagation, there is an indication of northwestward propagation from the equatorial western Pacific near 150°E towards the southern China coast, as can be seen in phases 2-6. This is similar to the propagation path of the synoptic 8-day waves represented by MCC modes 2-3 in this study, which was related to tropical cyclone activities by Chang et.al., (1994). The relationship between the two types of motions is unclear, as they have distinctively different time scales.

Compared to the V_{850} MCC mode 1 (Fig. 2) structure and the correlation pattern (Fig. 8a), it can be seen that phases 5-6 resemble the positive phase of mode 1 and phases 2-3 resembles the negative phase.

Fig. 28 shows the composite of U_{850}. As is the case with the mode 1 correlation structure (Fig. 8b), the westerly and easterly anomaly areas are much more elongated in the zonal direction than the v850 pattern. However, the near 20-day composite has a slightly larger zonal orientation (a west-southwest to east-northeast tilt) than both the mode 1 correlation and the monthly-mean seasonal change patterns. The 180° phase reversal can again clearly be seen between phase pairs 1-4, 2-5 and 3-6, respectively. Westward propagation patterns can be traced by

following individual positive, anomaly cells.

From phases 1 to 3 the northwestern subtropical Pacific is dominated by an anticyclonic (ridge) axis whose orientation rotates cyclonically from near zonal to WSW-ENE as it propagates westward. The westerly anomaly center north of this ridge propagates from 150°E in phase 1 to 105°E over Indochina in phases 3-4, when the pattern appears to grow and extend westward to produce another, stronger center over India. The propagation speed of this center is approximately 45° over 2/6 to 3/6 of a cycle, or about 4.5-7° per day. On the other hand, there is another westerly anomaly cell to the southeast of a cyclonic axis that propagates from the northern equatorial western Pacific in phase 2 to an expanded area centered in the Philippine Sea in phase 6. The center of this propagation path moves at most 20° longitude over 2/3 of 20 days, or approximately 1.5° per day, much slower than the first cell. This propagation also has a northward component resulting in a west-northwestward direction. The difference in the two propagating speeds appears to be due to the zonally elongated u cells that make the determination of the longitudinal center of the motion system very sensitive to case selection. Therefore, the u component is not suitable for determining the zonal propagation characteristics. Rather, it can be used to estimate the meridional propagation. Following the westerly cell in the northern equatorial zone in phase 2, which moves to a belt extending from eastern Indian Ocean to 25°N, 150°E in phase 6, the northward propagation speed appears

to be around 1° per day.

Comparison of the near 20-day composite with the U_{850} mode 1 correlation pattern (Fig. 8b), phase 2 is a good resemblance of the negative phase and phase 5 corresponds to the positive phase. The adjacent phases (3 and 6, respectively), still appear to correlate highly with the negative and positive phases, but there is a cyclonic rotation of the main axes.

Fig. 29 provides a wind vector plot for the near 20-day composite series. A series of anticyclonic and cyclonic cells propagating westward in the subtropical latitudes, and an orientation that is slanted to the west-northwest from the equatorial western Pacific, can be seen. As may be expected, only the subtropical propagation is indicated in the Φ_{850} composite (Fig. 30). Here the center of the high anomaly cell can be traced from about 145°E in phase 1 to around 100°E in phase 6. This 45° movement over 5/6 of a cycle, or a propagation speed of 2.7° per day, agrees with the speed determined from the V_{850} composite series (Fig. 27). The location of the anomalous high center is also consistent with the gradient wind relationship with both V_{850} and U_{850}. The westward propagation speed can also be determined from the track of the low anomaly center, which moves westward into the region of the southern Tibetan Plateau in phase 4. This is, of course, artificial as 850 hPa is below the ground surface. Nevertheless, the hydrostatic extrapolation of Φ_{850} under the surface is determined locally. Therefore, Fig. 30 indicates that a 20-day motion system

characterized by near surface air temperature and height anomalies continues a westward propagation from the western Pacific to the South Asian monsoon region. As is true with both U_{850} and V_{850}, a comparison to the P_{sfc} mode 1 correlation pattern (Fig. 15), shows that phase 2 of the near 20-day oscillation closely resembles the negative phase, and phase 5 resembles the positive phase.

Other fields in the near 20-day composite follow the same patterns as described for the 850 hPa fields, with generally good agreements between phase 2 and the negative phase of MCC mode 1, and between phase 5 with the positive phase. The composite D_{700} series, shown in Fig. 34, has a general 180° out-of-phase relationship with the V_{850} composite (Fig. 27), in that the low-level southerlies transport moist air northward and the northerlies transport drier air equatorward. This is the same relationship shown in the mode 1 correlation pattern and the seasonal change of monthly means. The composite T_{300}, shown in Fig. 33, is basically 180° out of phase with Φ_{850}. Thus, the system is deep, warm core with upper tropospheric warm center over low-level cyclonic, low pressure system and cold center over low-level anticyclonic, high pressure system.

At 200 hPa, the u and v wind composites (Figs. 32-31) respectively) show somewhat noisier structures than the 850 hPa, but the general relationship that phase 2 corresponding to negative mode 1 and phase 5 corresponding to positive mode 1 still hold in the core domain. A westward propagation pattern

does not show up clearly, except in V_{200} (Fig. 31) where an indication of westward propagation may be traceable by following the northerly anomaly areas.

As is found in the mode 1 correlation patterns, both v and u show a tendency of negative correlation with their 850 hPa counterparts south of 25°N, although the correlation is not high and the phase difference varies.

Unlike the more zonally oriented cells in the V_{200} mode 1 correlation and the seasonal-change patterns, which implies a significant north-south divergence component, the 20-day composite series of V_{200} show more steep southwest-northeast tilted anomaly areas whose orientations are similar to those of v850 composite. Therefore significant rotational shear of V_{200} is present.

In the tropics, the weak divergence shear of V_{200} does provide the correct sign of anomalous outflow in the upper anticyclonic area (phase 5) and anomalous inflow in the upper cyclonic area (phase 2).

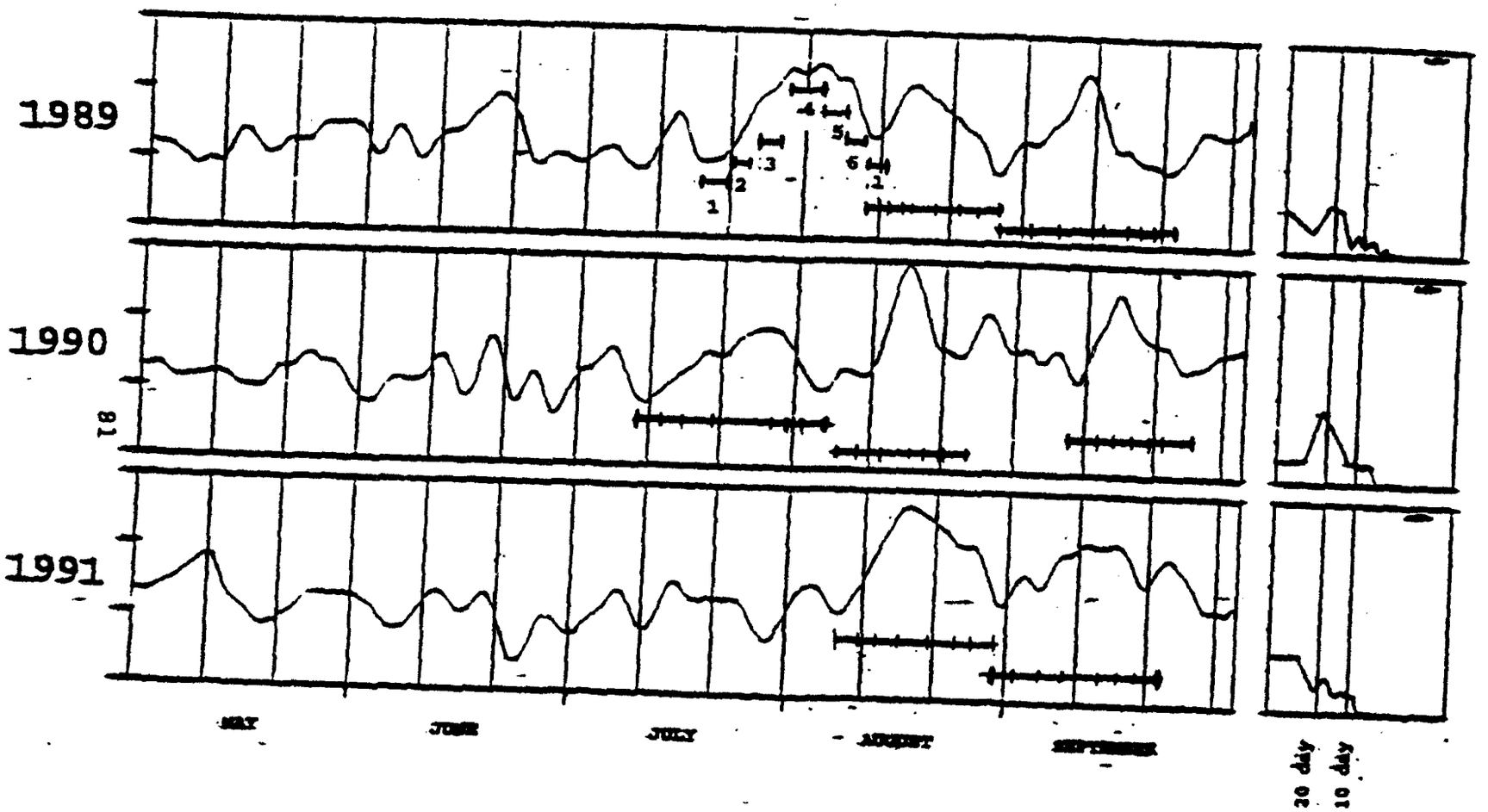

Figure 26: Selection of cases (each case marked by 6 phases categories) for the three summers of MCC mode#1 used in the near 20 day composite structure.

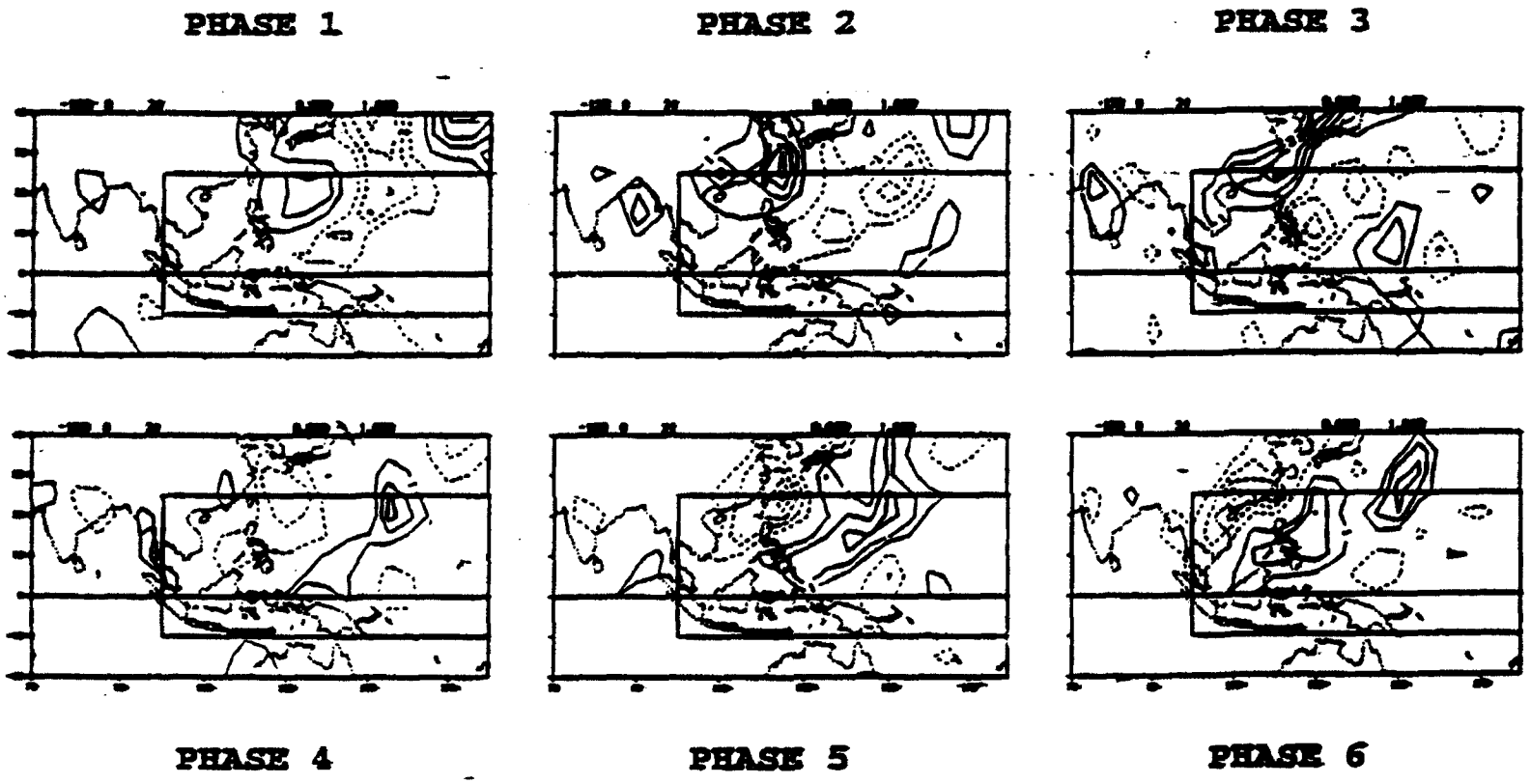

Figure 27: Departures of V_{850} from the case means for each phase. Contour interval is 1.0 m/sec. and negative values are dashed.

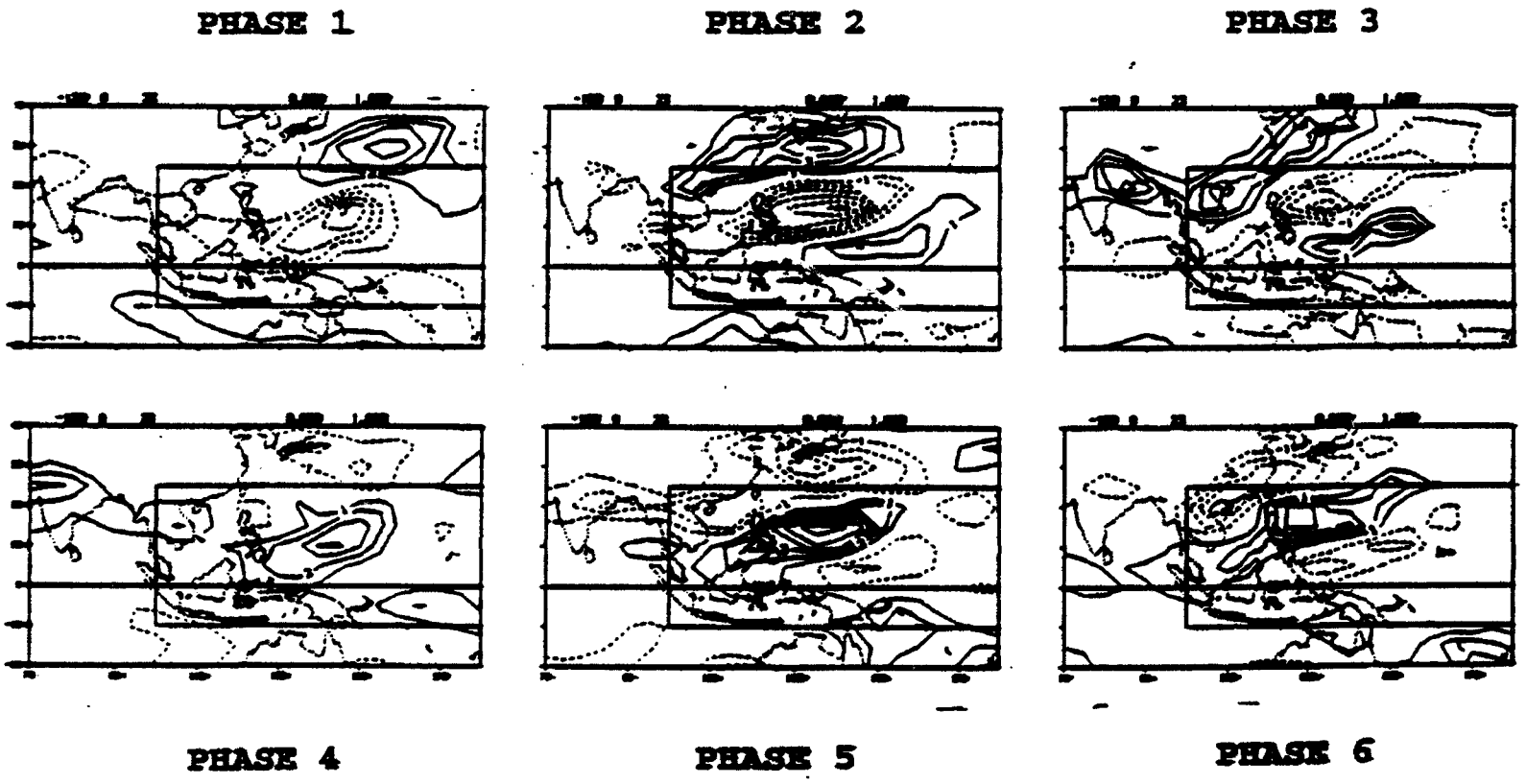

Figure 28: Departures of U_{850} from the case means for each phase. Contour interval is 1.0 m/sec. and negative values are dashed.

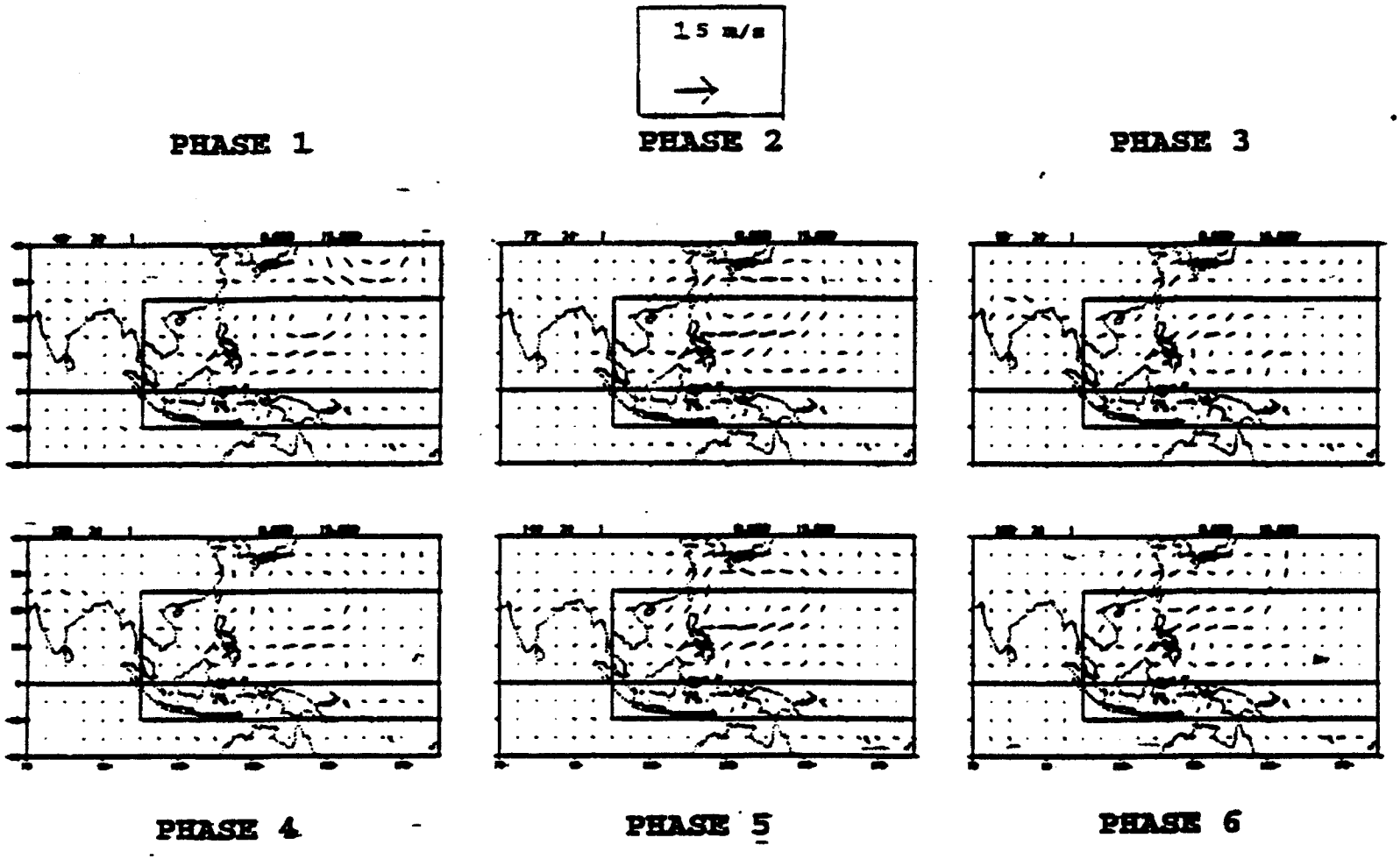

Figure 29: 850 hPa wind vector plot (from figures 27 and 28).
Vector scale shown on center of diagram.

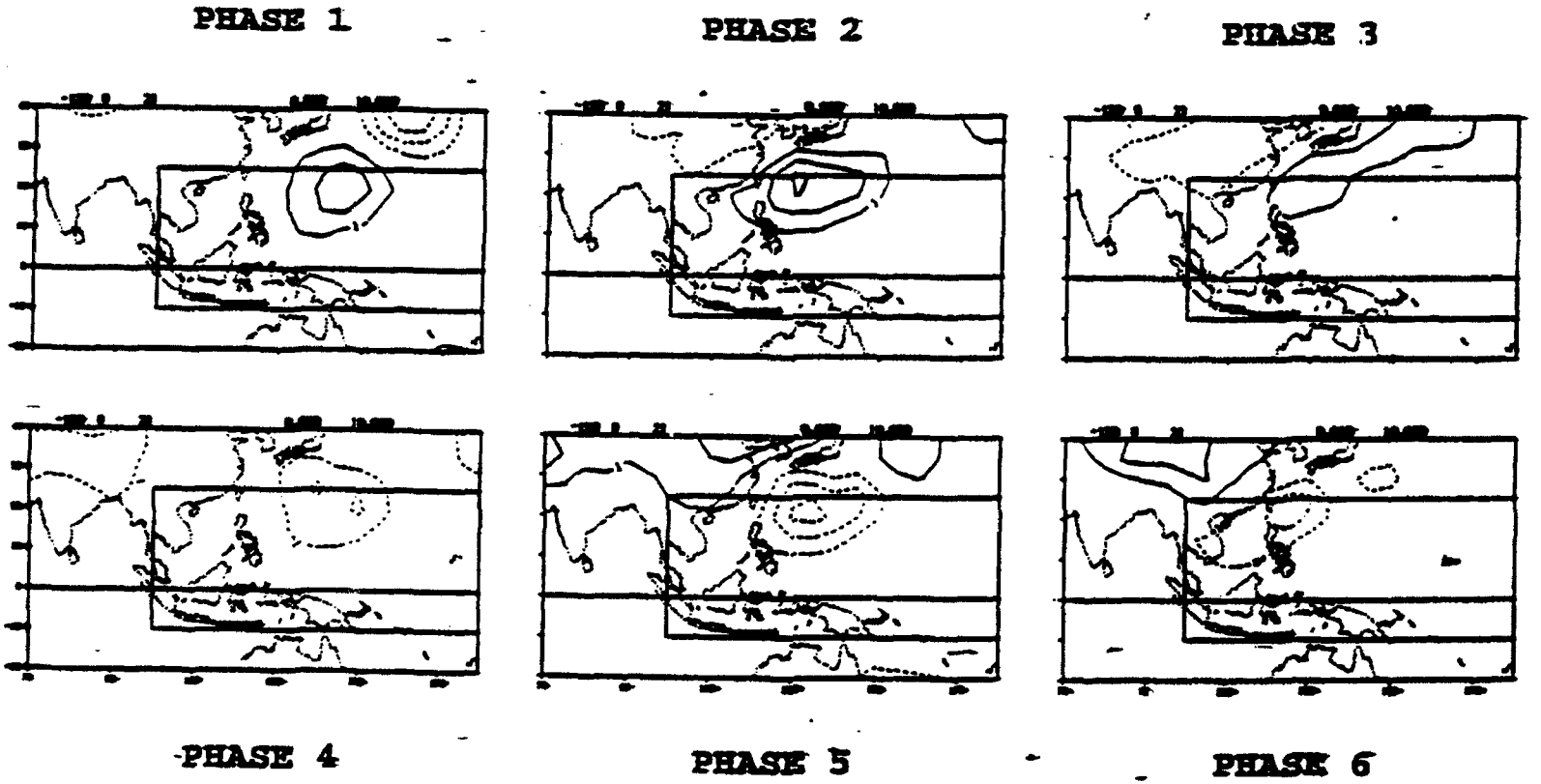

Figure 30: Departures of Φ_{850} from the case means for each phase. Contour interval is 10 m/sec. and negative values are dashed

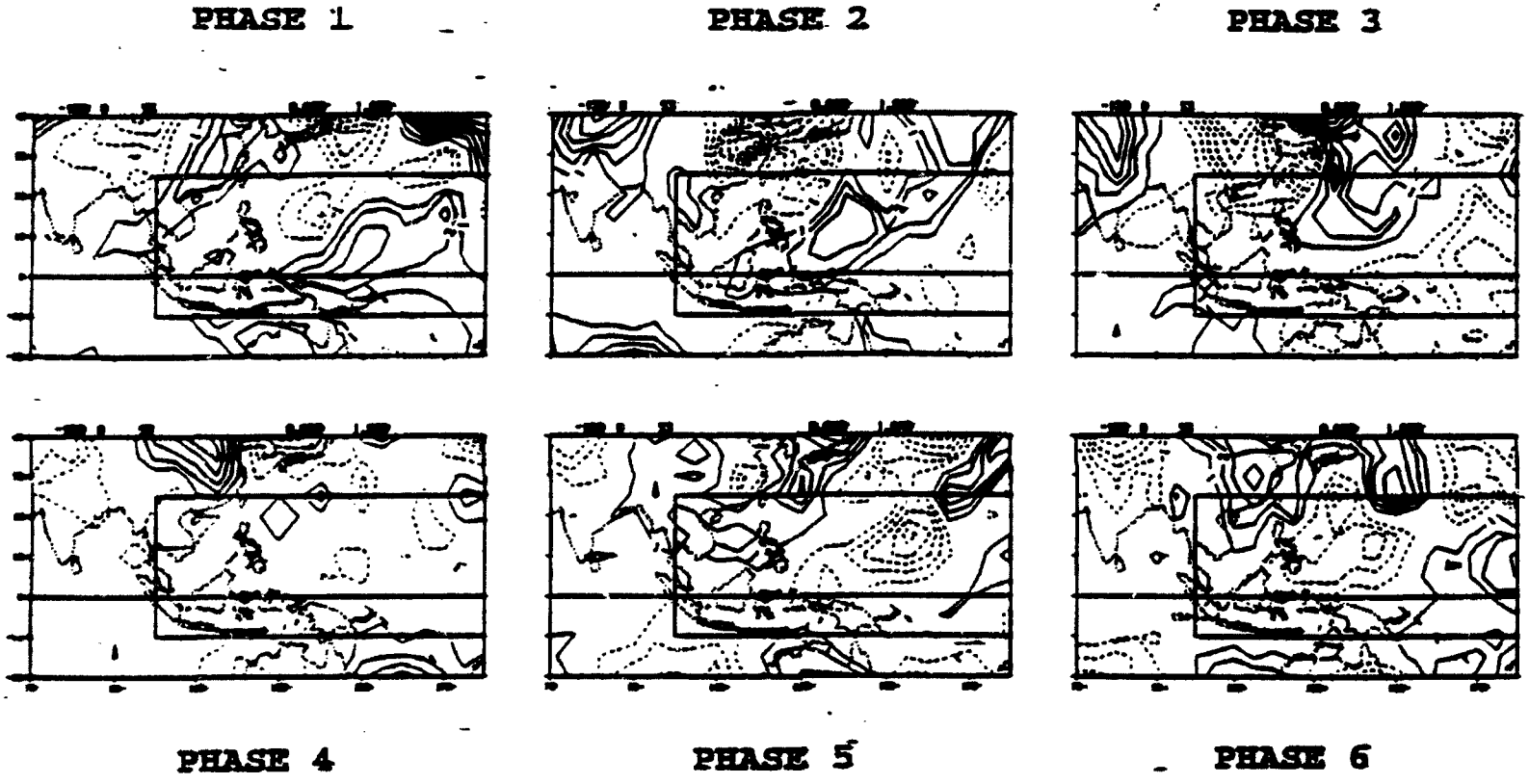

Figure 31: Departures of V_{200} from the case means for each phase. Contour interval is 1.0 m/sec. and negative values are dashed

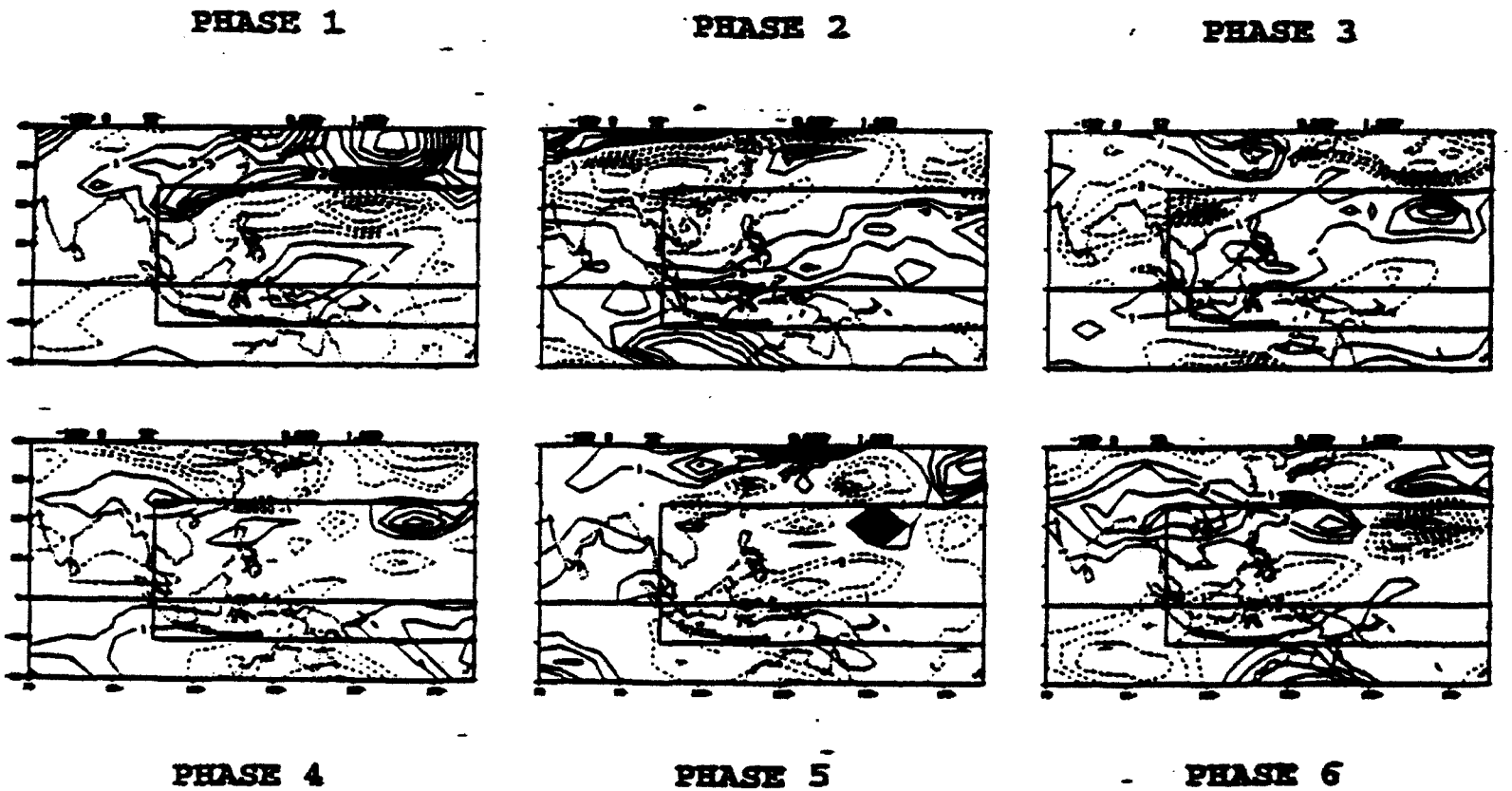

Figure 32: Departures of U_{200} from the case means for each phase. Contour interval is 1.0 m/sec. and negative values are dashed

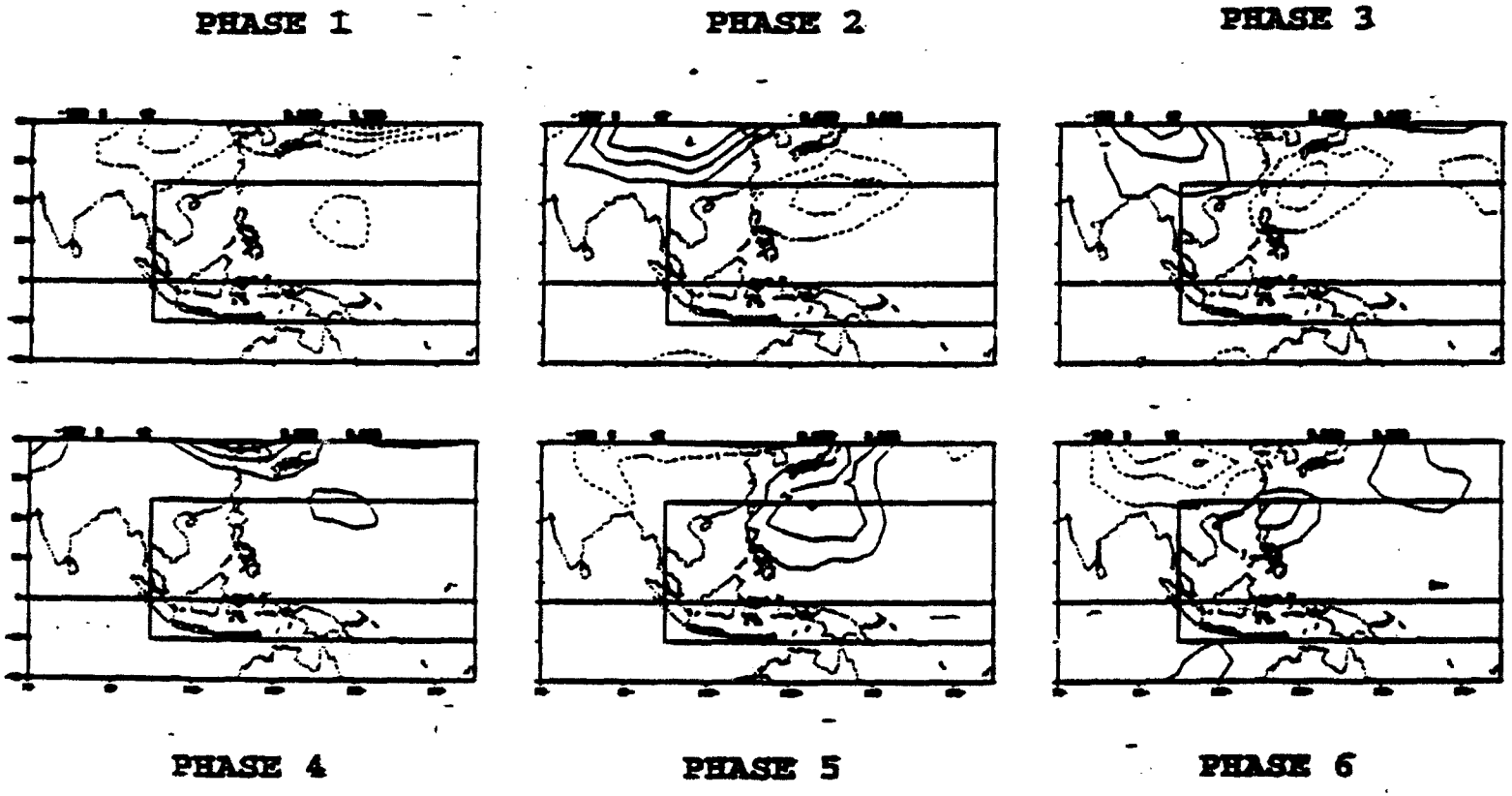

Figure 33: Departures of T_{300} from the case means for each phase. Contour interval is 0.005 °C. and negative values are dashed

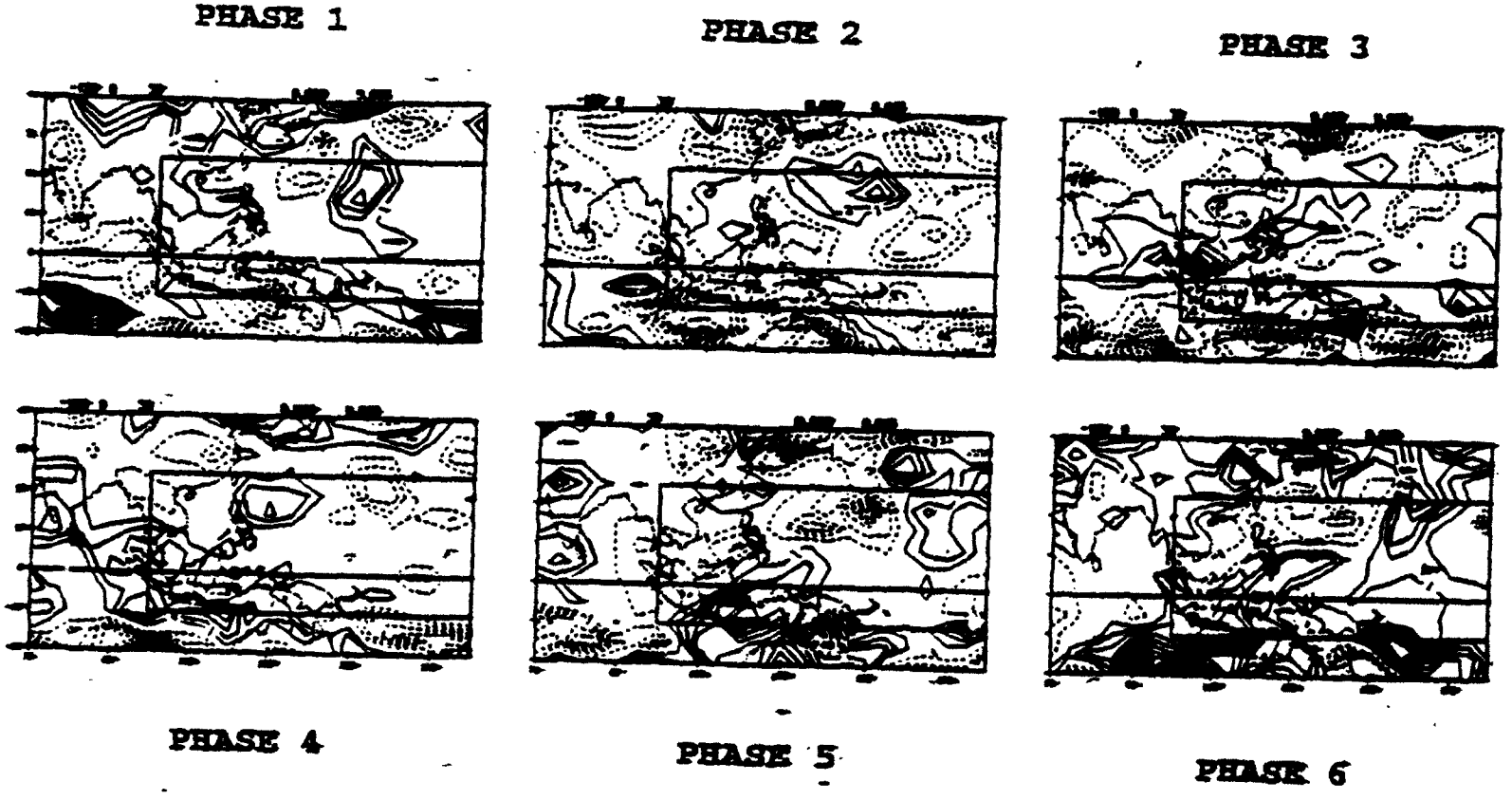

Figure 34: Departures of D_{700} from the case means for each phase. Contour interval is 0.005 °C. and negative values are dashed

VI. SUMMARY AND CONCLUSIONS

In this research we study the intraseasonal oscillations over the tropical western Pacific-eastern Indian Ocean region using the NOGAPS analyzed fields during the summers of 1989-1991. For each year, the data from May to September are included. The focus of the research is on oscillations other than the 30-50 day Madden-Julian Oscillation. Since the main signals of the MJO are in the u velocity, the motion systems studied here are chosen by identifying their basic structure from spatial principal components of the meridional velocity. The identification is done by using the multiple-set canonical correlation analysis (Chen and Chang 1993; Chen et al., 1994) on the v component at 850 hPa. The application of the technique is the same as that used by Chang et. al.,(1994) on the same data set for studying the synoptic scale wave patterns. Twelve sets of data are constructed by a forward sliding time window, which consists of 12 twice-daily time frames of the V_{850} field, through the five months of each year. The resulting MCC modes are ranked by the geometrically-averaged correlation between V_{850} fields of adjacent times within the 12 time frames, or 5.5 days.

The first MCC mode shows two pairs of opposite V_{850} centers in the western North Pacific and the maritime continent region. The four centers line up approximately in four corners of a rectangle, with the northeastern and the southwestern anomalous centers connected into a northeast-southwest tilted structure.

The pattern produce cyclonic shear in the northern subtropics along 25°N and anticyclonic shear just north of the equator during the positive phase. The half wavelength determined from the subtropical centers is about 3000 km, and is slightly shorter for the tropical centers. The entire pattern is quasi-stationary with an indication of a slight westward propagation. The averaged fractional variance is 17.6%. Its time coefficient exhibits strong intraseasonal characteristics on two time scales. The first is a seasonal trend that increases from early summer to late summer, the second is an oscillation with a period around 20 days.

The second and third MCC modes, with a 90° phase difference between them and comparable variances, form a synoptic-scale, northwestward propagating wave pattern from the equatorial central-western Pacific towards southern China coast. It has a periodicity of 8-9 days and a combined fractional variance of 31.3%. This synoptic wave pattern was studied extensively by Chang et.al.,(1994). Excluding the combined fractional variance of the synoptic wave pattern which dominates the V_{850}, the first mode has more than one quarter of the remaining variance, and is selected as the basic intraseasonal mode for further analysis.

The three dimensional dynamic and thermodynamic structure of the first mode is determined by a single-point correlation analysis between all fields and the time variation of the mode coefficient. The fields include sea-level pressure, and u and v velocities, dew point depression, and temperature at various

levels. For the positive phase of MCC mode 1, the correlation patterns describe a slowly westward propagating system of a low-level trough in the subtropical western North Pacific and a low-level ridge near the maritime continent north of the equator. The propagation speed is between 2.5°-3° per day. North of 25°N the entire troposphere is near barotropic. South of 25° a sharp vertical phase shift occurs in the middle troposphere, starting from 600 hPa near the dateline. Above 400 hPa the entire domain south of 25°N is near 180° out-of-phase with the lower troposphere. This equivalent barotropic, or first baroclinic mode, vertical structure is consistent with a warm core between 850-200 hPa, with maximum temperature fluctuations near 300 hPa.

At all levels the u field is more elongated in the zonal direction and the v field shows a tendency of a southwest-northeast tilt. There is also a slight equatorward vertical tilt in the upper troposphere. At lower levels the subtropical system transports moisture towards northern midlatitudes and drier air equatorward. At 200 hPa a north-south divergent flow near the upper-level ridge is clearly indicated by the meridional gradient of v. This divergent zone is in the general vicinity of the upper-level outflow associated with the northern summer ITCZ between the maritime continent and the subtropical western North Pacific. However, it has a west-southwest to east-northeast orientation, which is contrary to the climatological mean, west-northwest to east-southeast, orientation of the western Pacific ITCZ during the northern

summer monsoon.

Since the basic MCC mode is associated with two different intraseasonal time scales: a seasonal change from early to late summer and a near 20-day oscillation, a composite study is carried out to compare the averaged structure of these two time scales with the MCC mode 1. The seasonal change composite is done simply by first averaging all data fields within each of the five months, and then subtracting the summer-mean (3 summers of 5 months each) from the monthly averages. The resultant monthly departure fields indicate that the motion associated with the seasonal change is a reasonable reproduction of the basic mode dynamic and thermodynamic structures deduced from the correlation patterns. The oscillation is quasi-stationary, with May and June corresponding to the negative phase of MCC mode 1, and August corresponding to the positive phase of mode 1. In addition, the August departure fields exhibit the most complete spatial structure of the MCC mode, including all major features of the circulations over the entire domain.

The composite of the near 20-day oscillation is done by selecting the eight strongest cases during the three summers, which all occur in the July-September period. For each oscillation cycle six sequential phases are identified, with phase 1 being the
minimum in the MCC coefficient time series and phase 4 being the maximum. The composites of the six phases clearly indicate a near 180° out-of-phase reversal between , phases 1-4, 2-5 and

3-6. A westward propagation of 2.5°-3° per day can be seen in most fields, with phase 2 corresponding to the negative phase of MCC mode 1 and phase 5 corresponding to the positive phase of MCC mode 1.

It is obvious that the seasonal change structure is the result of the development of the northern summer monsoon. During the development, the monsoon trough extends eastward into the subtropical western Pacific, and the western front of the subtropical ridge there withdraws to the east. This leads to the largest changes to occur near 20°-25°N in the western Pacific, where the largest amplitude and the most distinctive feature are shown in the basic MCC mode. The question that is raised by this study is: what is the mechanism of the 20-day oscillations? The coincidence in the spatial structure between the near 20-day oscillation and the seasonal change suggests a hypothesis: While the seasonal change represents the development of the summer monsoon as a stationary response to the land-sea forcing, the near 20-day oscillation is a propagating response to the same land-sea forcing. The fact that the strongest cases of the near 20-day oscillation occur around August, which is the phase in the seasonal change that has the most complete MCC mode 1 structure, further supports this conjecture. The deep warm core shown in mode 1 indicates that the development of this mode is likely to depend on latent heat release associated with deep cumulus convection. Since latent heat release is not a symmetric forcing (no negative heating), only the positive phase of mode 1 provides

actual forcing. August is the month at the peak of the positive phase of the seasonal change and also has the best mode 1 response structure. Therefore, it is likely to be the period where the propagating response is also most prominently excited. The westward propagation and the spatial scale suggest that the near 20-day oscillation is a Rossby wave. Further studies, both observational and modeling, are needed to verify this hypothesis.

REFERENCES

Burpee,R.W.,1974: Characteristics of north African easterly waves during the summers of 1968 and 1969. *J.Atmos.Sci*,**31**,1556-1570.

Carlson,T.N.,1969: Some remarks on African disturbances and their progress over the tropical Atlantic. *Mon.Wea.Rev.*,**97**,716-726.

Chang,C.P. and C.R.Miller III,1977: Comparison of easterly waves in the tropical Pacific during two periods of contrasting sea-surface temperatures anomalies. *J.Atmos.Sci.*,**34**,615-628.

Chang,C.P., V.F.Morris and J.M.Wallace,1970: A statistical study of easterly waves in the western Pacific: July-December 1964: *J.Atmos.Sci.*,**27**,195-201.

Chang,C.P., J.M.Chen, P.Harr and L.Carr,1994: Northwestward propagating synoptic wave patterns over the tropical western Pacific and the periodicity of tropical cyclone activity. Submitted to *Mon.Wea.Rev.*

Chang,C.P. and H.Lim,1988: Kelvin wave CISK: A plausible mechanism for the 30-50 day oscillation. *J.Atmos.Sci.*,1709-1720.

Chang,C.P., T.C.Yeh and J.M.Chen,1993: Effects of terrain on the surface structure of typhoons over Taiwan. *Mon.Wea.Rev.*,**121**,734-752.

Chang,C.P.,1977: Viscous internal gravity waves and low frequency oscillations in the tropics. *J.Atmos.Sci.*,**34**,901-910.

Chen,J.M. and C.P.Chang,1994: A tecnique for analyzing optimal relationships among multiple sets of data fields.Part II: A reliability study. Submitted to *Mon.Wea.Rev.*

Chen,J.M.,C.P.Chang and P.A.Harr,1994: A tecnique for analyzing optimal relationships among multiple sets of data fields. Part I: The method. Submitted to *Mon.Wea.Rev.*

Chen,T.C., R.Y.Tzeng and M.C.Yen,1988: Development and life cycle of the Indian Monsoon: Effect of the 30-50 day oscillation. *Mon.Wea.Rev.*,**116**,2183-2199.

Dunn,G.E.,1940: Cyclogenesis in the tropical Atlantic. *Bull.Amer.Met.Soc.*,vol **21**,215-229.

Glahn,H.R.,1968: Canonical correlation and its relationship to discrimant analysis and multiple regression. *J.Atmos.Sci.*, **25**,23-31.

Harr,P.A.,1993: *Large-scale circulation regimes and tropical cyclone characteristics over the western Pacific ocean.* Ph.D.thesis,Dept.of Meteorology,Naval Postgraduate School,275pp.

Holton,J.R.,1971: A diagnostic model for Equatorial wave disturbances: The role of vertical shear of the mean zonal wind. *J.Atmos.Sci.*, **28**,55-64.

Horst,P.,1965: *Factor analysis of data matrices*. New York: Holt,Rinehart and Winston,730 pp.

Hotelling,H.,1933: Analysis of a complex of statistical variables into principal components. *J.of Edu.Psych.*, **24**,417-441,498-520.

_____,1935:The most predictible criterion. *J.of Edu.Psych.*, **26**,139-142.

_____,1936: Relations between two sets of variates. *Biometrika*, **28**,321-377.

Ketterning,J.R.,1971: Canonical analysis of several sets of variables space. *Phil.Biometrika*, **58**,433-460.

Krishnamurti,T.N.,J.Molinari,H.Pan,and V.Wong,1977: Downstream amplification and formation of Monsoon disturbances. *Mon.Wea.Rev.* **105**,1281-1297.

Krishnamurti,T.N.,1985:Summer Monsoon experiment -A review. *Mon.Wea.Rev.*, **113**,1590-1626.

Krishnamurti,T.N.,and H.N.Bahlme,1976: Oscillations of a Monsoon Sytem: Part I: Observational aspects. *J.Atmos.Sci.*, **33**,1937-1954.

Krishnamurti,T.N.,and D.Subrahmanyan,1982: The 30-50 day mode at 850 mb during MONEX. *J.Atmos.Sci.*, **39**,2088-2095.

Krishnamurti,T.N.,and P.Ardanuy,1980: The 10-20 day westward propagating mode and "breaks in the Monsoon". *Tellus*, **33**,15-26.

Krishnamurti,T.N.,P.K.Jayakaumar,J.Sheng,N.Surgi,and A.Dumar,1985: Divergent circulation on the 30-50 day time scale. *J.Atmos.Sci.*, **42**,364-375.

Lau,K.M.,and P.H.Chan,1986: Aspects of the 40-50 day oscillation during the northern summer as inferred from outgoing longwave radiation. *Mon.Wea.Rev.*, **114**,1354-1367.

Lau,K.H.,and N.G.Lau,1990: Observed structure and propagation characteristics of tropical summertime synoptic scale disturbances. *Mon.Wea.Rev.*, **118**,1888-1913.

Lau,K.H.,and L.Peng,1987: Origin of low frequency (intraseasonal) oscillations in the tropical atmosphere. Part I: Basic theory. *J. Atmos.Sci.*, **44**,950-972.

Li,C.Y.,and Y.P.Zhou,1992: The quasi-biweekly (10-20day) oscillation in the tropical atmosphere. *Sci.Atmos.Sinica*, **16**(in Chinese).

Libemann,B.,and H.H.Hendon,1990: Synoptic scale disturbances near the equator. *J.Atmos.Sci.*, **47**,1463-1479.

Lorenc,A.C.,1984: *The evolution of planetary scale 200 mb divergence during the FGGE year*. Meteorological Office Tech.Note II/ 210,1-23. [Available from Dynamical Climatology Branch, Meteorological Office,London road, Bracknell, Berkshire,England.]

Lorenz,E.N.,1956: *Empirical orthogonal functions and statistical weather prediction*. Sci.Report No.1 Statistical Forecasting Project,MIT,Dept.of Meteoroloy,Cambridge,Mass.,49 pp.

Madden,R.,and P.Julian,1971: Detection of a 40-50 day oscillation in the zonal wind. *J.Atmos.Sci.*, **28**,702-708.

_____,and_____,1972: Description of global scale circulation cells in the tropics with a 40-50 day period. *J.Atmos.Sci.*, **29**,1109-1123.

Nitta,T.,and Y.Takayabu,1985: Global analysis of the lower tropospheric disturbances in the trioucs during the northern summer of the FGGE year. Part II: Regional characteristics of the disturbances. *Pure Appl.Geophys.*, **123**,272-292.

_____,Y.Nakagomi,Y.Suzuki,N.Hasegawa,and A.Kadokura,1985: Global analysis of the lower tropospheric disturbances in the tropics during the northern summer of the FGGE year. Part I: Global features. *J.Meteorol.Soc.Japan*, **63**,1-19.

Norquist,D.C.,E.E.Recker and R.J.Reed,1977: The energetics of African wave disturbances as observed during phase III of GATE. Mon.Wea.Rev., **105**,334-342.

Pearson,K.,1901: On lines and planes of closest fit to points in space. *Phil.Magazine*, **2**,559-572.

Piersig,W.,1936: Schwankungen von luftdruck and luftbewengung sowie ein ein beitrag zum wettergesschehen in passatgebiet des ostlichen nordatlantischen ozeans. *Arch.Dent.Seewarte*, **54**(6). [Parts II and II have been translated and printed,1944: The cyclonic disturbances of the subtropical eastern north Atlantic. *Bull.Amer.Meteor.Soc.*, **25**,2-17.

Prohaska,J.T.,1976: A tecnique for analyzing the linear relationship between two meteorological fields. *Mon.Wea.Rev.*, **104**,1345-1353.

Reed,R.J.,and E.E.Recker,1971: Structure and properties of synoptic scale wave disturbances in the equatorial western Pacific. *J.Atmos.Sci.*, **28**,1117-1133.

_____,D.C.Norquist,and E.E.Recker,1977: The structure and properties of African wave disturbances as observed during phase II of GATE. *Mon.Wea.Rev.*, **105**,317-333.

_____,E.Klinker and A.Hollingsworth,1988: The structure and characteristics of African easterly wave disturbances as determined from the ECMWF operational anlysis/forecast system. *Meteor.Atmos.Phys.*, **38**,22-33.

Regula,M.,1936: Druckschwandungen und tornados and der wesduste von Africa. *Ann. Hydrog.Mar.Meteor.*, **64**,107-111. [Original quote from Burpee (1972,1974)]

Riehl,H.,1945: *Waves in the easterlies and the polar front in the tropics*. Misc.Rep.No. 17 Dept.of Meteorology, University of Chicago,79 pp.

Saha,K.,F.Sanders,and J.Shukla,1981: Westaward propagating predecessors of Monsoon depressions. *Mon.Wea.Rev.*, **109**,330-343.

Steel,R.G.D.,1951: Minimum generalized variance for a set of linear functions. *Ann. Math.Statist.* **22**,456-60.

Takayabu,Y.N.,and T.Nitta,1993: 3-5 day period disturbances coupled with convection over the tropical Pacific ocean. *J.Meteor.Soc.Japan*, **71**,221-246.

Tao,S.Y.,and L.X.Chen,1987: *A review of recent research of the east Asian summer monsoon in China*. Monsoon Meteorology. Chang and Krishnamurti,eds.,Oxford Univ.Press.,60-92.

Wallace,J.M.,and C.P.Chang,1969. Spectral analysis of large scale wave distrubances in the tropical lower troposphere. *J.Atmos.Sci.*, **26**,1010-1025.

Wang,B.,1988: Dynamics of tropical low frequency waves: An analysis of the moist Kelvin waves. *J. Atmos.Sci.*, **45**,2051-2065.

Wu,P.L.,and C.Y.Li,1990: The 10-20 day oscillation in the atmosphere. *Proceedings on Atmospheric Sciences*,Scientific Press,Beijing,149-159 (in Chinese).

Yanai,M.,T.Maruyama,T.Nitta and Y.Hayashi,1968: Power spectra of large scale disturbances over the tropical Pacific. *J. Meteorol.Soc.Japan,* **46**,308-323.

INITIAL DISTRIBUTION LIST

1.	Defense Technical Information Center Cameron Station Alexandria,Virginia 22304-6145	2
2.	Superintendent Atnn:Library,Code 52 Naval Postgraduate School Monterey,CA 93943-5000	2
3.	Chairman (Code OC/co) Department of Oceanography Naval Postgraduate School Monterey,CA 93943-5000	1
4.	Chairman (Code MR/Hy) Department of Meteorology Naval Postgraduate School Monterey,CA 93943-5000	1
5.	Prof. Chih-Pei Chang (Code MR/Cp) Department of Meteorology Naval Postgraduate School Monterey,CA 93943-5000	2

6. Prof. Jeng Ming Chen (Code MR/Ch) 1
Department of Meteorology
Naval Postgraduate School
Monterey,CA 93943-5000

7. Dr. Patrick Harr (Code MR/Hp) 1
Department of Meteorology
Naval Postgraduate School
Monterey,CA 93943-5000

8. Ms. Bao Fong Jeng (Code MR/Jg) 1
Department of Meteorology
Naval Postgraduate School
Monterey,CA 93943-5000

9. LT. Jorge Cardenas A. 2
GMC box 1707
Naval Postgraduate School
Monterey,CA 93943-5000